8-1954

Calorimetric Measurements on High Purity Iron and Eutectoid Steels

Marion Lewis Picklesimer
University of Tennessee - Knoxville

To the Graduate Council:

I am submitting herewith a dissertation written by Marion Lewis Picklesimer entitled "Calorimetric Measurements on High Purity Iron and Eutectoid Steels." I have examined the final electronic copy of this dissertation for form and content and recommend that it be accepted in partial fulfillment of the requirements for the degree of Doctor of Philosophy, with a major in Materials Science and Engineering.

E. E. Stansbury, Major Professor

We have read this dissertation and recommend its acceptance:

John H. Fryer Jr. Lawrence K. Jetler, Walter S. Snyder, Anton Besaumas, H. K. Garber

Accepted for the Council:

Carolyn R. Hodges

Vice Provost and Dean of the Graduate School

(Original signatures are on file with official student records.)

August 10, 1954

To the Graduate Council:

I am submitting herewith a thesis written by Marion Lewis Picklesimer entitled "Calorimetric Measurements on High Purity Iron and Eutectoid Steels." I recommend that it be accepted in partial fulfillment of the requirements for the degree of Doctor of Philosophy, with a major in Metallurgy.

E. E. Stansbury
Major Professor

We have read this thesis and recommend its acceptance:

John F. Fogl Jr.

Lawrence K. Jetter

Walter S. Landis

Anton deS Brasunas

H. J. Garber

Accepted for the Council:

E. G. Watters
Dean of the Graduate School

CALORIMETRIC MEASUREMENTS ON HIGH PURITY IRON AND EUTECTOID STEELS

A THESIS

Submitted to
The Graduate Council
of
The University of Tennessee
in
Partial Fulfillment of the Requirements
for the degree of
Doctor of Philosophy

by

Marion Lewis Picklesimer

August 1954

ACKNOWLEDGEMENT

The author wishes to express his appreciation to Dr. E. E. Stansbury for the many ways in which he has contributed to this work; his encouragement and example, the original design of the calorimeter, his constant help and suggestions in the construction and operation of the calorimeter and in the course of the work, and for his supervision and help in the preparation of this manuscript.

The author wishes to acknowledge and express his appreciation to the Department of Chemical Engineering of the University of Tennessee for the appointment of the author as Research Assistant under Atomic Energy Commission Research Grant No. AT (40-1) - 1068.

Sincere appreciation is extended to Glenn E. Elder, coworker and fellow Research Assistant, for his help in the design, construction, testing, and operation of the calorimeter used in this work; and to E. H. Honeycutt, Sr., and the members of the Chemical Engineering Shop for the manufacture of the parts of the calorimeter.

TABLE OF CONTENTS

LIST OF TABLES

LIST OF FIGURES

CHAPTER I

SUMMARY

The investigation reported in this dissertation was concerned with the determination of the thermodynamic properties of certain Fe-Mn-C alloys so that the effect of manganese on the Fe-C alloy system might be evaluated.

The metals investigated were (1) a 0.75% C - 1% Mn high purity eutectoid steel whose transformation kinetics had been previously investigated by the author; (2) a 0.87% C Fe-C binary high purity alloy; and (3) a high purity electrolytic iron.

The calorimeter used in this investigation was designed and built in the Chemical Engineering Department of the University of Tennessee. The basic design of the calorimeter was that of a specimen, heated by an internal resistance element dissipating essentially constant power, surrounded by an adiabatic shield consisting of a cylinder of highly polished copper and heated by external power. The temperature difference between the specimen and the adiabatic shield was kept to within 0.01°C by feeding the amplified emf of a differential thermocouple into a D.A.T.-Speedomax control system controlling the A.C. power input to the adiabatic shield. The calorimeter was operated at a vacuum of 0.1 microns or better and was capable of operation from room temperature to 950°C.

The adiabatic calorimeter was used to determine the apparent specific heats (not corrected for the specimen heater) and the enthalpies of transformation of the three metals. Comparison of the data for the three metals permitted the determination of the effect of manganese on

the thermodynamic properties.

The specific heat and enthalpy of transformation of high purity iron were determined and compared to values reported in the literature. The enthalpy of transformation determined by the author to be 211 calories per mol, and the temperature of transformation, 912°C on heating and 909°C on cooling, compare favorably with the accepted literature values of 215 calories per mol and 910°C respectively. The estimated true specific heat of iron is in agreement with two prior determinations, Awberry and Griffiths, and Pallister, but not in agreement above 500°C with the collation of Darken and Smith. The enthalpy of transformation of iron at subcritical temperatures was determined by the use of the specific heat data. The value at 720°C was found to be 700 calories per mol as compared to the value of 950 calories per mol reported by Darken and Smith.

The specific heat and enthalpy of transformation of a 0.87% C Fe-C binary alloy were determined. The enthalpy of transformation at 720°C was found to be 875 ± 10 calories per mol. The specific heat of pearlite in the alloy was somewhat greater than that for ferrite in the high purity iron while the specific heat of austenite in this alloy was essentially the same as for austenite in the iron. The maximum temperature of transformation reached in recalescence during a very slow transformation of austenite to pearlite was 709.4° C.

A series of the 0.75% C-1% Mn steel specimens was isothermally transformed to pearlite at 680, 660,640, and 620° C. The specific heats and enthalpies of transformation of these specimens were determined in the calorimeter. The enthalpies of transformation at 720°C ranged from 885 to 910 calories per mol for specimens isothermally transformed from

620 to 680°C respectively. From room temperature to the neighborhood of 530°C, the specific heats of the specimens were the same. Above 530°C to 700°C, a decrease in the specific heat was caused by the partitioning of Mn in the pearlite with the greatest deviation occurring for the 620°C specimen and none for the 680°C Specimen. Above 700°C no differences in the specific heat of pearlite or austenite could be detected for the different specimens. The enthalpy of partitioning of Mn in this steel was found to be approximately 30 calories per mol of steel. This value may be in error by 50%. The maximum recalescence temperature reached during a very slow transformation of austenite to pearlite was 690.8°C for this steel.

The enthalpy of tranformation of austenite to pearlite in the 0.87 % C binary alloy may be calculated at 720°C from the value of 700 calories per mol for the enthalpy of transformation of pure iron and the value of 7500 calories per mol for the enthalpy of formation of cementite from austenite as reported by Darken and Gurry. Such a calculation yields a value of 885 calories per mol of steel which may be compared to the experimental value of 875 calories per mol. A similar calculation using Darken and Smith's value of 950 calories per mol for the enthalpy of transformation of pure iron at 720°C yields a value of 1063 calories per mol of steel. This is 188 calories per mol higher than the experimental value.

The conclusions that were reached in this dissertation are as follows:

1. Manganese has little if any effect on the specific heat of austenite and pearlite except as it partitions in the pearlite during the

specific heat determination, for the steel investigated.

2. Manganese increases the enthalpy of transformation of austenite to pearlite at all temperatures.

3. Manganese will partition in pearlite with a pronounced heat effect, amounting to approximately 30 calories per mol of steel for the 0.75% C - 1% Mn steel.

4. The enthalpy of transformation of pearlite to austenite at 720°C was determined to be 875 ± 10 calories per mol for the 0.87% C binary alloy and 890 ± 10 calories per mol for the 0.75% C-1% Mn alloy.

5. The true specific heat of pearlite is unaffected by the interlamellar spacing, low percentages of alloying elements, and partitioning or lack of partitioning of the alloying element except as the partitioning occurrs during the specific heat determination, within an accuracy of determination of ± 0.5% for the specific heat.

6. The specific heat of austenite is a linear function of temperature, slowly increasing with temperature, and is not detectably different between several alloys containing relatively small amounts of alloying elements.

7. The agreement of the experimentally determined specific heats, enthalpies of transformation, and temperature of transformation of high purity iron with the literature values, and the self-consistency of the experimental data lend considerable support to the author's determinations.

8. The conclusion of Darken and Smith that the specific heats of iron above 500°C as reported by Awberry and Griffiths and by Pallister were too low is incorrect. The tables of enthalpies of ferrite and austenite as given by them are therefore incorrect, and the enthalpies of

transformation of iron as found in their table are too large at all temperatures below 910°C.

9. The interfacial energy between ferrite and cementite cannot be as great as that of 6.8×10^{-5} cal/cm^2 as calculated by Zener and probably is not as great as that of 3.3×10^{-5} cal/cm^2, experimentally determined by Thompson.

10. The free energy (chemical) of the reaction of austenite to form massive cementite plus massive ferrite for both the binary 0.87% C alloy and the 0.75% C - 1% Mn steel, as a function of the degree of supercooling may be represented by the equation

$$\Delta F = 0.7179 \ (\Delta T)^{1.0935}$$

This leads to the conclusion that changes in the chemical free energy by the addition of 1% Mn to form an eutectoid Fe-Mn-C alloy cannot cause the large differences in the rates of growth of pearlite in the two alloys.

11. The basic design of the calorimeter is satisfactory but improvements in the detailed design will be required for better operation and accuracy.

CHAPTER II

INTRODUCTION

One of the most important metallurgical problems of industry has been the investigation of the effect of alloying elements and heat treatment on the properties of steels. Most important in establishing these properties is the response of steels to the effects of alloying elements and other factors on the transformation of the high temperature phase, austenite, to various products at subcritical temperatures.

Many have contributed to the intense investigation of this difficult and interesting problem over the past seventy-five years. Many of the investigations have been empirical, yielding solutions to immediate industrial problems, several have been empirical investigations of wide scope and covering many years of work, while others have been based on various theories, improving as the basic knowledge increased, but always limited by the incomplete knowledge of the basic factors involved and the inaccuracy and lack of fundamental data.

The transformation of austenite, the face centered cubic high temperature single phase solid solution of iron, carbon, and the alloying elements, at appropriate subcritical temperatures, gives (a) pearlite, the equilibrium decomposition product composed of alternate plates of ferrite (essentially body centered cubic iron with a very small amount of dissolved carbon) and cementite, an intermetallic compound of iron and carbon having the nominal chemical formula of Fe_3C; (b) bainite, a lower temperature decomposition product, composed of essentially needles of ferrite containing particles of cementite; and (c) martensite, a still lower temper-

ature decomposition product, very hard, composed of ferrite supersaturated with carbon so that the ferrite lattice is greatly distorted. The rates of formation and the products formed are dependent on the alloy content and the temperature of transformation of the parent austenite.

All of the decomposition products have been investigated, pearlite and martensite more intensely than bainite. For most practical purposes, the pearlite transformation is of greatest importance, since it may be completed to yield the softest steel for machining and forming or suppressed to permit the martensite reaction to take place to yield the hardest and strongest steel.

Of the many investigations of the austenite-pearlite reaction, perhaps the most important have been those of Davenport and Bain (1)[1] who first proposed the addition of a time axis to the iron-carbon phase diagram, of Grossman (2) on the suppression of the reaction to give martensite, and of Mehl and coworkers (3, 4, 5, 6, 7, 8, 9) on the mechanism and kinetics of the formation of pearlite.

Davenport and Bain (1) first utilized time and temperature axes to picture the progress of the austenite transformation at constant temperature. The "S" curves, actually time-temperature-Transformation (TTT) diagrams, so derived permitted the condensation of an extremely large amount of experimental data in one diagram, and conclusively proved that the decomposition of austenite to pearlite and bainite was time dependent and was one of nucleation and growth of the product. The utilization of TTT diagrams permitted the convenient expression of many of the effects of

---

[1]The numbers in parentheses refer to numbered references in the bibliography.

alloying elements on the decomposition of austenite. One of the striking results demonstrated is the "bay" in the TTT diagrams of certain alloy steels where there is a temperature range between approximately 500 and 600°C in which the austenite may be held for weeks without transforming. Above and below this temperature range, the austenite decomposes to pearlite and bainite, respectively.

Grossman (2), using commercial steels, evaluated the effects of alloying elements, singly and in combination but always with the commercial impurities present, on the hardenability of steels, i.e., the maximum diameter of rod which could be quenched to half hardness in the center under ideal conditions. These definitive empirical investigations covered all of the normal commercial alloying elements and impurities over a range of compositions. Multiplying factors for each alloying element and impurity were determined so that the hardenability of a steel could be calculated approximately if the chemical composition was known. The results were of great and immediate significance to industrial applications, but only posed more problems to the academic and theoretical investigators.

Johnson and Mehl (8) derived mathematically, the equation representing the fraction of starting material transformed as a function of time at constant temperature for any reaction proceeding by a process of nucleation and growth. This equation was applied to the decomposition of austenite to pearlite with excellent results when the restriction of grain boundary nucleation was used, demonstrating the effect of variation of the rates of nucleation and growth on the time dependency of the reaction. However, the use of the equation does not permit the direct evaluation of nor does it predict the effect of temperature and alloying elements on the rate

of reaction. The equation is given below for the case of grain boundary nucleation with constant rates of nucleation and growth throughout the transformation at a constant temperature.

$$F(z) = 4\pi\lambda \int_0^z e^{-4\pi\lambda\alpha}\, \xi(z-\alpha)\, d\alpha$$

Where

$F(z)$ = fraction transformed at time "t"
z = Gt/a
λ = $a^3 N_s/G$
a = grain radius (austenite)
G = rate of growth of a nodule of pearlite
N_s = the rate of nucleation of pearlite nodules per unit area of grain surface
t = time
α = integration variable $\quad 0 \leqq \alpha \leqq \infty$

$$\xi(z) = \begin{cases} 3\int_{1-z}^{1} y^2\left[1 - \omega(y,z)\right] dy & \text{when } z \leqq 1 \\ 3\int_{0}^{1} y^2\left[1 - \omega(z,y)\right] dy & \text{when } z \geqq 1 \end{cases}$$

$$\omega(z,y) = \begin{cases} 1 \text{ when } \quad 0 \leqq z \leqq (1-y) \\ \left[\frac{(1+y^2) - z^2}{4y}\right] \left\{(y)^{1+y-z} \left[\frac{1+y+z}{1+y-z}\right]^{(1+y)} \left[\frac{(1+y^2)^2 - z^2}{4}\right]^{z} e^{\frac{2(1+y)}{}}\right\}^{4\pi\lambda} \\ \qquad \text{when } (1-y) \leqq z \leqq (1+y) \\ 0 \quad \text{when } z \geqq (1+y) \end{cases}$$

y = integration variable $\quad 0 \leqq y \leqq 1$

From this equation, a series of master curves were derived to which the experimental reaction curves may be fitted to permit the determination of N_s and G.

Hull, Colton, and Mehl (6), using commercial steels and a high purity binary Fe-C alloy, investigated the general reaction kinetics of the austenite-pearlite reaction. They determined (a) the effect of austenization

time and temperature (austenite grain size and homogeneity) on the overall transformation rate, (b) the rate of growth of pearlite nodules at isothermal subcritical temperatures, and (c) the rate of nucleation of pearlite as affected by grain size, homogeneity, subcritical temperature, and time at subcritical temperature. While elucidating much of the mechanism and reaction kinetics of the pearlite transformation, the actual interface mechanism of the transformation was not found.

Mehl and Roberts (7) determined the effect of undissolved carbides and of undissipated carbon gradients in austenite on the austenite-pearlite reaction. They also determined a method for finding the time of austenization required for complete homogenization of the austenite with respect to carbon.

Zener (10) has proposed, on a thermodynamic basis, a theory of the transformation of austenite to pearlite and has derived an expression for the rate of growth of pearlite from austenite. From arguments based on the iron-carbon phase diagram, thermodynamics, diffusion equations, and equilibrium solubilities of solutes across a curved interface, he concluded that the radius of curvature of a cementite plate of a growing colony of pearlite is twice the critical radius at which growth would stop, that one-half of the available free energy of the transformation is dissipated in the diffusion of carbon, and that the other half of the free energy available is used to form the interface between ferrite and cementite. From these conclusions, he derived equations for the interlamellar spacing and the rate of growth of pearlite, both as functions of temperature. The equations are

$$V_b = (\Delta T)^2 \, e^{-Q'/RT}$$

$$S_o = \frac{2\ T_e\ S}{\rho Q(T_e - T)}$$

where

V_b = rate of growth of pearlite . . . . . mm/sec
ΔT = degree of undercooling (T_e-T). . . . . ^oK
T = temperature of transformation . . . . . ^oK
T_e = equilibrium eutectoid temperature . . . . . ^oK
Q' = activation energy for diffusion of carbon. . . . . .cal/mol
Q = enthalpy of transformation of austenite to pearlite . cal/mol
S_o = interlamellar spacing. . . . . mm
S = interfacial energy between ferrite and cementite . . .cal/mm^2
ρ = density of austenite . . . . . .grams/mm^3

The equation for the rate of growth is of the correct form for it predicts the "C" curve for pearlite that is shown by an experimental rate of growth versus temperature curve. However, the theory has been severely criticized on the grounds that several assumptions used in the calculations were invalid, calculations were not checked against experimental data available in the literature, the theory was derived in terms of curved interfaces but the equations used were for plane interfaces, semi-quantitative relations were derived from purely schematic diagrams, several definitions were incorrect, and that some good experimental data directly invalidate the theory and some of the assumptions.

Using the data of Mehl et al (5) on the interlamellar spacing of pearlite, Zener has calculated the ferrite-cementite interfacial energy to be 6.8×10^{-5} cal/cm^2. The only experimental determination of the ferrite-cementite interfacial energy know to the author is that of Thompson (11) who found a value of 3.3×10^{-5} cal/cm^2 by comparing the electrical resistance of a steel of known carbon content in an annealed condition showing fine spheroids of cementite to a fully annealed condition showing coarse spheroids of cementite.

Frye (12,13) has derived theoretically from the Eyring rate theory an equation for the rate of growth of pearlite as a function of temperature, that should be general for all steels. The equation is

$$r = \frac{k\Delta T \Delta F}{chR} \exp\left(\frac{\Delta S^*}{R} - \frac{\Delta E^*}{RT}\right)$$

where

r	= rate of growth of pearlite	mm/sec
c	= a constant	^oK/mm
ΔT	= amount of undercooling	^oK
ΔF	= free energy difference between austenite and pearlite at the reaction temperature	cal/mol
h	= Planck's constant	cal·sec
R	= gas constant	cal/mol ^oK
ΔS^*	= entropy of activation	cal/mol ^oK
ΔE^*	= internal energy of activation	cal/mol
T	= temperature of reaction	^oK
k	= Boltzmann's constant	cal/^oK

The equation was derived on the assumption that there was an activated complex with an activation energy for the transformation of austenite to pearlite at the austenite-pearlite interface. A plot of $\log(\Delta T \Delta F/r)$ versus $1/T$ utilizing the experimental rate of growth data should result in a straight line whose slope is an evaluable constant times the activation energy of the complex. The equation is of the correct form in that it predicts a maximum in the rate of growth curve at some subcritical temperature. The equation gave fair results when tested with the experimental rates of growth of high purity Fe-C binary eutectoid alloys (Hull (6), McElroy(13,14)) but poor results for the high purity Mn eutectoid steels of McElroy(13,14) and the author(15). The equation was evaluated using specific heat and enthalpy of transformation data of doubtful accuracy to determine the free energy differences between austenite and pearlite. Also, the temperature dependence of the interlamellar spacing is uncertain.

None of the theories to date have explained all of the known facts of the transformation, partially, at least, because of the lack of accurate and detailed data on the specific heat, enthalpy of transformation, rate of growth, interlamellar spacing, and the effect of alloying elements on these. These data must be determined for it is known that the effects of alloying elements are much greater than can be explained by any of the theories.

Some of the known facts of the austenite-pearlite transformation are:

1. The rate of growth of a pearlite nodule is apparently constant from the time it is large enough to be distinquished by the highest magnification of the optical microscope to the time that impingement with the neighboring nodules prevents further measurement (3,6).

2. The first few tenths of a per cent of an alloying element are seemingly more effective in changing the rate of transformation to pearlite than the same amount added to a steel containing a larger amount of the same alloying element(2). This is not true for the rate of growth of pearlite, as the effect seems to be a linear function of the alloy content.

3. Almost all alloying elements decrease the rate of growth of pearlite, some more effectively than others. Only cobalt is known to increase the rate of growth (6).

4. All alloying elements change the eutectoid composition and temperature.

5. For a given alloy, the interlamellar spacing seems to be a function of the rate of growth and the amount of undercooling. However, the function is changed, sometimes drastically, by variation in alloying element so that the interlamellar spacing is not a characteristic of the rate

of growth nor of the amount of undercooling (5).

6. There is an increase in the volume of the metal whenever austenite decomposes.

7. The order of effect of the alloying elements on the rate of growth of pearlite is the same as the order of the effect on the creep strength of ferrite.

8. The effect of an alloying element on the rate of growth of pearlite is much greater in magnitude than its effect on the diffusion rate of carbon in austenite can explain.

9. The rate of nucleation of pearlite nodules is greatly affected by alloying element and content. Some alloying elements are much more effective than several times the same percentage of other elements (6).

10. The pearlite nodules are nucleated in the grain boundaries and grain corners in the austenite in clean homogeneous steels (6).

11. The pearlite nodule tends to be spherical, hemispherical, or sphere sectors in shape (6).

12. A nodule of pearlite is composed of many colonies with the ferrite and cementite lamellae being parallel in the individual colony but not from one colony to its neighbor (3,6).

13. The orientation relationship of the pearlite lamellae to the parent austenite grain is complex and is a plane of irrational indices. However, it has been determined that the cementite of the pearlite has the same orientation relationship to the parent austenite that proeutectoid cementite has and that ferrite does not have the same orientation as that of proeutectoid ferrite (9).

14. In a given alloy, at subcritical temperatures, the rate of re-

action starts slowly, increases, as the temperature is lowered, to a maximum rate in the neighborhood of 600°C and then decreases with a further lowering of the temperature. The rate of growth of pearlite follows the same pattern. Alloying elements decrease the maximum rate of transformation and growth and shift the temperature at which the maximum occurs(3, 4,5,6,7,8).

From a kinetic point of view, the possible variables are:

1. The rate of diffusion of carbon and the effect of alloying elements on this.

2. The rate of diffusion of the alloying elements themselves.

3. The thermodynamics of the system.

4. The mechanism of the transformation.

Investigations have been made to determine the rate of diffusion of carbon and the effect of alloying elements on the rate of diffusion. The effects found cannot explain the change in the rate of transformation or the rate of growth of pearlite. Other investigations have been made to determine the rate of diffusion of the alloying elements. These rates cannot explain the effect on the rate of growth of pearlite except in those pearlites where a complex alloy carbide is formed instead of the normal $(Fe,X)_3C$. The mechanism of the transformation has not been found. Those proposed have not been able to account for the effects of the alloying elements. The thermodynamics of the system are not known accurately. The data that do exist are of doubtful accuracy and have not been correlated to composition, microstructure, or heat treatment.

A consideration of the thermodynamics of the system will show that the possible independent or interrelated variables of the system are:

1. The chemical free energy relationships and the effects of the alloying elements on these.

2. The work required in the volume expansion during the transformation.

3. Since an interface is formed, the effect of temperature, interlamellar spacing, and alloying elements on the total interfacial energy involved.

4. Activation energies and entropies and the effects of alloying elements on these if the transformation can be considered as one of an activated complex, formed in the austenite, that decomposes to pearlite.

5. The partitioning or lack of partitioning of the alloying elements between ferrite and cementite in pearlite.

The application of Frye's equation to the calculation of activation energies and the effects of alloying elements on these shows that the equation is not adequate for determining the effect of manganese (13,14,15) when the chemical free energy change is used for computing ΔF in the equation. The probable reason is that the composition of the complex changes as the reaction temperature is lowered. It has been shown that (14,15) at the higher temperatures of reaction, manganese partitions in the pearlite, and that partitioning in the austenite-pearlite interface, decreasing as the temperature of reaction decreases, probably stops at approximately 650° C for an eutectoid steel containing 1% Mn. If Frye's equation is applied to the rates of growth of the 1% Mn steel below 650° C, a straight line in the plot of log ($\Delta T \Delta F/r$) versus 1/T is found as the theory would predict for a complex of unchanging composition.

Calculations of the total work done in the volume expansion accomp-

anying the transformation, shows that the total energy required is very small compared to the amount of energy released by the transformation. Unfortunately, there is no theory at present which can determine the work done at the austenite-pearlite interface and the effect it would have on the rate of growth. However, since the order of effect of alloying elements on the rate of growth and formation of pearlite is the same as that on the creep strength of ferrite, the work and strain at the interface may be important.

There exist no data of sufficient accuracy and properly correlated to heat treatment and alloy content, which can be used to calculate the thermodynamics of the system. Darkin and Gurry (16,17) have collated the data on the specific heat and enthalpy of transformation of ferrite and austenite in high purity electrolytic iron and have used the collation to calculate the thermodynamic properties of iron. There are some data (19,18) of doubtful accuracy on the specific heat of commercial steels but these have not been correlated to heat treatment or alloy content, making them almost worthless in estimating the thermodynamic properties of steels. Several values have been reported (29,30) for the enthalpy of transformation of eutectoid steels, but there is wide scatter and considerable doubt about the accuracies of the determinations. A thorough knowledge of the thermodynamics and the change with alloy content is necessary before proper evaluation of the present theories may be made and on which new theories may be based and evaluated.

The determination of the thermodynamics of a steel require a knowledge of the specific heat and enthalpy of transformation of the steel as affected by heat treatment and alloy content. From these, the free energy

of the reaction may be calculated and the effect of the variables determined.

A study of the known facts of the reaction reveals the following possible variables and effects.

1. The interlamellar spacing of pearlite decreases with increased undercooling, requiring more and more energy to create the ferrite-cementite interface. This energy must be subtracted from the chemical free energy of the system. The alloying element may or may not affect the interfacial energy per unit area.

2. The alloying elements generally partition in the pearlite at equilibrium. Any deviation from this partitioning raises the energy level of the reaction product and decreases the free energy available for the progress of the reaction. It is known that the partitioning of the alloying element seems to be a function of the rate of growth of pearlite in that as the rate of growth increases, there is not sufficient time for the diffusion to occur and the alloying element is trapped in the position it occupied in the parent austenite at the time the austenite-pearlite interface overtook it. This has been experimentally shown, but cannot as yet be calculated as the effect of strain existing in the interface on the rate of diffusion is not known, although it can be predicted that the rate of diffusion will increase.

3. The alloying element may cause a change in the enthalpy of transformation partly because of the change in the eutectoid temperature and composition, and partly because of the change in the chemical composition of ferrite and cementite.

4. With the above in mind, the specific heat and enthalpy of trans-

formation as determined for the non-equilibrium conditions should be different from those for equilibrium conditions. A specimen isothermally transformed at 620° C will have a finer interlamellar spacing and less partitioning of the alloying element than one reacted at 680°C. These effects should show up as a change in the specific heat or enthalpy of transformation or both. Two specimens of differing alloy content, reacted at the same temperature, should have different specific heat curves, or different enthalpies of transformation, or both, because of the different interlamellar spacings, different eutectoid temperatures, and different amounts of partitioning. Two specimens of the same composition, reacted at the same temperature but for different times, should show differences in specific heat or enthalpy of transformation or both because the one reacted for a longer time should be closer to an equilibrium partitioning of the alloying element. Thus, most if not all of the possible variables and effects should be evaluable from the determination of the specific heats and enthalpies of transformation of a properly selected series of steels of controlled composition and heat treatment.

The general interest in the austenite-pearlite reaction from both the practical and theoretical viewpoints plus the interest of the author in eutectoid decomposition led to the desire to determine the thermodynamics of the reaction. The prior investigation of the author on the kinetics of the reaction in a 1% Mn eutectoid steel (15) caused the selection of the particular alloys used so that the kinetic and thermodynamic characteristics of the reaction in one steel might be known. The availability of and the author's part in the design and operation of an adiabatic dynamic calorimeter of sufficient accuracy and flexibility in the Chemical

Engineering Department of the University of Tennessee led to the initiation of the investigation reported herein.

CHAPTER III

THE CALORIMETER

The basic calorimeter design has been reported in two reports, one (32) a Master's Thesis by G. E. Elder, and the other (31), a progress report under A.E.C. Reasearch Grant No. AT-(40-1)-1068, June 1952. However, a number of major improvements have been made in the calorimeter since those reports and a description of the calorimeter will be given.

The basic design of the calorimeter is that of a specimen heated internally and continuously, surrounded by an adiabatic shield continuously maintained at the temperature of the specimen. Time and power measurements (of the specimen heater) were made at predetermined temperature intervals to permit the direct calculation of the mean specific heat over each succeeding temperature interval. Convectional heat transfer between the specimen and its surroundings was minimized by maintaining a high vacuum (0.01 - 0.1 microns) in the calorimeter, conduction heat transfer by minimizing surface contact areas, and radiation heat transfer by polishing the inside of the adiabatic shield and the outside of the specimen. Temperature measurements were made by means of thermocouples fastened to the specimen and the shield, and the differential thermocouple fastened to both the specimen and shield. Maintenance of the shield temperature and rate of rise of temperature, to that established by the specimen, whether increasing, constant, or decreasing, was accomplished by the use of recently developed electronic control instruments, of great sensitivity and stability, actuated by the differential thermocouple between the specimen and the shield.

The calorimeter was designed to meet the following operational requirements:

1. Be continuously measuring from room temperature to 950° C.

2. Be capable of determining the specific heats by the power pulse method as a check on the continuous method of measurement.

3. Provide completely adiabatic conditions for the specific heat determination so that a minimum correction would be necessary for heat loss or gain.

4. Permit accuracies of determination of the specific heat of approximately 0.25% with reproducibility of at least 0.25%.

5. Permit a maximum of ease and accuracy of assembly with a maximum of reproducibility of conditions of operation, combined with a maximum of flexibility for design changes as operating conditions required.

Shortly after the calorimeter was described in the above reports, requirements 1 and 5 dictated a major change in the construction of the calorimeter base. The old calorimeter design made connection of the power and thermocouple leads from the shield to the outside very difficult due to a lack of operating space and the resulting connections were difficult to inspect visually. The calorimeter base was redesigned so that all thermocouple and power connections could be made and inspected quickly and easily. This was accomplished by making the base of one piece of brass plate 3/4 inches thick and 13 1/2 inches square. The base was water cooled by copper tubing soft soldered in a spiral groove machined in the bottom of the plate. The top of the plate was grooved to take the outer water jacket and a copper radiation shield. A number of holes were drilled to permit the entrance of the power and thermocouple leads into the vacuum

chamber. Others were drilled in the top of the plate to accomodate the thermocouple connections. The thermocouple connections from the specimen and shield were made, to the corresponding leads from the cold well, on top of the calorimeter base. The connections were made by lapping the bare wire from the specimen or shield over the proper bare wire from the cold well, with the joint electrically shielded from the calorimeter base by a thin mica shield, and from the screw applying pressure to the lap joint by a fiber bushing. The holes in the calorimeter base received a portion of the fiber bushing and were threaded at the bottom to receive the clamping screw. The power connections to both the specimen heater and the shield were made by the insertion of the power lead into a brass coupling rod and tightening a screw in the coupling. The rod from the coupling was led to the outside of the calorimeter through a machined lavite plug in the calorimeter base. The thermocouple leads to the cold well were led out through ceramic tubes cemented into brass bushings threaded into the calorimeter base, with the tubing holes containing the thermocouples leads sealed with vacuum sealing wax. The vacuum connection to the calorimeter was a 3 inch copper tubing tee silver soldered to the base from the bottom and located as close as possible to the outer water jacket. The vacuum port, the thermocouple connections, and the power connections were shielded thermally from the upper part of the calorimeter by a copper radiation shield, in thermal contact with water cooled base, which in turn was shielded from the adiabatic shield by four highly polished stainless steel radiation shields. There were three cylindrical stainless steel radiation shields interposed between the adiabatic shield and the outer water jacket to minimize the heat lost by the adiabatic shield to its surroundings.

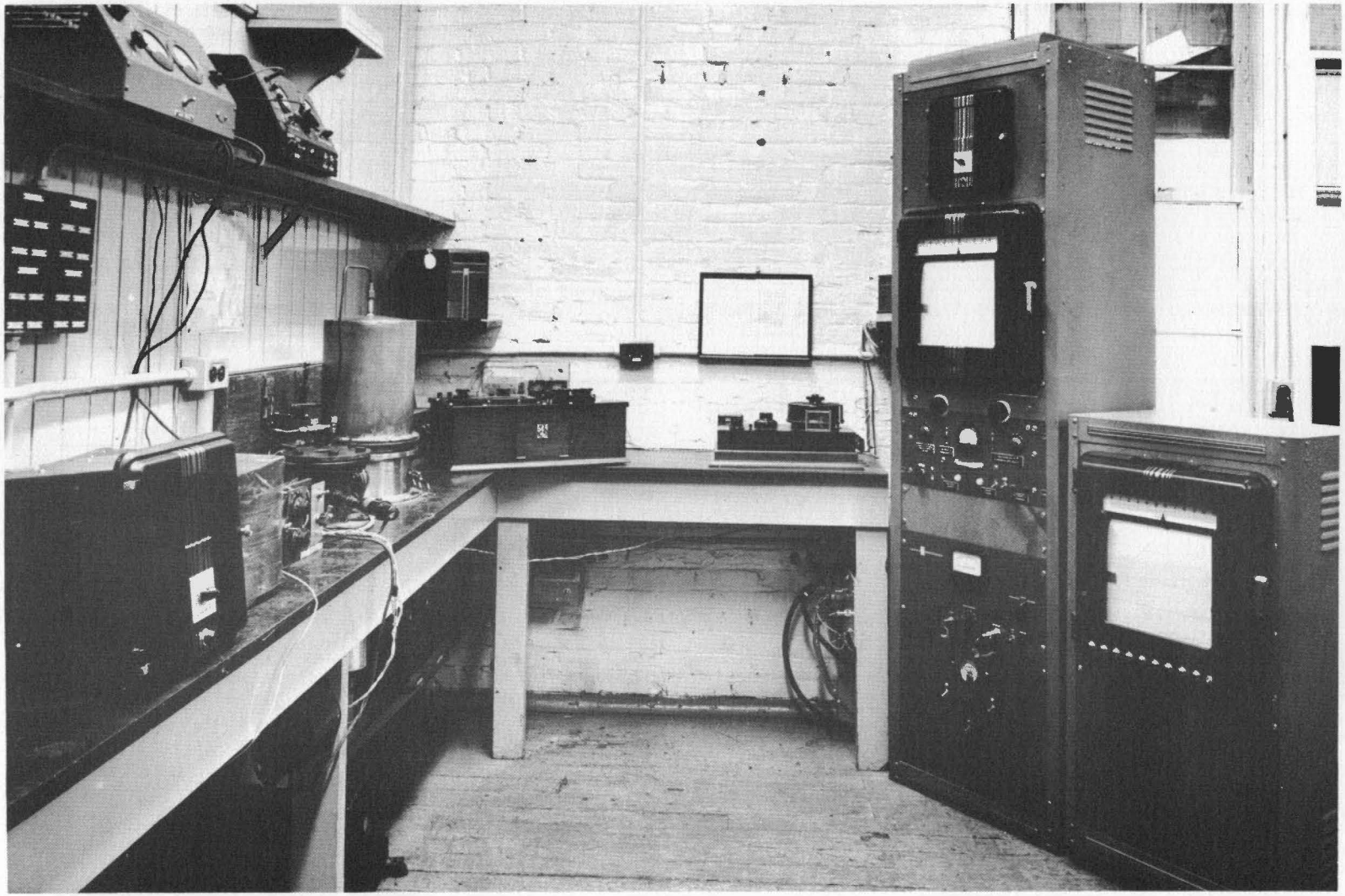

Figure 1. Assembled Calorimeter and Associated Equipment

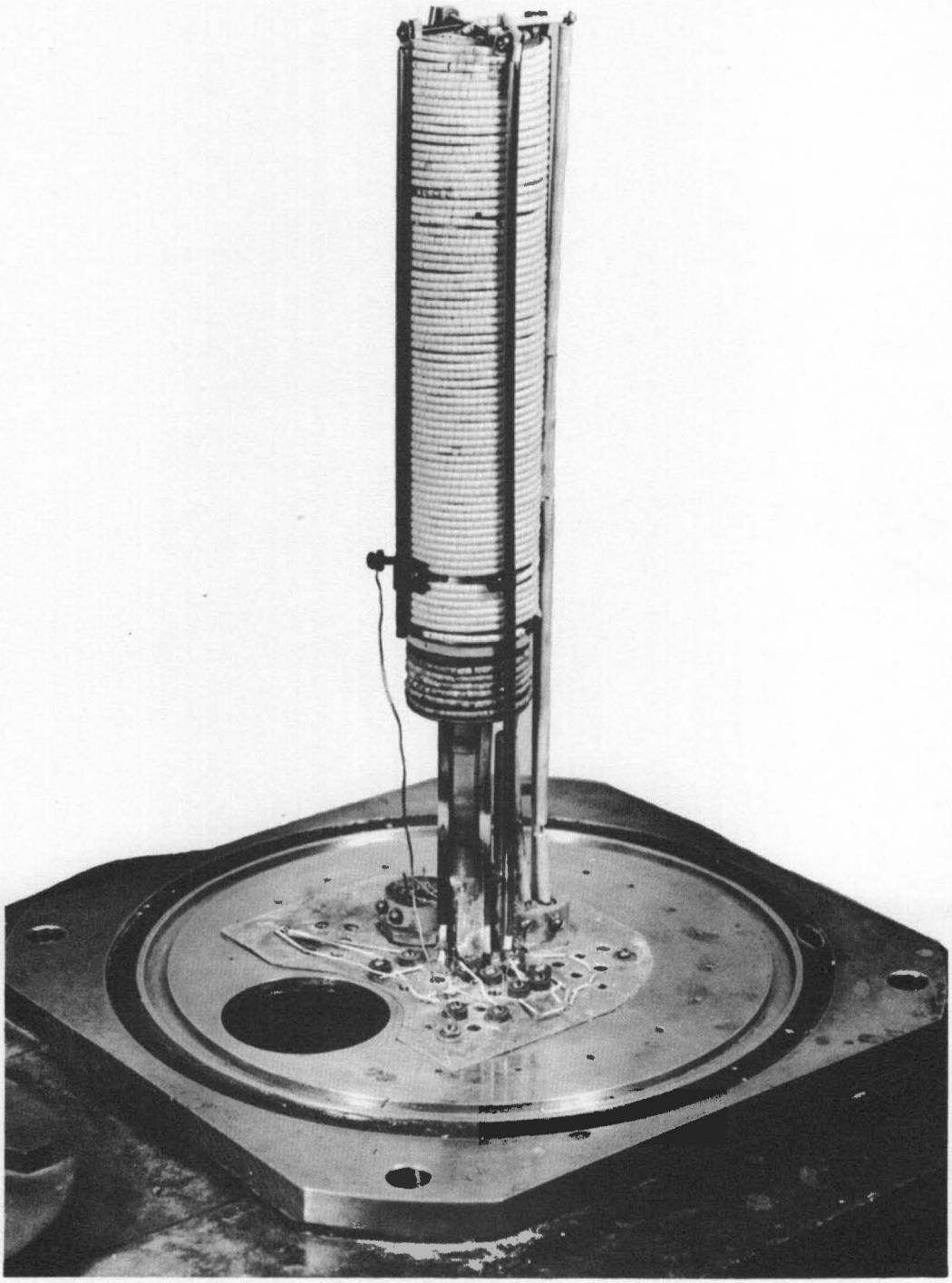

Figure 2. Calorimeter with Outer Radiation Shields Removed

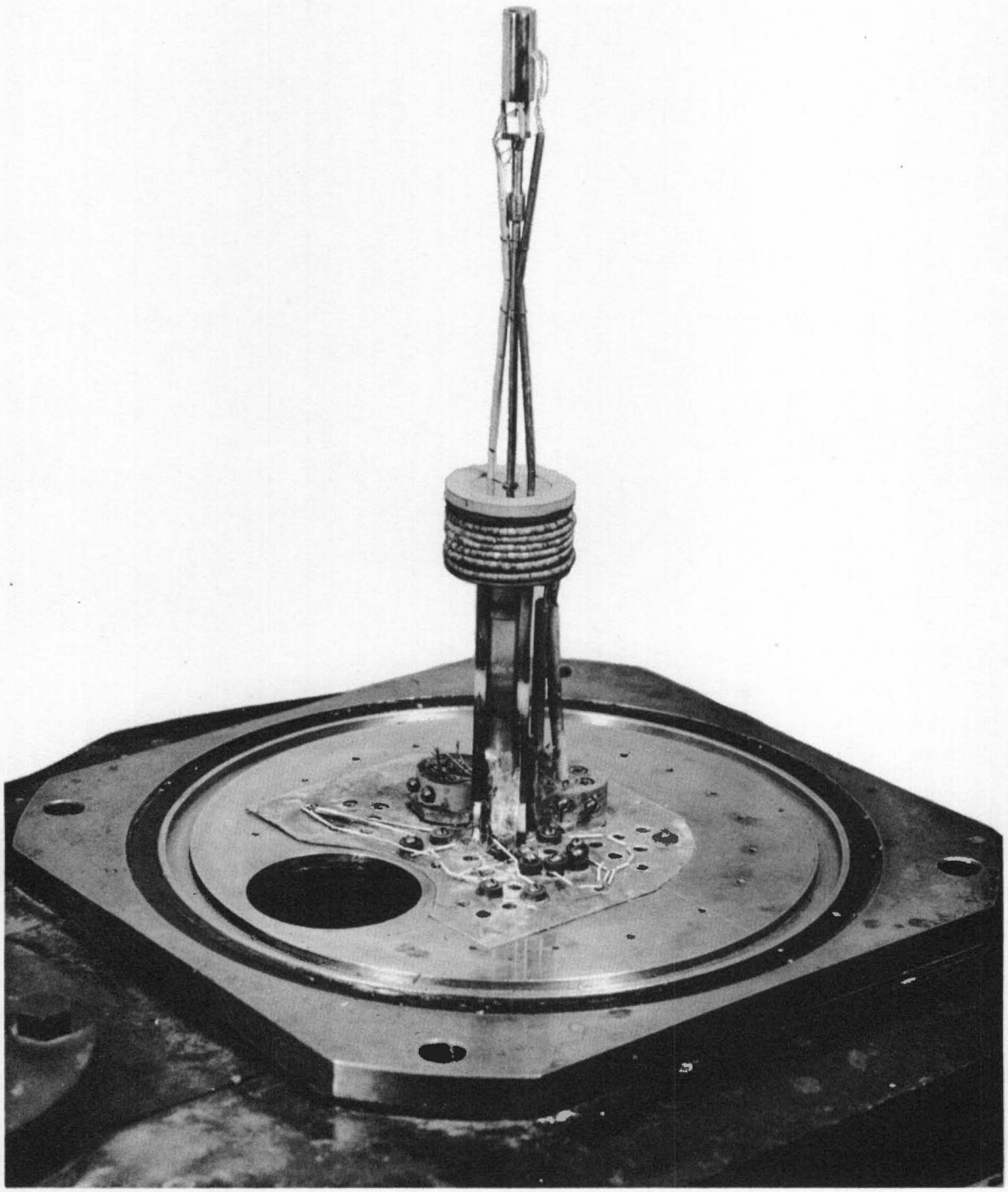

Figure 3. Calorimeter with Adiabatic Shield Removed

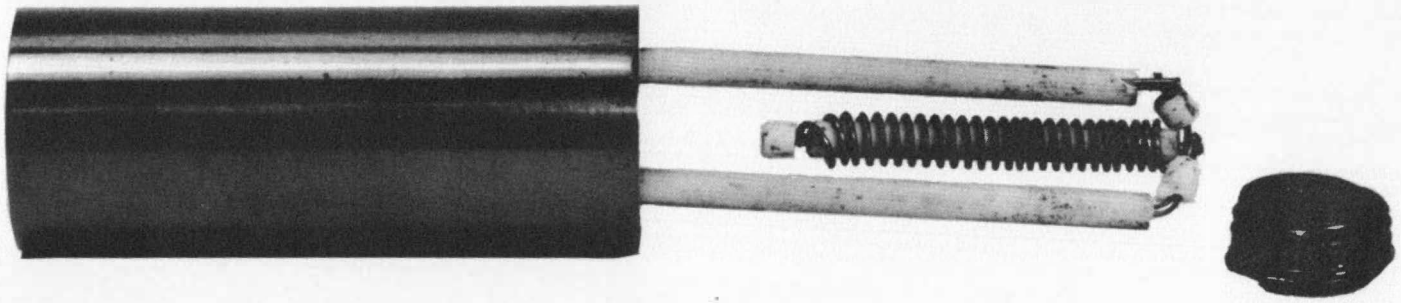

Figure 4. Specimen and Heater Assembly

The cylindrical adiabatic shield surrounding the specimen was redesigned to eliminate several faults of the older design. The overall length was increased to 9 inches so that the specimen was farther from the shield base, decreasing the amount of the specimen seen by the base, and the shield thermocouples were relocated to a spot opposite the specimen by means of a 1/8 inch diameter hole 3 inches deep in the vertical wall of the shield. An access hole was drilled radially to meet the bottom of the 3 inch hole and tapped to receive an allen screw as a plug. The thermocouple beads (the two platinum wires were beaded together as were the Pt-13% Rh wires) were inserted in two small holes drilled radially in the bottom of the plugging hole. These small holes were then peened shut so that a tight mechanical and electrical connection was made between the beads and the shield. The shield itself actually formed the thermocouple junction. The allen screw served only to shield the junction from the shield windings. The vacuum ports and mounting holes in the copper shield were placed 1 inch from the bottom of the shield. The cylindrical adiabatic shield sat on the shield base which was controlled to the cylindrical shield temperature by a control system similar to that for controlling the adiabatic shield temperature to that of the specimen.

The specimen and specimen heater designs were changed to minimize losses from the heater down the heater leads and the heater base. The heater coil was entirely enclosed by the specimen and the power leads were led from the outside through the wall of the specimen almost the entire length of the specimen before fastening to the heater coil. The open top of the specimen was closed by a threaded plug. In this manner heat losses by conduction down the power leads was minimized since the

power leads were essentially at the specimen temperature at the point of exit from the specimen. Heat losses by radiation from the coil were eliminated since no part of the coil could "see" the outside. The potential leads for measuring the voltage drop across the heater were fastened at the point where the power leads entered the specimen. The heating coil was located in the center of the specimen by ceramic tubing, covering guide pins welded to the coil, in locating holes in the specimen and plug. No vacuum ports were drilled in the specimen. The heater coil and power leads contained in the specimen were oxidized in open air by electrically heating the coil to a bright red heat for five minutes. This greatly increased the emissivity of the heater coil so that the temperature differential between the coil and the specimen was considerably reduced, again decreasing the conduction losses down the power leads.

The control system was not changed. It consisted essentially of a Leeds and Northrup D.A.T. and Speedomax control system, actuated by the differential thermocouple between the specimen and the adiabatic shield whose output was amplified by a Leeds and Northrup Microvolt D.C. Amplifier. The D.A.T. is a duration adjusting type control instrument which pulses power to the furnace unit according to the demands of the system. The Speedomax is both a recorder and the sensing unit for the D.A.T., sensing the temperature differential, and causing the electronic and electrical circuit of the D.A.T. to sense the direction as well as the rate of change of the temperature differential between the specimen and the shield, with the consequent adjustments of the pulsing of the power to the furnace to bring both the temperature differential and the rate of change of temperature differential to zero. The Speedomax was of the zero center, 10 milli-

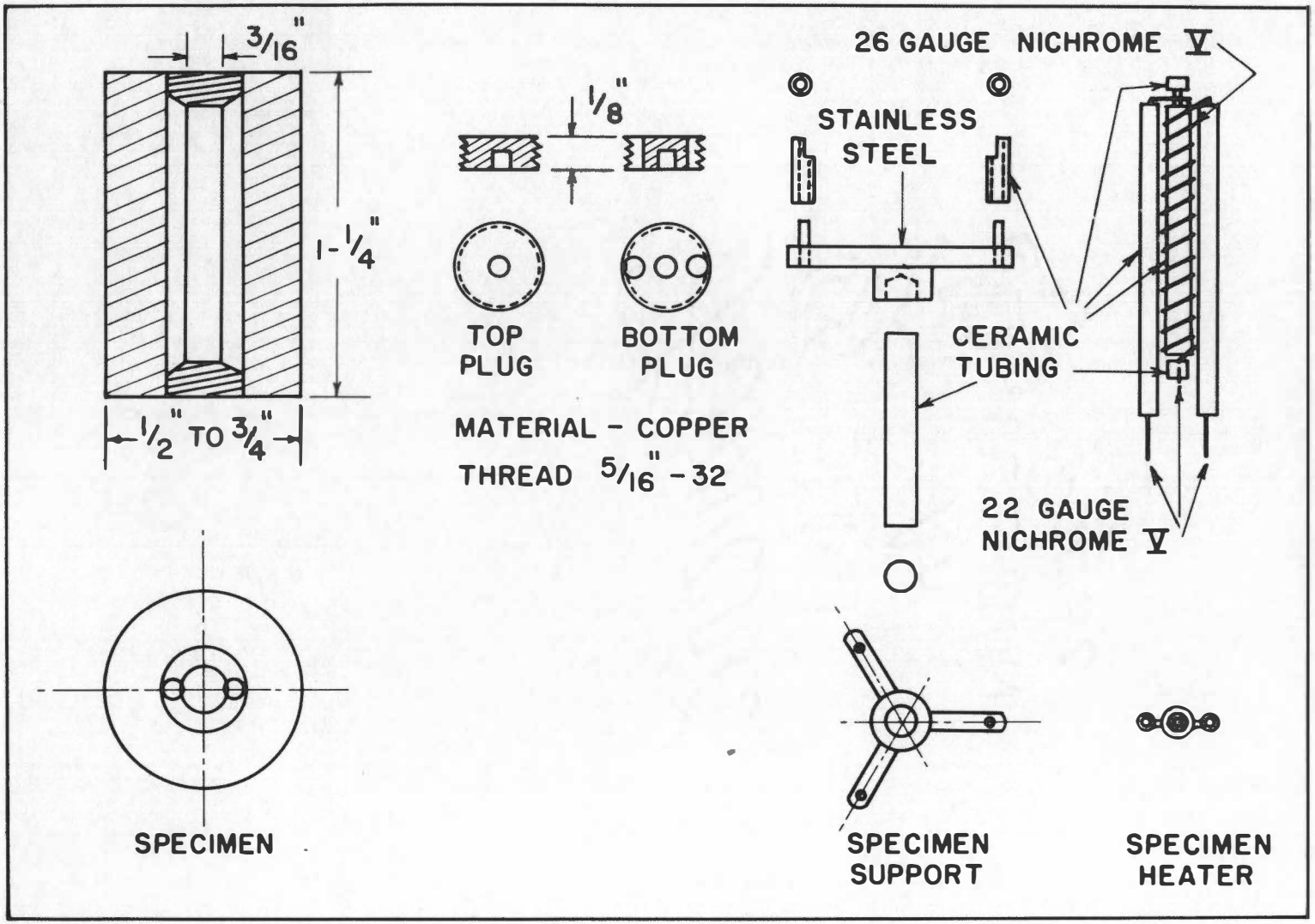

Figure 5. Specimen, Plugs, Heater, and Support Design

volt range type, providing operating control with temperature differentials both positive and negative for the shield temperature over that of the specimen. The D.C. Microvolt Amplifier was provided with an amplification selector, which when set on a scale number of 2, caused the full range of the Speedomax to correspond to 100 microvolts output of the differential thermocouple. For the Pt-Pt 13% Rh thermocouple used, this amounted to approximately ten degrees Centigrade at 500° C.

The adiabatic shield base temperature was controlled to that of the adiabatic shield by a control system using the D.A.T. as above but with the Speedomax replaced by a null balance system similar to it. A D.C. Microvolt Amplifier was used to amplify the differential thermocouple output as before.

Because of the much higher heat losses of the adiabatic shield to the surroundings at the higher temperature, the D.A.T.-Speedomax control system was unable to maintain proper control at the higher temperatures with the amount of power proper for the lower temperatures. Because of this and the fact that the D.A.T.-Speedomax control is most stable when the D.A.T. is pulsing at a rate such that the power on-off times are equal, a variable transformer was used to provide the power for the adiabatic shield. The setting of the variable transformer was continuously and automatically adjusted to supply the necessary power by a null balance system using a thermocouple on the shield.

When the calorimeter was previously reported, the specimen heater power was supplied by a constant voltage source to minimize power changes during the runs. The voltage control unit proved too unstable to permit consistently accurate and rapid readings. The circuit was redesigned to

contain only two resistances, variable in steps, the standard resistance for measuring the amperage of the circuit, the specimen heater, and the 6 volt battery. This circuit proved sufficiently stable for use, with a slow and steady drift that was small enough to permit comparison of successive runs on the basis of specimen power.

The approximate temperature of the specimen was continuously recorded by a Leeds and Northrup recorder having 1 millivolt full scale and indexing to 10 millivolts in one millivolt steps.

The specific temperature of the specimen was measured by a Rubicon Thermofree Microvolt Potentiometer and the voltage and amperage of the specimen heater was measured by a Leeds and Northrup Type K-2 Potentiometer.

When compared to the older designs of calorimeters (20-29), this calorimeter had the following advantages:

1. Only one operator was required.

2. Heating rates from zero to 5°C per minute could be set by simple adjustment of the variable resistances in the specimen heater circuit.

3. Specific rates of heating and cooling by radiation between the specimen and shield could be established by offsetting the shield control to establish the desired temperature differential. Corrections for heat losses and thermocouple errors could be made in this manner during a run. Small corrections amounting to 0.5 to 5 microvolts were generally necessary during a run. The offset required could be determined by opening the specimen heater circuit and allowing the control system to stabilize. Generally, the offset required during the run was the offset necessary to prevent any drift in the specimen temperature. Above 700°C, the increas-

ing electrical conductance of the insulating refractories in the calorimeter permitted an emf from the specimen heater circuit to be impressed on the differential thermocouple, causing an error in the control. The offset necessary to correct for this impressed emf could be determined by momentarily opening the specimen heater circuit and determining the amount of movement of the control Speedomax pen.

4. Specimen machining and installation were made quite simple when compared to some of the older calorimeters.

5. Specific heats could be measured as mean specific heats computed over any temperature interval greater than five degrees from approximately 60°C to 950°C.

6. The calorimeter could be opened, the new specimen installed, all connections made, the calorimeter closed, and the vacuum reduced to operating conditions in four hours or less.

7. The thermocouple connections were easily, quickly, and positively made on the base of the calorimeter and could be visually inspected. Parasitic thermal effects were minimized by careful choice of wire, by careful annealing, by handling the thermocouple wire so as to prevent contamination (by the use of surgeon's rubber gloves), and by the fact that there was no intervening metal in the connections of the thermocouple wires made on the calorimeter base.

8. The operating inaccuracies were reduced to those of measurement of the temperature interval and time. The absolute accuracies of the true specific heats were determined, however, by the accuracy of the determination of the calibration of the specimen heater, since this was far greater than the errors involved in the measurement of the temperature interval.

9. Cooling rates varying from zero to a maximum of 12°C per minute at 900°C and 5°C per minute at 400°C could be set and held for any desired temperature interval. For example, one transformation in an eutectoid steel on cooling required seven hours from the start to the completion of the transformation while another transformation on cooling in the same steel specimen required less than five minutes. The only difference in the calorimeter in the two cases was the differential offset of the Speedomax control for cooling.

10. The entire specific heat curve from room temperature to 950°C could be determined in as little as seven hours for an eutectoid steel specimen containing approximately 1/3 mol of steel.

11. Specimen sizes could be varied from 7/16 inches in diameter by 1 inches long to 3/4 inches in diameter by 3 inches long with no change in the calorimeter with the exception of the specimen heater.

12. The thermocouples were welded to the specimen as separate wires by condenser discharge (Federal Tweezer Weld) for all specimen metals except copper so that the specimen surface completed the thermocouple junction. For the copper specimens, the platinum wires were beaded together and welded to the specimen as were the Pt-13% Rh wires with the specimen still serving as the thermocouple junction. The weld in this case was made with a specially built welding gun and condenser welder which caused an arc to flash from the wires to the specimen as the gun tip contacted the specimen.

The limitations of the calorimeter were:

1. The lowest temperature at which the specific heat could be determined was somewhat greater than 60°C, depending on the time required for

the temperature control system to maintain the shield temperature to within 0.2°C of that of the specimen. If a refrigeration system was incorporated into the calorimeter jacket, the starting temperatures could be lowered and the specific heats near 0°C determined.

2. The accuracy of the calorimeter measurements was greatly limited by the thermocouples used. All base metal thermocouples proved to be too inhomogeneous, to change composition by preferential vaporization, or to be too sensitive to cold work during installation with the severe thermal gradients present in the calorimeter. All pure metal thermocouples investigated proved to be too sensitive to contamination. The Pt–Pt 13% Rh thermocouples were insensitive to small amounts of cold work in the thermal gradients, and showed no apparent composition change due to preferential vaporization. However, they were seriously limited in the thermal emf generated per degree was so low that measurements of the temperature intervals were limited to 0.01°C. For a 20°C interval, this represents an error of ± 0.1% while for a 5°C interval, it is an error of ± 0.4%. In this regard, the pure metal thermocouple, palladium–molybdenum, is undergoing investigation. It should be stable, not too easily contaminated, and generates approximately 40 microvolts per degree relative to 10 for the Pt–Pt 13% Rh thermocouple used. This will increase the accuracy of the measurement of the temperature interval by a factor of four and will require improvement in the method of measuring the time of the temperature interval.

3. The calorimeter was limited in the maximum temperature practically attainable by the copper used in it in the adiabatic shield and the copper leads for power to the specimen. The temperature was limited to 950°C for fear of damage to the adiabatic shield and the shield base. The limitation

of 950°C may be removed by eliminating all copper in the calorimeter and making the shield of molybdenum.

4. While the accuracy of measurement of the apparent specific heat, defined herein as the total heat input per degree divided by the total weight of the specimen and heater, as determined in the calorimeter was ± 0.5% or better (considering reproducibility of the measurement), the accuracy of the true specific heat of the specimen was limited by the accuracy of the calibration of the specimen heater and of the calorimeter for heat losses by the specimen. The problem of calibration of the calorimeter is a difficult one. No metallic specific heats have been determined with sufficient accuracy for use in the calorimeter, and non-metallic materials cannot be used for calibrating since the conditions of operation would be quite different than those for metals. If the specimens of the same metal and different weights are used to calibrate by the method of differences, the effect of different heating rates for the same power level, or of different power levels for the same heating rate must be considered. In such calibrations, a major difficulty is encountered in correcting for heat losses from the specimen heater under these various conditions of operation. At the same energy input, different heating rates give different time intervals over which heat may be lost by conduction down the heater leads, etc. Different energy inputs, on the other hand, result in different operating temperatures for the heater and hence to different losses again. It should be possible to investigate these variables systematically and thus arrive at a calibration.

CHAPTER IV

MEASUREMENTS AND ERRORS

In the original design of the calorimeter, the limiting accuracies of the measurements of the variables of the system were carefully considered so that the total error of measurement of the specific heat would be dominated by one error, i.e., if the error of temperature measurement is to be $\pm$ 0.1%, then the total of all other errors is to be 0.05% maximum.

The mathematical equation for the calculation of the apparent specific heat in the calorimeter is

$$C_p^a = \frac{EItk}{\Delta T\, w}$$

where

C_p^a = apparent mean specific heat at constant pressure over the temperature interval of ΔT °C
ΔT = the temperature interval in °C
E = voltage across the specimen heater in volts
I = amperage in the heater circuit in amperes
t = time required to traverse the temperature interval in seconds
k = conversion factor of watt-seconds to calories
w = weight of the specimen, heater, and plugs in grams

With the power in the specimen heater being measured by a Leeds and Northrup Type K-2 Potentiometer to 2 parts in 10,000, time (300 or more seconds for a 20°C interval) to 0.2 seconds, weight to 0.001 grams for approximately 20 grams weight, and the temperature interval to 0.2 microvolts, the error of determination of the apparent mean specific heat is fixed by the measurement of the microvolts per temperature interval and of the time of the interval. If the temperature interval is long or the microvolts per interval are large, the error in the measurement of the temperature interval will be of the same magnitude as that of time. If

the temperature interval is short or the microvolts per degree small, the error in the measurement of the temperature interval will dominate the others. Since only the Pt-Pt 13% Rh thermocouple proved acceptable for reasons previously discussed, the temperature interval measurement was limited to the accuracies of measuring the emf of the thermocouple used by the potentiometer used. The Rubicon Thermofree Microvolt Potentiometer used was accurate to ± 0.1 microvolts. For a temperature interval of 20°C in the neighborhood of 500°C, the emf change of the thermocouple is approximately 200 microvolts. An error of ± 0.1 microvolts at each end of the interval causes an error of ± 0.1% in the measurement of the 20°C temperature interval. At a heating rate of 4°C per minute, the time required for the 20°C interval is 300 seconds which when measured to ± 0.2 seconds yields an error of ± 0.067% in the time interval. The errors in power and weight measurements are negligible in comparison. Therefore, the total maximum error for the above conditions is ± 0.17%. If the heating rate is cut to 2°C per minute, then the error in the time measurement of the interval is only ± 0.033% and the total error is then ± 0.133%. If the heating rate is still slower, the total error is not greatly improved for the limiting error is that of temperature measurement. Only an improvement in the thermal emf of the thermocouple or an increase in the accuracy of the measurement of the emf will improve the total error of measurement. Both of these improvements will be more thoroughly discussed in the section on recommendations.

Initial specific heat measurements on copper indicated consistently reproducible jumps of 1 to 2% in the apparent specific heat in the neighborhood of 500°C. A check of the methods of measurement revealed no cause,

and nothing in the calorimeter operation could be detected which might explain the reproducible errors. An examination of the temperature-emf tables used (Table 4, Bulletin No. 508, Bureau of Standards) showed that in the neighborhood of 500°C, the microvolts for each successive 20°C. interval did not increase smoothly but jumped in the same way as the errors in the apparent specific heats. A thorough check of the tables showed that all of the discrepancies occurring in the apparent specific heat curves were caused by the errors in the microvolts per successive 20°C interval as listed in the tables. It was then realized that the accuracy being demanded of the tables was considerably greater than that with which the tables had been derived. Smoothing of the tables was required. Since this smoothing is quite critical in adjudging the accuracy of the final results, the process will be described in detail.

Reference to the literature cited in the Bureau of Standards Bulletin No. 508, Tables 4 and 5, gave the details of the methods by which those tables were derived. A group of Pt-Pt 10% Rh thermocouples was calibrated against standard melting points, established by gas thermometry in terms of the International Standard Temperature Scale, and their readings averaged for each point. Between successive points, the temperature-emf relationship was assumed to follow second order polynomials, which were so related that the slopes (derivatives) of the successive equations were the same at the calibration point serving as their junction, as well as giving the same value of the emf for that point. These equations were then used to calculate the emf for each degree of temperature over the range from 0°C to 1300°C. These calculated emf values were rounded off to the nearest microvolt. For the determination of the tables for the Pt-Pt 13% Rh thermo-

couples, five Pt-Pt 10% Rh thermocouples and six Pt-Pt 13% Rh thermocouples were fastened to a metal block, the block heated by a furnace, the temperature determined by averaging the readings of the 10% Rh thermocouples, and the average reading of the 13% Rh thermocouples was taken as the value of the emf at that temperature. Apparently the tables determined for the 10% Rh thermocouples were used for the entire range of temperature as no mention was made of calibrating the 13% Rh thermocouples by the standard melting point method. No mention of any assumption of equations was made for the 13% Rh thermocouples. This work was done in 1911 and 1913. The only changes made by the Bureau of Standards since has been the adjustment of the tables to allow for the redefinition of some of the melting points and for the change in the volt standard. No determinations have been made against the platinum resistance thermometer although this thermometer is the defined standard from 0°C to 630°C.

As no equation could be found which would approximate the emf-temperature curve for the Pt-Pt 13% Rh thermocouple for more than a 50°C interval above 200°C with the required accuracy, it was decided to smooth the tables by the process of successive differences.

The assumption was made that the temperature-emf values at the standard melting points were correct as listed in the tables 4 and 5, and these values were used to test the smooth tables.

To apply the method of differences, the emf differences for each successive 10°C interval, divided by 10, in Table 4, Bulletin No. 508, starting at 0°C, were plotted against the mean temperature for the interval. A smooth curve was drawn between the points from 0°C to 1100°C. No section of the curve was drawn that did not cover at least 200°C and smooth into

the other sections, both above and below. The emf per degree was read off in thousandths of a microvolt for each degree and tabulated. The differences of these values were tabulated. The differences were again taken and tabulated. This amounted to taking the numerical values of the third derivative of the temperature-emf curve. These last differences were adjusted to give as smooth a succession of values as possible. These adjusted differences were then totaled successively, these totaled successively, etc., until the values of the emf-temperature curve were given. These values were checked against the values assumed correct at the standard melting points. Any discrepancy of more than 2 microvolts at any calibration point caused an adjustment of the drawn curve and the adjusted differences, with the redetermination of the table until, in the final table, the smoothed values did not vary more than 2.2 microvolts from the assumed values at the standard melting points from the ice point to the melting point of gold, 1063°C. No further adjustment of the curve would yield a lower variation at all of the standard calibration points. This final table was smooth to 0.001 microvolts, but is only smooth to that value. The absolute accuracy of the table cannot be greater than that of the emf values at the standard melting points that are listed in Table 4, Bulletin No. 508, Bureau of Standards, which have been assumed to be correct. An example of the calculations is given in Table I. The final smoothed table is given in Appendix A.

A comparison of the apparent specific heat curves of copper, one using the values of Table I, Bulletin No. 508, and the other using the values from the smoothed tables to recalculate the same data, is shown in Figure 6. It is to be noted that in the curve for the smoothed table, the

TABLE I

CALCULATIONS FOR SMOOTHING THE EMF-TEMPERATURE CURVE FOR Pt-Pt 13% Rh THERMOCOUPLES BY SUCCESSIVE DIFFERENCES

1 °C	2 μv	3 μv/°C	4 $3_{i+2}-3_i$	5 $4_{i+2}-4_i$	6 adjusted 3rd diff.	7 7_i+6_{i+1}	8 8_i+7_{i+1} μv/°C	9 9_i+8_{i+1} μv at °C	10 line no. i
		5.621					5.620		20
10	55		0.022	-0.001	0	0.022		55.210	21
		5.643		0	0		5.642		22
11	61		0.022			0.022		60.582	23
		5.665		+0.001	0		5.664		24
12	66		0.023			0.022		66.516	25
		5.688		-0.001	0		5.686		26
13	72		0.022			0.022		72.202	27
		5.710		0	0		5.708		28
14	78		0.022			0.022		77.910	29
		5.732		0	0		5.730		30
15	83		0.022			0.022		83.640	31
		5.754		0	0		5.752		32
16	89		0.022			0.022		89.392	33
		5.776		0	-0.001		5.773		34
17	95		0.022			0.021		95.165	35
		5.798		0	+0.001		5.795		36
18	101		0.022			0.022		100.960	37
		5.820		0	0		5.817		38
19	106		0.022			0.022		106.777	39
		5.842		-0.001	-0.001		5.838		40
20	112		0.021			0.021		112.615	41
		5.863					5.859		42

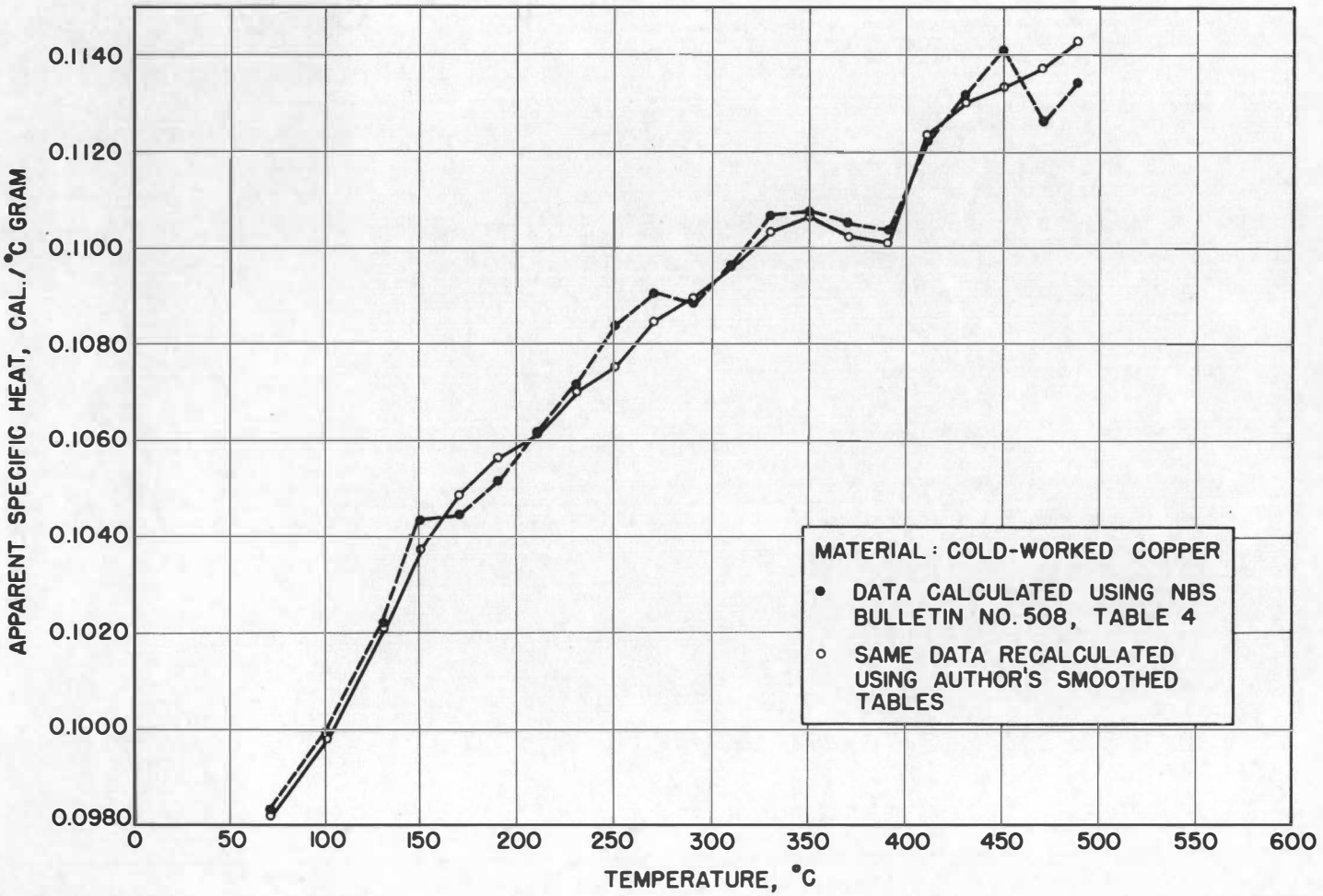

Figure 6. Apparent Specific Heat Curves of Cold-Worked Copper Using NBS Bulletin No. 508 and Author's Smoothed Tables to Calculate the Temperature Interval

points for each 20°C interval do not deviate from the smooth curve by more than 0.25% for any point and less than this for the majority of points.

A table of differences of the emf values for each degree of temperature between the smoothed table and Table 4, Bulletin No. 508, is given in Appendix A. An examination of this table shows that the curves for the two tables cross several times between 0°C and 310°C. Above 310°C and particularly above 470°C, the tables deviate up to 5 microvolts at 509°C, then gradually approach each other until the deviation is as low as 1.3 microvolts at 640°C. They again deviate considerably near 750°C, but not as greatly, and again near 950°C. At 1063°C, the deviation is only 0.940 microvolts. It is believed that the values in Table 4, Bulletin No 508, are in error. If the emf values at 380, 430, and 480°C are used to evaluate a second order polynomial equation, it will be seen (Appendix A) that the values in Table 4, Bulletin No. 508, do not deviate from this equation by more than 1.3 microvolts at any temperature. If this equation is extrapolated to 500°C, the difference of values is 0.8 microvolts. If the emf values for 500,550, and 600°C are used, and this equation extrapolated to 480°C, the difference is 2.8 microvolts. These differences indicate that the emf values in Table 4, Bulletin No. 508, increase too rapidly between 480 and 500°C.

The apparent specific heat of copper, given in Figure 6, shows that no experimental point deviates from the smooth curve by more than 0.25%, and that the curve is smooth and continuous from 60 to 500°C. This demonstrates that the new table is consistent and smooth to a degree greater than the error of measurement of the temperature interval.

The assumption is made that while the actual thermocouples will

deviate from the table, the deviation will be smooth and reproducible in each thermocouple.

For differences of specific heat in the same specimen, caused by cold working, heat treatment, age hardening, etc., a calibration of the calorimeter to yield true specific heats is not necessary. However, if different specimens are to be compared, or the data used in thermodynamic calculations, the true specific heats are required and a calibration is necessary.

To perform this calibration, the apparent specific heat of a heavy copper specimen was determined. The specimen was removed from the calorimeter and some mass removed by machining. The lighter specimen was replaced in the calorimeter and the apparent specific heat determined. Since the true specific heat must be the same in both runs, the difference in the apparent specific heats must be in the energy required for the heater and the heat losses. To determine the heat losses, several runs were made at heating rates of 1, 2, and 4°C per minute on the same specimen. No differences greater than the reproducibility of the runs at the same rate of heating on the same specimen, were detected. This meant that the effect of the heating rate was negligible and the heat losses from the heater were small. Several runs were made to check the reproducibility of installation by removing the specimen from the calorimeter, reinstalling the same specimen including rewelding of the thermocouples, and redetermining the apparent specific heat curve. No differences were detected greater than the reproducibility of rerunning an undisturbed specimen.

The heater calibration was determined by substituting the smoothed values of the apparent specific heats of the two runs using the same

heater but different weight specimens, in a formula derived as follows.

The apparent specific heat equation for this calorimeter is

$$C_p^a = \frac{EItk}{\Delta Tw} \tag{1}$$

Since the weight of the specimen and heater combined is in the above equation, the equation can be rearranged to separate the energy going to the specimen and that going to the heater, provided the assumption is made that the heat losses from the heater are negligible.

$$EItk = (C_p^t w_s + C_h w_h)\Delta T \tag{2}$$

where

C_p^t	= true specific heat of copper	cal/gram °C
C_h	= true specific heat of the heater	cal/gram °C
w_s	= true weight of copper	grams
w_h	= true weight of the heater	grams

If the values for the run of the heavy specimen are designated with the subscript 1, and the values for the light specimen with 2, the equation for the true specific heat of the specimen and heater may be derived as follows.

From equation (2)

$$E_1 I_1 t_1 k = (C_p^t w_{s1} + C_h w_h)\Delta T \tag{3}$$

$$E_2 I_2 t_2 k = (C_p^t w_{s2} + C_h w_h)\Delta T \tag{4}$$

Rearranging

$$C_h w_h = E_1 I_1 t_1 k/\Delta T - C_p^t w_{s1} \tag{5}$$

$$C_h w_h = E_2 I_2 t_2 k/\Delta T - C_p^t w_{s2} \tag{6}$$

Rearranging (1)

$$EItk = C_p^a w \Delta T \tag{7}$$

Combining (5),(6), and (7), and rearranging

$$C_p^t = \frac{C_{p1}^a w_1 - C_{p2}^a w_2}{w_1 - w_2} \tag{8}$$

In determining the specific heat of the heater and of the specimen, smooth curves were drawn through the experimental points, and the values on the smooth curves used for C^a_{p1} and C^a_{p2}. This minimized the error in the specific heat curve of the heater due to experimental errors in the apparent specific heats. The values for the true specific heat of the specimen and heater are given in Figure 7 and tabulated in Appendix B.

Unfortunately, errors in the correction for the heater are so great they overshadow the experimental error of 0.25%. For this reason, the absolute accuracy of the true specific heats as given in this dissertation may be in error by 2 to 3%. However, the relative accuracy for comparison of specimens of similar weight is still that of the experimental accuracy, ± 0.25%.

CHAPTER V

PLAN OF THE INVESTIGATION

The data needed to determine the thermodynamics of the transformation of a steel are: (1) the specific heat of austenite from above the critical temperature to the transformation temperature, (2) the specific heat of the transformed product from the reaction temperature to room temperature, (3) the enthalpy change at the transformation temperature, and (4) the variation of these with temperature of reaction.

Since the calorimeter could not be used to determine these data directly, that is, during the transformation of austenite to pearlite at temperatures well below the critical temperature, the problem was approached from the reverse transformation. If the specific heat of the pearlite and austenite are known throughout the temperature range over which the transformations are to be studied, and the enthalpy of transformation of pearlite to austenite is known at one temperature, then the thermodynamics of the reaction of austenite to pearlite may be calculated as a function of temperature.

In order to determine the effect of the variation of the reaction temperature on the transformation of austenite to pearlite, specimens of known alloy content were completely transformed at various subcritical temperatures, for times just long enough to complete the transformation. These were run in the calorimeter to determine the specific heat of the pearlite from room temperature to the reaction temperature, pearlite to austenite, the enthalpy of transformation of pearlite to austenite, and the specific heat of austenite from the reaction temperature to approxi-

mately 900°C. Any differences in the specific heat of the pearlite to the reaction temperature would be due to differences in interlamellar spacing, to any partitioning of the alloying element between ferrite and cementite in the pearlite, and to inherent differences in the pearlite itself since pearlite reacted at a lower temperature may be in a higher energy state than pearlite of the same physical structure reacted at a higher temperature. Any differences in the enthalpy of transformation of pearlite to austenite would be due to the differences in the partitioning of the alloying element, the interlamellar spacing, and possibly due to the energy state of the pearlite. By comparison of the specific heats and the enthalpies of transformation of the specimens that had been treated to different conditions, the effect of each of the possible variables and conditions could then be determined.

Since the kinetic data for a high purity 0.75% C-1% Mn steel (15) had been determined and the specimens of the proper size and shape had been transformed to 100% pearlite at several subcritical temperatures for this investigation, the primary object of this investigation was a determination of the thermodynamics of this steel. In order to help evaluate the effect of the addition of the manganese as an alloying element, specimens of high purity iron, carburized to eutectoid carbon content were to be isothermally transformed at the same subcritical temperatures and the thermodynamics of this alloy determined. Also, a specimen of high purity electrolytic iron was to be run to determine the specific heat for comparison with the alloy steels. The enthalpy of transformation of iron was to be determined to provide a check for the self consistency of the data for the steels and to compare with the values for the specific heat

and enthalpy of transformation reported in the literature since a fairly wide scatter exists in the reported values.

From the above specimens it would be possible also, by knowing the interlamellar spacing of the pearlite for each specimen, to determine the interfacial energy of the interface between ferrite and cementite and the effect of the alloying element on the interfacial energy.

By running hyper- and hypo- eutectoid steels in the calorimeter, and comparing to the eutectoid alloys, the heat of solution of ferrite and cementite in austenite could be determined.

CHAPTER VI

RESULTS AND DISCUSSION

The apparent mean specific heats and enthalpies of transformation of high purity electrolytic iron, a 0.87% C high purity Fe-C binary alloy, and a series of specimens of 0.75% C - 1% Mn high purity eutectoid steel were determined in the adiabatic dynamic calorimeter. The 0.75% C-1% Mn steel specimens were isothermally transformed from austenite to pearlite at 620, 640, 660, and 680°C. The 0.87% C binary alloy was furnace cooled. The data are compared to determine the effect of manganese content and heat treatment on the specific heats and enthalpies of transformation.

The apparent mean specific heat as used in this dissertation is defined by the equation

$$C_p^a = \frac{EItk}{\Delta T w_a}$$

where

C_p^a = apparent mean specific heat at constant pressure
E^p = volts across the specimen heater
I = amperage in the specimen heater circuit
t = seconds required to traverse the temperature interval
ΔT = temperature interval in °C
k = conversion factor of watt-seconds to calories
w_a = total weight of the specimen, heater, and plugs

Time, power, and temperature were read at every 20°C interval from 80 to 800 or 950°C.

The reproducibility of the apparent mean specific heat, as affected by rerunning an undisturbed specimen, heating rate, installation of the specimen, dissassembly of the calorimeter, and specimen weight was determined by repeated measurements on copper specimens. Only the specimen

weight was found to affect the apparent specific heat. The scatter of individual points of any one determination from its smooth curve was not more than ± 0.25%. The reproducibility of the smooth curve for different runs for the same specimen and under the same conditions or for different conditions was about ± 0.3%.

A calibration of the calorimeter to yield true specific heats was attempted but was not successful. As no metallic specific heats have been determined with sufficient accuracy to permit direct calibration of the calorimeter, the following method of differences of weights of specimens for the same metal was used. The apparent specific heat curve for a copper specimen weighing 41.5408 grams was determined and compared to the curve for the same specimen machined to a weight of 26.1160 grams, using the same heater and plugs in both runs. The equations used for the calculation of the true mean specific heat of copper and of the heater and plugs are given in Chapter IV. The data are given in Figure 7. The true mean specific heat of copper as determined is considerably less than the values reported in the literature. The true specific heat curve for the specimen heater is considerably higher than that calculated from the materials of construction(Appendix B). The discrepancy between these two corrected specific heat curves and previously reported data is not evident, making further work necessary before reliable true specific heats may be reported. However, if the specific heat curve calculated from the materials of construction is accepted, the true specific heat as calculated from the data is in reasonable agreement with literature values.

For the major purpose of the investigation reported in this dissertation, knowledge of the true specific heats is not necessary as the

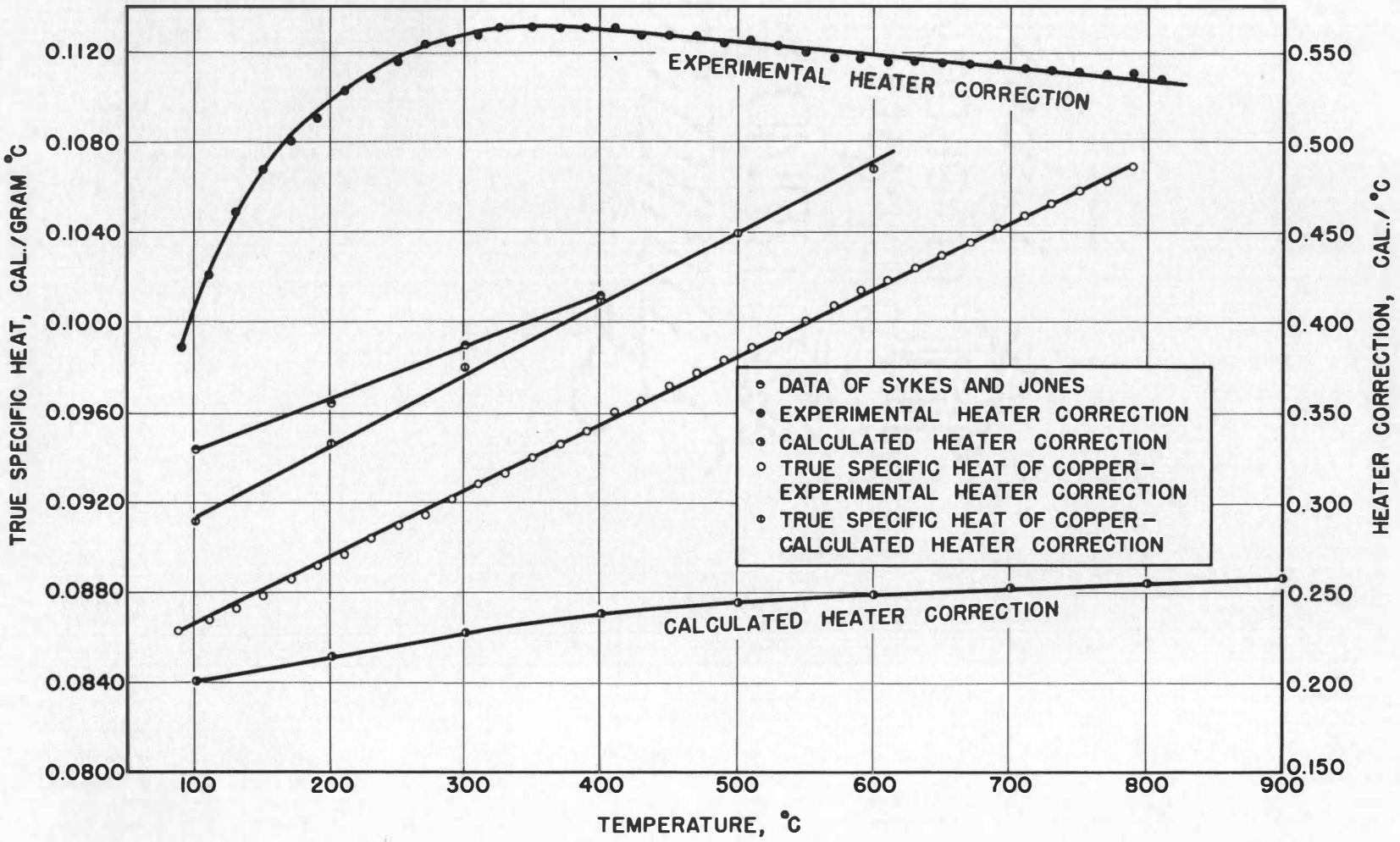

Figure 7. Heater Corrections and True Specific Heat of Copper

apparent mean specific heats may be compared to determine the information desired.

The enthalpies of transformation of the steels and the iron were determined by calculating the total heat input over a temperature range including the temperature of transformation, subtracting the energy required for the apparent mean specific heat over that range of temperature, and converting to calories per mol. The accuracies of determination were at least ± 1% for the steels and ± 0.5% for the iron.

The accuracy of control of the temperature difference between the specimen and the adiabatic shield was determined by cutting off the power to the specimen heater and permitting the calorimeter to stabilize at temperature. Any drift of the specimen temperature was corrected by offsetting the differential temperature control. The offset required was determined every 100°C above 400°C and the runs made accordingly. The offset was checked wherever possible on each run. For specimens in an equilibrium state, the check was made every 200°C and the data redetermined if an error had occurred. For specimens in a non-equilibrium state the offset could not be checked until the austenitic region was reached. The data were weighed accordingly.

Incorrect readings by the thermocouples may be primarily attributed to two sources. First, small differential thermocouple errors are almost inherent in the calorimeter design, since the techniques of manufacture and annealing of thermocouple wire are not sufficiently perfect to insure perfect thermocouples. There will always be slight composition and/or cold work gradients along the wire. These, when placed in several thermal gradients, will generate spurious parasitic emfs that will affect the

reading of the thermocouple. Obviously, such temperature gradients cannot be eliminated from the calorimeter. Second, a source of error arises from the changing electrical conductivity of the electrical insulation in the specimen heater. Since the specimen is unavoidably grounded through the differential thermocouple, any leakage from the specimen heater circuit will produce an emf across the differential thermocouple wire. While the electrical resistivity of most insulators is very high at room temperature, the resistivity drops very rapidly with increasing temperature, especially so above 700°C. This effect could not be eliminated in the calorimeter used but may be by an improved design.

Another source of error, giving inexplicible jumps in the apparent specific heat of copper near 500°C, was found to be in the temperature-emf tables used (Bulletin No. 508, Bureau of Standards) in the early determinations. A check of the tables showed that the accuracies demanded for use in the specific heat calculations were greater than the table permitted. The use of the smoothed tables, explained in Chapter IV and tabulated in Appendix A, resulted in smooth curves with no inexplicible effects. The curves given in Figure 6 are calculated from the data for the same calorimetric determination, using both tables to calculate the temperature intervals. The jumps evident in the curve for the specific heat using Bulletin No. 508 are smoothed out when the temperature intervals are calculated using the smoothed tables of temperature-emf values. All specific heat data reported were determined using the smoothed emf-temperature tables.

While it was impossible to calibrate the thermocouples in place in the calorimeter, the use of a standardized procedure of annealing the

thermocouple wire and using only one batch of wire throughout the experiment insured comparable results. This was checked by replacing one section of the thermocouple wire and redetermining the apparent specific heat of a specimen. Two points in the specific heat determination served to grossly check the thermocouples. These points were the Curie temperature of iron and the ferrite to austenite transformation temperature of pure iron. The values found were 768°C and 912°C on heating and 909°C on cooling respectively as compared to 768°C and 910°C respectively, the accepted literature values. Thus the maximum temperature error was not more than 2°C. This was sufficiently accurate for use, since the accuracy of measurement of the temperature interval is the important requirement.

In order to determine the effect of Mn on the thermodynamic properties of steel, specimens of high purity electrolytic iron, a 0.87% C high purity Fe-C binary alloy, and a series of isothermally transformed specimens of a 0.75% C - 1% Mn high purity eutectoid steel were run in the dynamic adiabatic calorimeter to determine the specific heats and enthalpies of transformation.

While the true specific heat of the specimens could not be determined, the apparent specific heats could be compared to permit the determination of the information desired.

The apparent specific heat of pure iron was determined from 80 to 950°C on one specimen. The curve, Figure 8, was smooth and continuous over the entire range of temperature except for the peaking at the Curie temperature and at the ferrite-austenite transformation temperature. The estimated true specific heat calculated from the apparent specific heats

using a correction for the specimen heater based on the materials of construction, are in reasonable agreement with the prior determinations of Awberry and Griffiths (25) and of Pallister (23) but are somewhat lower than the values used in the collation of Darken and Smith (17) who believed the data of Awberry and Griffiths and of Pallister to be too low above 500°C. The Curie temperature was determined to be 768°C by extrapolation of the apparent mean specific heats of the specimen above and below this temperature. The value is in excellent agreement with the reported literature value of 768 to 770°C (16,17,18,19,20,21,23,25,29).

Portions of the time-temperature curves, recorded during the transformations, are given in Figure 9 for the ferrite to austenite transformations occurring on heating. On the first determination, the specimen superheated to 913°C, cooled to 912°C, and transformed at 912°C. On the second heating, the specimen started transforming at 912°C and did not superheat as on the first determination. Two transformations on cooling were recorded and the time-temperature curves are given in Figure 10. No attempt was made to determine the enthalpy change of the first cooling transformation. The rate of cooling was the maximum for the calorimeter. The specimen temperature dropped to 905°C before the transformation started, rose to 906.5°C, and the specimen very quickly reached the normal cooling rate for ferrite. The second cooling transformation was made at a cooling rate of 3/4°C per minute for austenite. The specimen undercooled to 907.3 °C, rose to 909.0°C, transformed at 909.0°C for 28 minutes, and then abruptly reached the normal cooling curve for ferrite.

The enthalpy of transformation on the pure iron was determined twice on heating and once on cooling. The three determinations were made on one

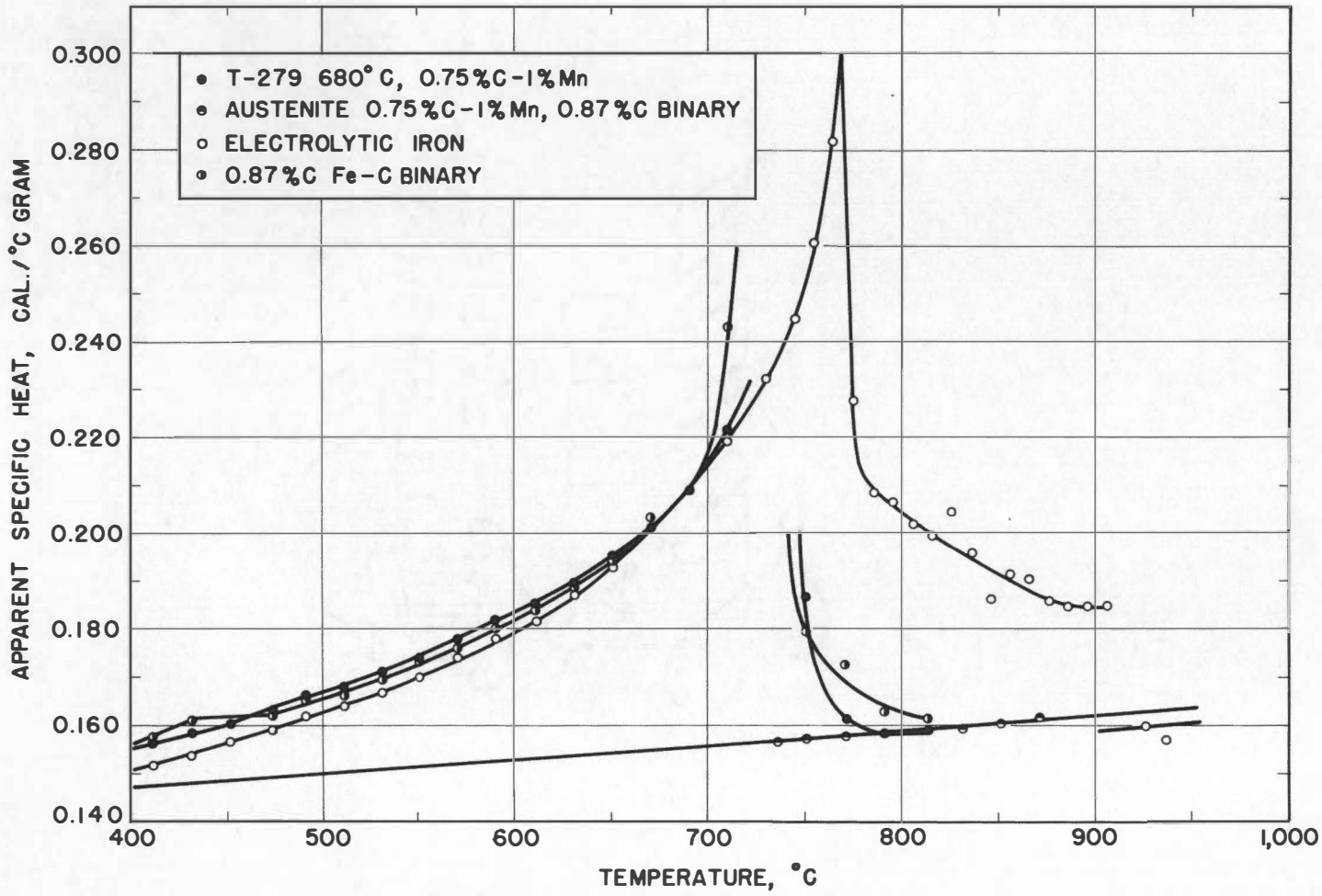

Figure 8. Apparent Specific Heats of Several Specimens

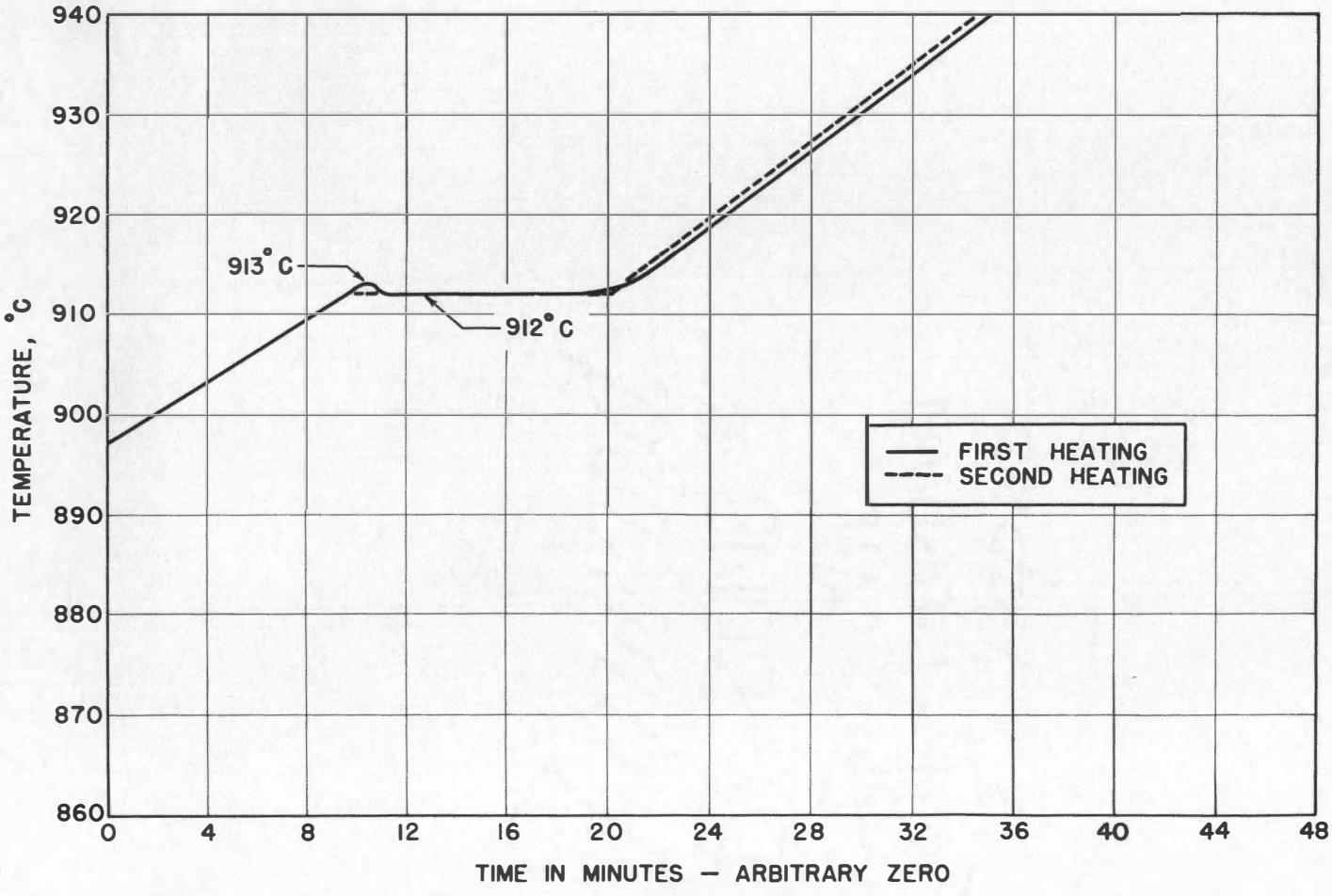

Figure 9. **Time - Temperature Heating Curves for the Ferrite to Austenite Transformation in High Purity Iron**

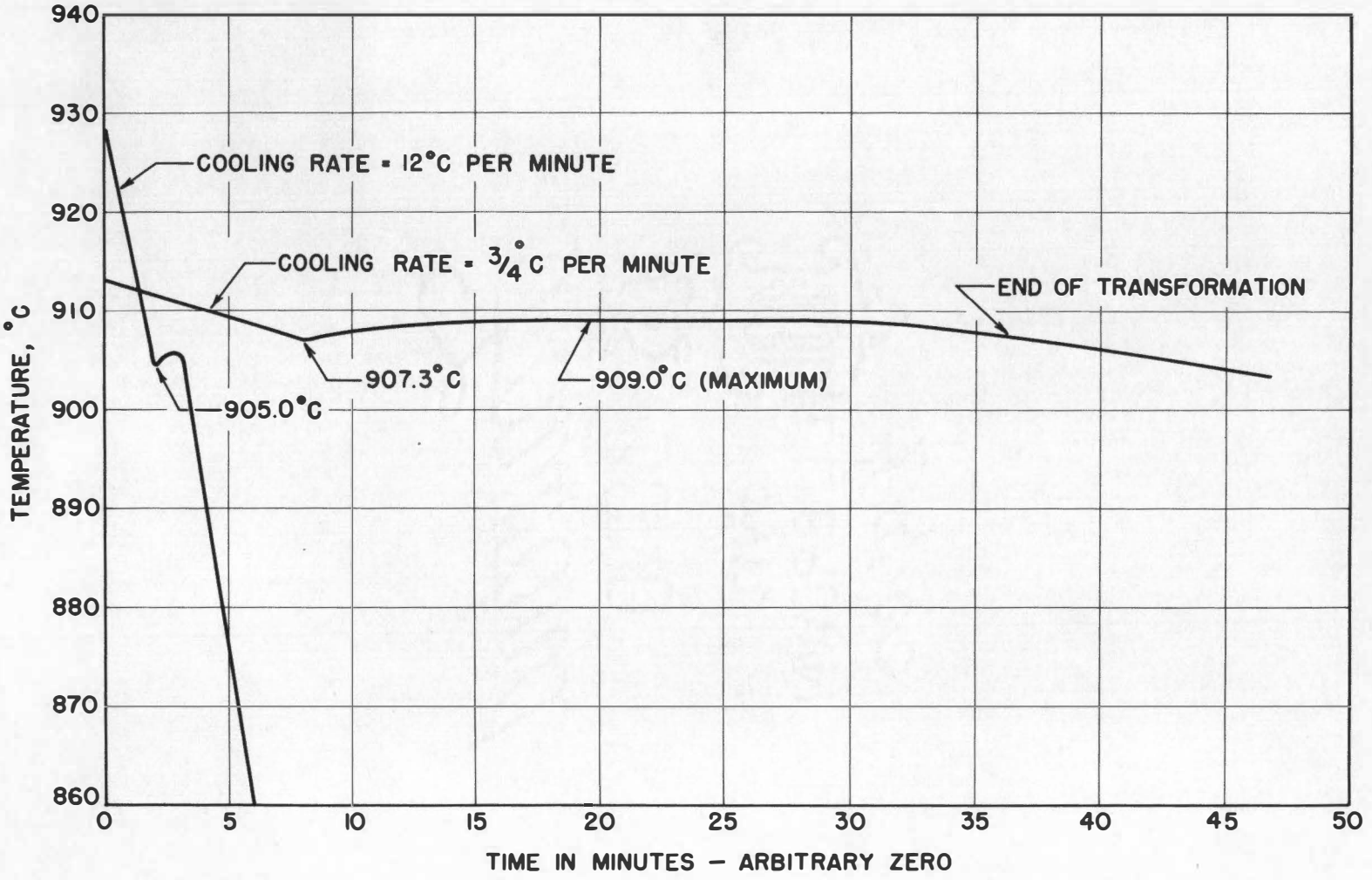

Figure 10. Time - Temperature Cooling Curves for the Austenite to Ferrite Transformation in High Purity Iron

specimen during one calorimeter run. The values determined are: first heating - 209.6 cal/mol; second heating - 211.1 cal/mol; and second cooling - 211.9 cal/mol. All values were corrected to 910°C. The average value of 211 cal/mol agrees surprisingly well with the reported value of 215 cal/mol. The reported value for the temperature of transformation is 910°C.

The apparent specific heat and enthalpy of transformation of the 0.87% C high purity Fe-C binary alloy, furnace cooled, were determined to provide a basis for the determination of the effect of the addition of Mn to an eutectoid steel. The apparent specific heat curve, Figure 8, was smooth from room temperature to the transformation temperature except for the peaking occurring above 200°C at the Curie temperature for cementite. The apparent specific heat curve for the specimen in the austenitic condition was smooth and increased linearly with increasing temperature. The rather abrupt increase in the apparent specific heat of pearlite starting at about 715°C and continuing into the transformation is believed to be due to the rapidly increasing solubility of cementite in ferrite as the eutectoid temperature is approached. The enthalpy of transformation of pearlite to austentite corrected to 720°C was determined to be 875 ± 10 cal/mol of alloy.

The time-temperature curves for the transformations of the 0.87% C binary alloy on heating and cooling are given in Figure 11. The curve for the transformation on heating started deviating from the expected curve at approximately 718°C, with the deviation increasing as the transformation temperature was approached. No superheating was observed and the specimen temperature increased continuously throughout the transform-

ation. The transformation was not complete until the temperature reached 740°C, due primarily to the dissipation of carbon gradients. The time-temperature curve for the transformation on cooling is given in Figure 11. The first deviation from the normal cooling curve for austenite occurred at 724°C, the deviation increasing slowly untilthe transformation caused the temperature to start rising at 708.3°C. The specimen temperature rose to 709.4°C. The total time between 720 and 700°C was 70 minutes. As this alloy was slightly hyper-eutectoid, a deviation above 720°C would be expected as the proeutectoid cementite was precipitated.

A series of specimens of the 0.75% C - 1% Mn high purity eutectoid steel were isothermally transformed from austenite to pearlite at the subcritical temperatures 680,660,640, and 620°C for times just long enough to permit complete transformation, to give specimens of different interlamellar spacings and different amounts of partitioning of Mn. The specific heat and enthalpies of transformation for these specimens were determined and compared, both with each other and with the binary alloy, to determine the effect of the addition of Mn, to an eutectoid alloy, on the specific heats and enthalpies of transformation, and to attempt to determine the ferrite-cementite interfacial energy in pearlite from a comparison of the enthalpies of transformation. A comparison of the curves given in Figure 12 shows that the differences of interlamellar spacing does not effect the specific heat within the accuracy of determination of ± 0.5%. However, the partitioning of Mn occurring during the specific heat determination does affect the specific heat between 530 and 700°C. The magnitude of the effect is dependent on the amount of partitioning occurring, that for the 620°C specimen being the greatest and that for the 680°C specimen

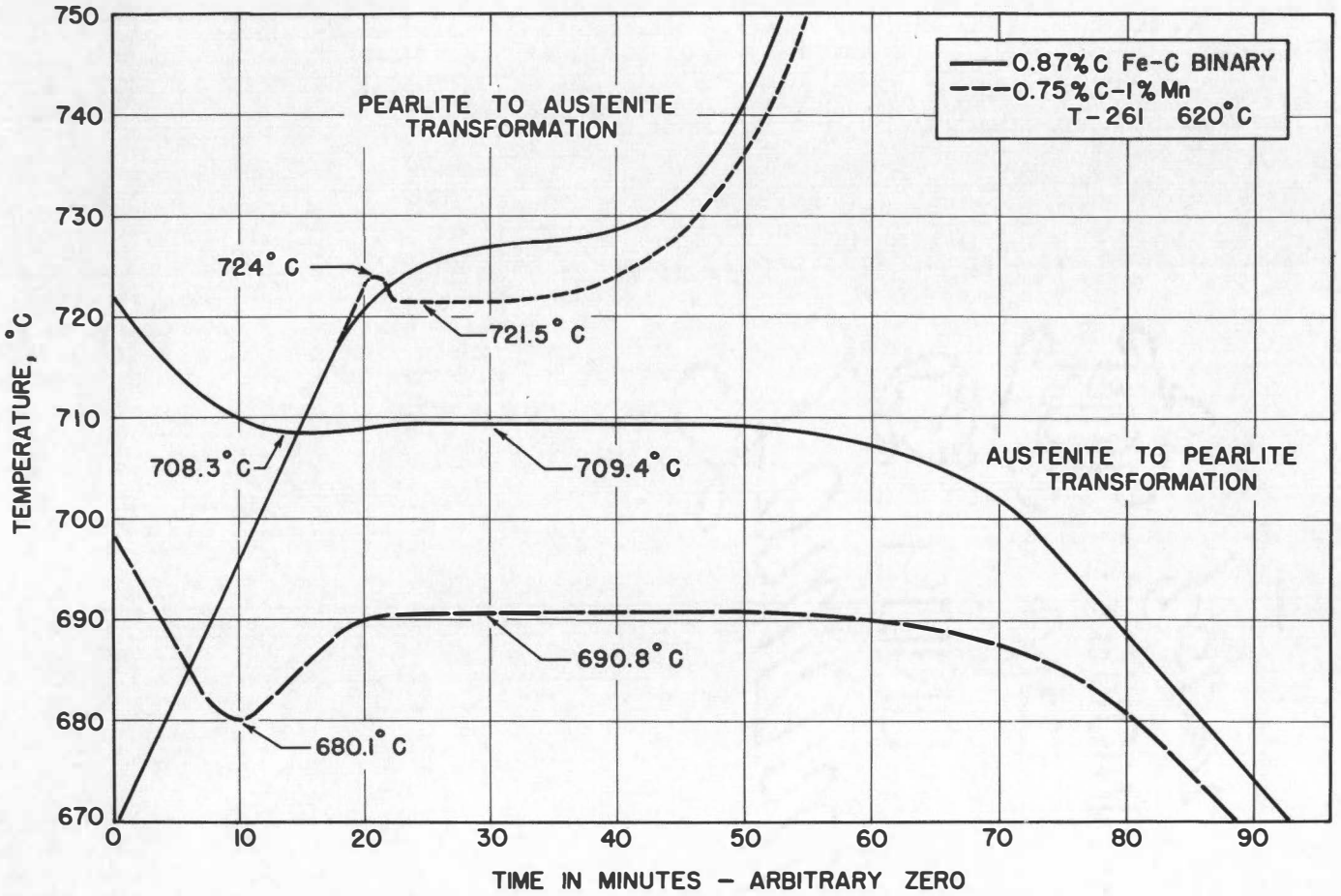

Figure 11. Time - Temperature Curves for Austenite and Pearlite Transformation in Two Steels

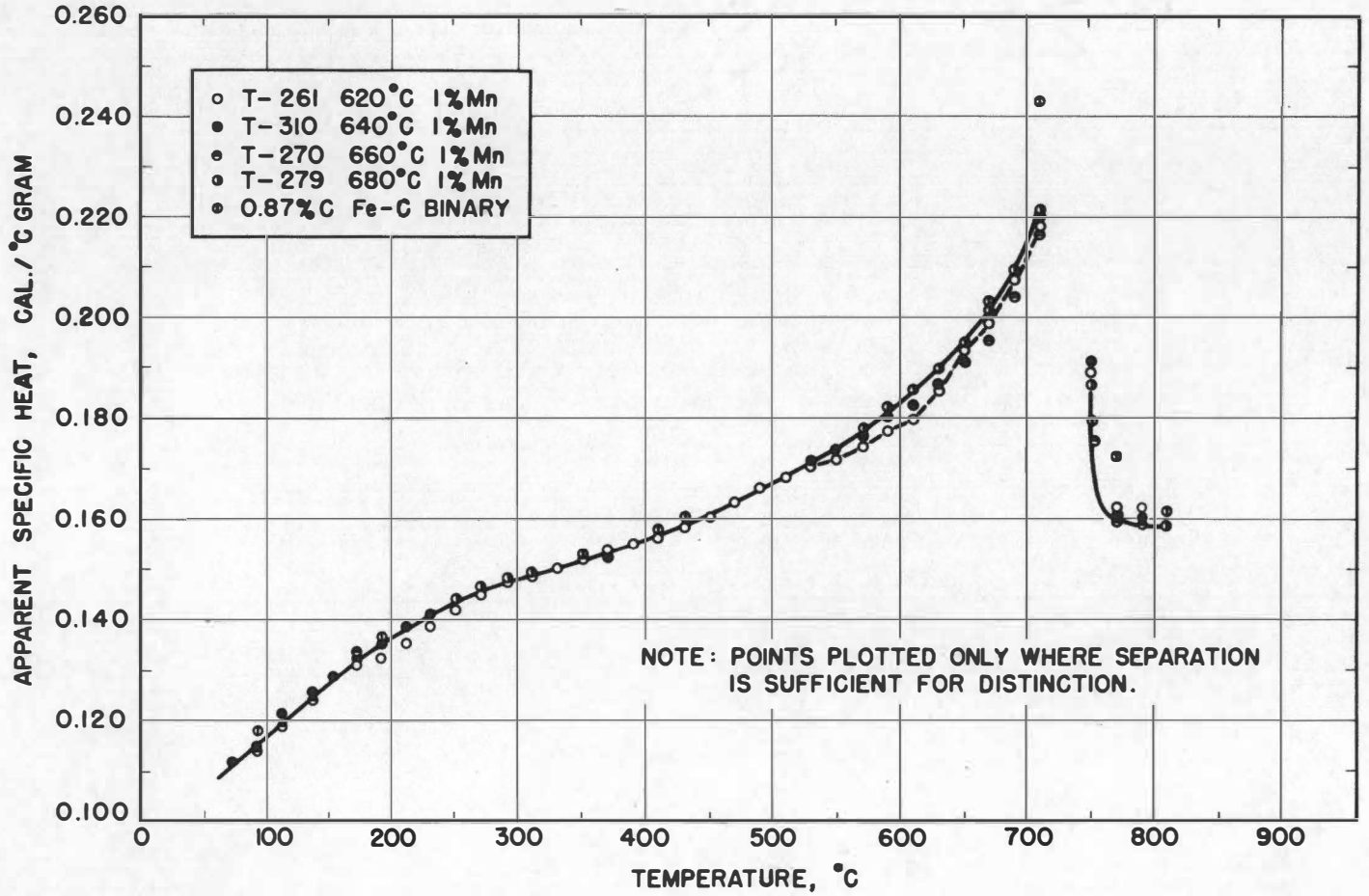

Figure 12. Apparent Specific Heats of a 0.75% C - 1% Mn Steel

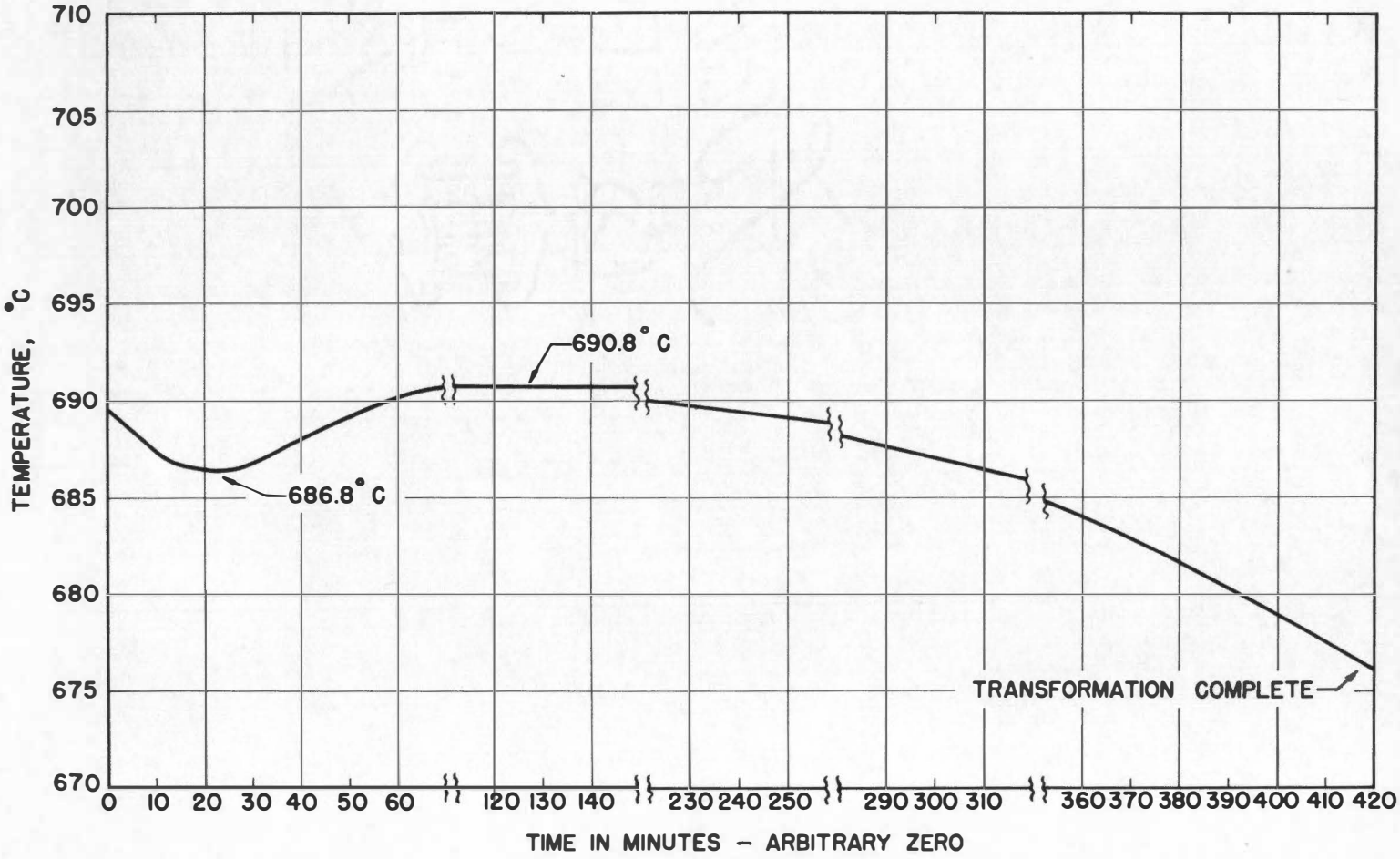

Figure 13. Time - Temperature Curve for the Transformation of Austenite to Pearlite in a 0.75% C - 1% Mn Steel Requiring Seven Hours for Completion

being zero. Other than this there are no differences between the apparent specific heat curves for the different isothermal treatments or for the two alloys except that the cementite Curie temperature peak is smoothed out or absent in the Mn alloy. A comparison of the apparent specific heat curves for the two alloys in the austenitic condition shows that the addition of Mn has no effect on the specific heat of austenite.

A portion of the time-temperature curve for specimen T-261, typical of all of the Mn steel specimens, during which the transformation of pearlite to austenite occurred, is given in Figure 11 where it is compared to the curve for the 0.87% C binary alloy. The specimen superheated to 724°C, cooled to 721.5°C, then the temperature gradually increased as the transformation progressed. The two curves were superimposed at 710°C. Above 740°C, the two curves, 1% Mn and 0.87% C binary, are parallel, indicating, as was found, that the apparent specific heat of austenite is not affected by the presence of the 1% Mn. Since the same heater and plugs were used, and the specimen weights were the same within 0.5%, the true specific heats of the two alloys in the austenite condition were the same.

The time-temperature curve for the transformation of austenite to pearlite in the 1% Mn steel on cooling at a rate of 1/5°C per minute is given in Figure 13. As the total time required for the transformation was seven hours, the curve as shown is broken at several points so that the interesting points may be shown on a reasonable scale. A time-temperature curve for the transformation on cooling requiring 3 1/2 hours for completion differed only in the minimum temperature reached before the transformation was well underway and the time required for the transformation to be completed. The critical and interesting points of both curves are compared,

TABLE II

ENTHALPY OF TRANSFORMATION

Specimen No.	Austenite to Pearlite Transformation °C	Enthalpy of Transformation Calculated Using Apparent C_p Cal/Mol			Temperatures During Transformation °C	
		Heating		Cooling		
		720-800°C	720-760°C		Max.	Min.
T-262	620	890.8	891.6		723.6	721.5[1]
T-261	620	891.7	880.1		723.3	721.2[1]
					690.8[2]	686.8[2]
T-311	640	893.1	890.6		723.7	721.7[1]
T-310	640	906.5	899.7		723.1	721.3[1]
T-270	660	835.5[3]	863.8[3]		724.0	721.9[3]
T-278	680	912.8[4]	889.9[4]		724.5	722.7[4]
T-279	680	897.1	891.5		724.0	722.0[1]
				995.8[5]	690.8	682.9[5]
0.87% C Steel		899.1	874.9		720 - 735[6]	
				900.6[7]	709.4	708.3[7]
Electrolytic Fe		209.6[8]			913.0	912.0[8]
		211.1[9]			912.0	912.0[9]
				211.9[10]	909.0	907.0[10]

All T- specimens are 0.75%C - 1% Mn steels and were isothermally transformed at the temperatures indicated.

(1) Transformation occurring on heating.
(2) Transformation occurring on cooling, time required 7 hours 40 minutes
(3) Transformation on heating, C_p at 730, 740°C, too low
(4) Transformation on heating, C_p above 740°C too high
(5) Transformation on Cooling, time required - 3 hours 20 minutes
(6) Transformation on heating, continuous rise in temperature, no superheat
(7) Transformation on cooling, time required - 55 minutes
(8) Transformation on first heating
(9) Transformation on second heating
(10) Transformation on second cooling

in Table II, with each other and with that for the transformation occurring for the maximum rate of cooling possible in the calorimeter.

The enthalpies of transformation of the Mn steels specimens were determined during the specific heat runs and are given in Table II. The values are in the approximate order that would be expected when the interlamellar spacings and associated interfacial energies are considered. This same order of values would be expected from the consideration of partitioning of Mn in the pearlite except that the heat evolution, amounting to approximately 30 calories per mol of steel for the 620°C specimen, due to the partitioning during the specific heat determination, is over at 700°C, i.e., the specific heats of the 620 and 680°C specimens are the same at 700°C, and therefore the partitioning of Mn did not affect the determination of the enthalpy of transformation. This was true for the transformation of pearlite to austenite but would not be true for the transformation of austenite to pearlite at subcritical temperatures where the transformation occurs so rapidly that the diffusion of Mn could not take place. Consideration of the errors of determination of the enthalpies of transformation of the non-equilibrium specimens, i.e., offset errors in the differential temperature control system, lead to an estimate of 890 $\pm$ 10 calories per mol of steel for the enthalpy of transformation of all of the Mn steel specimens tested. While there is a spread of 25 calories per mol in the enthalpies of transformation of the specimens, and the order is correct, no value for the interfacial energy may be calculated as the reproducibility of the enthalpy of transformation of the 680°C specimen was $\pm$ 10 calories per mol and that for the other specimens could not be determined due to control errors during the transformations.

However, the conclusion may be drawn that the interfacial energy is not as large as the value of 6.8×10^{-5} cal/cm^2 as deduced by Zener (10) and probably is not as large as the experimental value of 3.3×10^{-5} cal/cm^2 reported by Thompson (11). If the interlamellar spacings of the 620 and 680°C specimens are taken as 1000 and 5000 Å respectively (estimated from electron and optical micrographs), and the interfacial energy is 3.3×10^{-5} cal/cm^2, the total interfacial energies are 96 and 20 cal/mol respectively making a difference of 76 cal/mol in the enthalpies of transformation. The maximum difference that is possible to estimate from the data is approximately 40 cal/mol. This estimate does not consider the control errors known to be present during the determinations.

The apparent specific heat data for the steels, combined with the experimental enthalpies of transformation may be used to calculate the enthalpy of transformation as a function of subcritical temperature. The results of such calculations are given in Table III and Figure 14. In the case of pure iron, the assumption was made that within the accuracy of determination, the specific heat of austenite was not affected by the presence of the relatively small amounts of alloying elements present. The apparent specific heat of austenite in the steels was then used, with proper corrections for the differences in weights of the specimens, to calculate the apparent specific heat of austenite in pure iron at subcritical temperatures. The assumption of linearity between the austenitic specific heat and temperature was used to extrapolate the curve for the steels to 500°C. The derivation of the equations used and the calculations are given in Appendix C.

The self-consistency and accuracy of the data may be checked by

TABLE III

FREE ENERGY AND ENTHALPY OF TRANSFORMATION AT SUBCRITICAL TEMPERATURES

Temperature °C	Free energy and Enthalpy of Transformation Cal/Mol						
	0.75%C-1%Mn Steel		0.87%C Fe-C Binary		0.75%C Binary(Calculated)		Pure Iron
	ΔH	ΔF	ΔH	ΔF	ΔH	ΔF	ΔH
910							211
900							221
880							241
860							264
840							293
820							327
800							370
780							421
760							516
740							620
720	890		875	0	859	0	700
710	935	0					
700			984	18.7	968	18.4	767
690	1011	19.8	1020	28.8	1004	28.3	
680							823
670	1075	41.1	1084	50.1	1068	49.4	
660							870
650	1133	63.6	1139	72.6	1123	71.5	
640							909
630	1188	87.3	1187	96.2	1171	94.9	
620							942
610	1233	112.1	1230	120.9	1214	119.3	
600							
590	1274	137.8	1269	146.4	1253	144.4	
580							
570	1312	164.5	1304	172.9	1288	170.7	
560							
550	1345	192.0	1335	200.0	1319	197.3	
540							
530	1375	220.2	1363	228.0	1347	225.0	

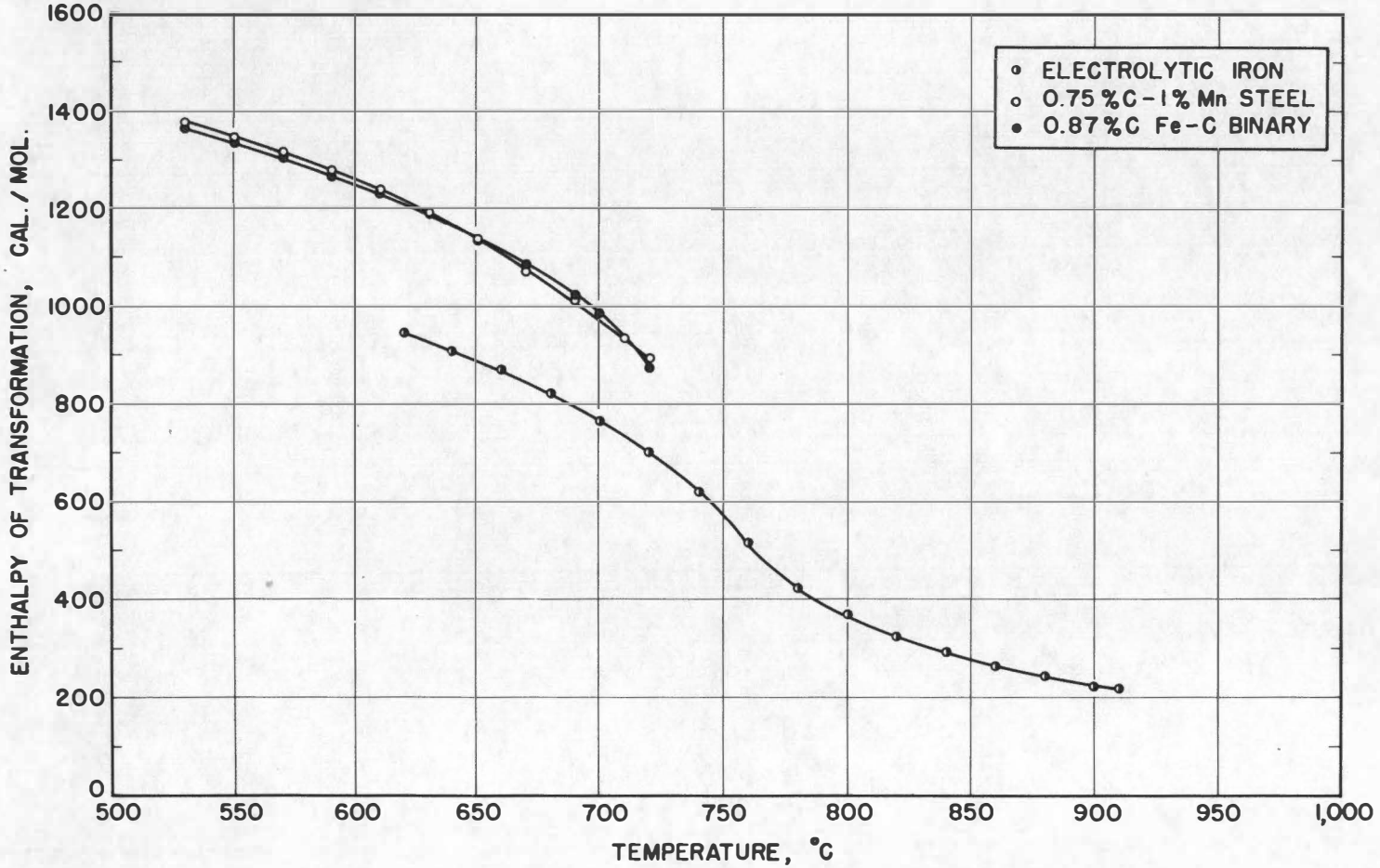

Figure 14. Enthalpy of Transformation of Austenite

calculating the enthalpy of transformation of the 0.87% C binary alloy at 720°C. The enthalpy of transformation of austenite to ferrite in pure iron is given in Table III to be 700 cal/mol at 720°C. Darken and Gurry (16) have reported a value of 7500 cal/mol for the enthalpy of formation of cementite from austenite at 723°C. For one mol of the 0.87% C binary alloy, there are 0.03926 mols C and 0.96074 mols Fe present. There are 0.03926 mols Fe_3C and 0.84296 mols ferrite formed when one mol of austenite transforms to pearlite. The enthalpy of transformation then is, neglecting the interfacial energy of the pearlite and the solution of the small amount of C in ferrite,

0.84296 mols ferrite transforming at 700 cal/mol	= 590 cal
0.03926 mols Fe_3C formed at 7500 cal/mol	= 294 cal
enthalpy of formation of one mol of pearlite	= 884 cal

This calculated value of 884 cal/mol agrees surprisingly well with the experimental value of 875 cal/mol. The calculated value would be less if the interfacial energy in the pearlite were included in the calculation.

The same calculation may be made for the 0.75% C - 1% Mn steel except that the heats of solution of Mn in austenite and ferrite are unknown. Using a value of - 3600 cal/mol for the enthalpy of formation of Mn_3C (33), assuming that there is no enthalpy of mixing of Fe_3C and Mn_3C, and ignoring the heat of solition of Mn in the two phases, the calculation yields a value of 842 cal/mol for the enthalpy of transformation of the 1% Mn steel as compared to the experimental value of 890 cal/mol. The value for the enthalpy of formation of Mn_3C, while the best available in the literature, is for the reaction of the elements and not for the formation from austenite containing dissolved Mn and C. Thus the disagreement of the

calculated and experimental values is not unexpected.

If the value of 950 cal/mol for the enthalpy of transformation of pure iron from austenite to ferrite at 720°C, as reported by Darken and Smith (17), is used to perform the above calculations, the values are 1067 cal/mol for the Mn steel and 1053 cal/mol for the binary alloy, much higher than the experimental values found.

For comparison to the 1% Mn alloy, the enthalpy of transformation of a 0.75% C Fe-C binary alloy may be calculated by the above means. For one mol of 0.75% C Fe-C alloy there are 0.03384 mols C, 0.96616 mols Fe, 0.03384 mols Fe_3C, and 0.86464 mols ferrite present. Therefore the enthalpy of transformation at 720°C is

0.03384 mols Fe_3C formed at 7500 cal/mol	=	254 cal
0.86464 mols ferrite formed at 700 cal/mol	=	605 cal
enthalpy of transformation to pearlite	=	859 cal

Since the specific heats of the 0.87% C and the 0.75% C Fe-C alloys should be the same, the enthalpies of transformation of the 0.75% C Fe-C binary alloy at subcritical temperatures may be calculated by subtracting the difference, 16 cal/mol, in the enthalpy of transformation at 720°C from the subcritical enthalpies of transformation of the 0.87% C binary alloy. The data are given in Table III.

The free energy of the reaction of austenite to pearlite at subcritical temperatures may be calculated from the enthalpy of transformation at subcritical temperatures and the specific heat of austenite and pearlite at these temperatures. The assumptions required are that the austenite specific heats may be safely extrapolated to 500°C as a straight line and in the case of the Mn steel, that the free energy of the reaction

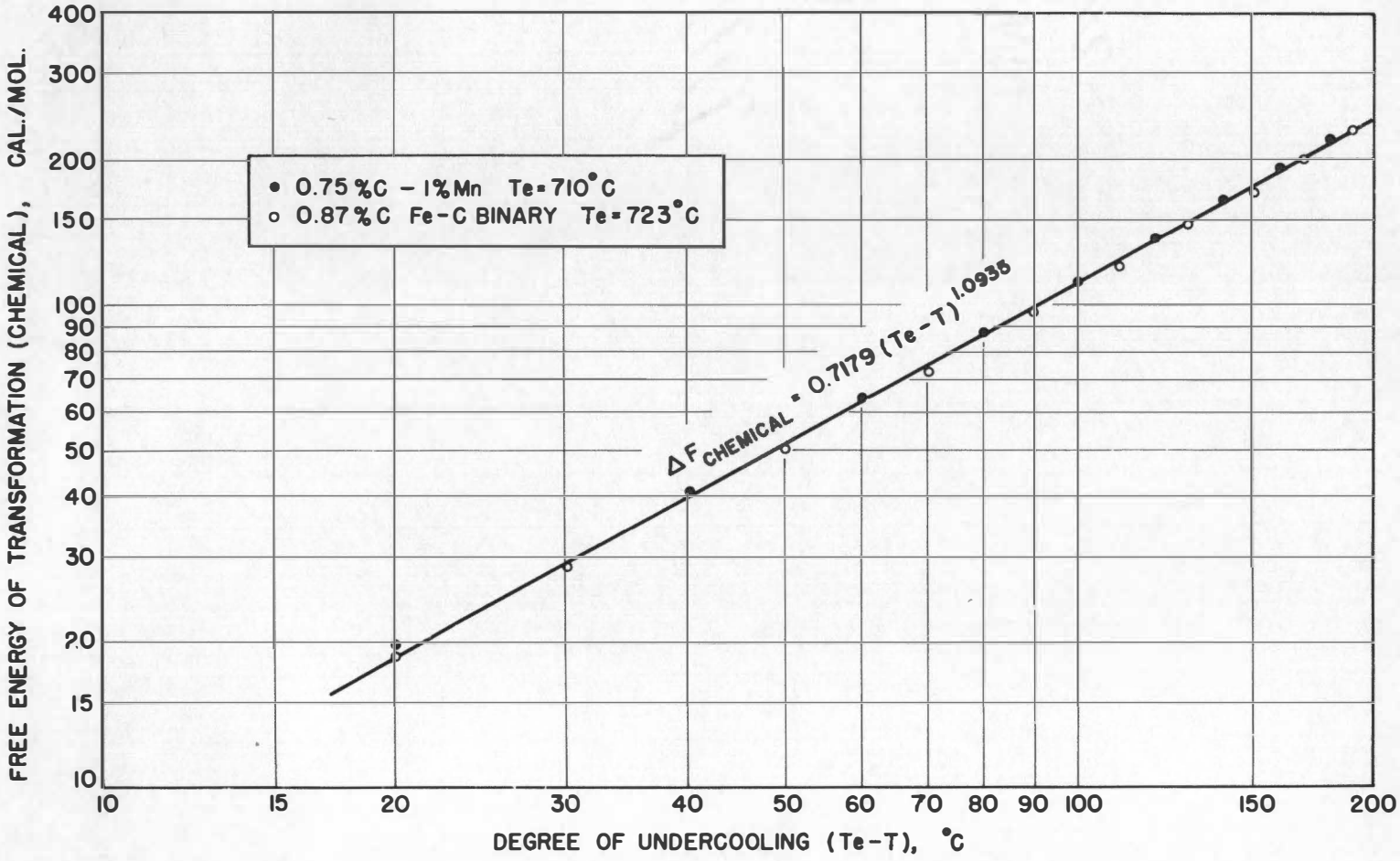

Figure 15. Free Energy of Transformation of Austenite to Massive Ferrite Plus Massive Cementite

of austenite to pearlite at the lowest temperature of the three phase region of the ternary phase diagram is zero. The thermodynamic equation used for the calculations is

$$\Delta F = \frac{\Delta H_o \, \Delta T}{T_o} + \int dT \int \frac{\Delta C_p \, dT}{T}$$

The calculations are given in Appendix B and the values are plotted in Figure 15. It seems remarkable that not only does a plot of log ΔF versus log $(T_e - T)$ yield a straight line but that the same line fits the data for both the 0.75% C - 1% Mn steel and the 0.87% C Fe-C binary alloy. The differences in the free energies of transformation of the 0.87% C and the 0.75% C binary alloys is more apparent than real. The calculations are hardly good to such accuracy. The equation of the line is

$$\Delta F_{chemical} = 0.7179 \, (\Delta T)^{1.0935}$$

This result leads to the conclusion that the chemical free energy, that is, the total amount of free energy liberated by the reaction of austenite to massive ferrite and massive cementite, cannot be the cause of the marked decrease in the rate of growth of pearlite shown when Mn is introduced into the alloy. The conclusion seems inescapable in the light of the self-consistency of the experimental data reported herein.

CHAPTER VII

CONCLUSIONS AND RECOMMENDATIONS

Although no true specific heats were determined in the work herein reported, those estimated from the apparent specific heats agree closely with the experimental values reported by Awberry and Griffiths (25) and by Pallister (23). This, with the self-consistency of the data reported, permit the conclusion that the table of enthalpies of pure iron as reported by Darken and Smith (17) are incorrect (too high). Therefore, the specific heats of iron which they used to determine the enthalpy of iron as a function of temperature are incorrect. Their conclusion that the reported values of Awberry and Griffiths (25) and Pallister (23) are too low above 500°C is therefore also incorrect.

Several general conclusions may be reached from the data. These are:

1. The addition of manganese to an eutectoid steel has little effect on the specific heats of austenite and pearlite.

2. Manganese will partition in pearlite with a pronounced heat effect. An unpartitioned pearlite will partition during a specific heat determination above 500°C, causing a decrease in the apparent specific heat. The deviation from the specific heat curve for a partitioned specimen represents a release of energy amounting to approximately 30 cal/mol of steel for a steel containing 0.75% C and 1% Mn.

3. The interfacial energy between ferrite and cementite in pearlite cannot be as great as that of 6.8×10^{-5} cal/cm^2 as calculated by Zener (10) and probably is not as great as 3.3×10^{-5} cal/cm^2 as experimentally determined by Thompson (11).

4. The true specific heat of pearlite in the 0.75% C - 1% Mn high purity steel is unaffected, within the accuracy of determination of ±0.5%, by the interlamellar spacing, the partitioning or lack of partitioning of the alloying element except as the partitioning occurs during the specific heat determination, and is not detectably different from that of a 0.87% C binary Fe-C alloy from 100 to 710°C.

5. The specific heat of austenite in the 0.75% C - 1% Mn steel and the 0.87% C Fe-C binary alloy is a linear function of temperature, slowly increasing with increasing temperature and is not detectably different in the two alloys. The true specific heat of pure iron (austenite) lies, within the accuracy of determination, on the extrapolated austenitic specific heat curve of the steels, indicating that the presence of the relatively small amount of alloying element has little if any effect on the specific heat of austenite.

6. The peak in the specific heat curve occurring at the Curie temperature of cementite for the 0.87% C Fe-C binary alloy is smoothed out in the 1% Mn steel so that it cannot be definitely located.

7. The basic design of the dynamic adiabatic calorimeter is very satisfactory and with improvements should become a major laboratory tool. The best accuracy obtainable in the present calorimeter is ± 0.5% but with the improvements, it should become at least ± 0.1%, leading to a more critical evaluation of the specific heat data and permitting the determination of effects on the specific heat that are too small to be detected with the present design.

8. There is evidence, shown by the time-temperature curve for the 0.87% C Fe-C binary alloy, that the solubility of carbon in ferrite changes

very rapidly in the temperature range of 713 to 723°C. No valid estimates of the solubility change may be made from the present data.

The specific conclusions that may be reached are:

1. The enthalpy of transformation of high purity electrolytic iron is 211 ± 2 cal/mol. The iron used in this experiment transformed at 912°C on heating and 909°C on cooling. These values are in excellent agreement with accepted literature values of 215 cal/mol and 910°C repectively. This agreement lends considerable support to the correctness of the experimental calorimetric work herein reported.

2. The enthalpy of transformation of pearlite to austenite in a 0.75% C - 1% Mn high purity eutectoid steel is 890 ± 10 cal/mol at 720°C, and is 875 cal/mol for a high purity 0.87% C Fe-C binary alloy at 720°C.

3. The maximum recalescence temperature reached during a very slow (seven hours) transformation from austenite to pearlite in a 0.75% C - 1% Mn steel was 690.8°C. That for a transformation requiring 3 1/2 hours for completion in the same steel was the same. The three phase field for this alloy has been established by prior work as from 709 to 714°C. The maximum recalescence temperature for the transformation in the 0.87% C binary alloy was 709.4°C.

4. The specific heat and enthalpy of transformation data herein reported may be used to calculate the enthalpy of transformation of the 0.87% C binary alloy at 720°C, utilizing the enthalpy of transformation of pure iron at 720°C as calculated from the specific heat data and the value at 910°C, and the enthalpy of formation of Fe_3C from austenite as reported by Darken and Gurry. The calculated value is 884 cal/mol and may

be compared with the experimental value of 875 ± 15 cal/mol.

5. The free energy as a function of the degree of supercooling for the reaction of austenite to pearlite in an eutectoid Fe-C binary alloy is the same as that for an eutectoid 0.75% C - 1% Mn steel. This does not say that the free energy of the reaction as a function of absolute temperature is unaffected. The free energy of the reaction versus the degree of undercooling may be plotted to yield a straight line on a log-log scale. The equation relating the chemical free energy to the degree of undercooling is

$$\Delta F = 0.7179\ (\Delta T)^{1.0935}$$

This leads to the conclusion that the change in chemical free energy with the addition of Mn cannot explain the large effect on the rate of growth of pearlite.

The experience obtained in the operation of the calorimeter in the determination of the data presented leads to the following recommendations on the detailed design of the calorimeter. The basic design is excellent and no recommendations need to be made.

1. Due to the changing resistivity of ceramics at temperatures near and above 700°C, with the consequent conductance of electrical current, it is recommended that the present calorimeter be inverted, so that the specimen is suspended and so that suspension may be electrically insulated from the rest of the calorimeter in the cold zone of the calorimeter. In this way, the electrical circuit from the specimen heater that impresses an emf on the differential thermocouple may be broken, and its effects on the differential thermocouple prevented. This would eliminate one of the major problems in control and in the evaluation of the data.

2. Other thermocouple materials, preferably pure metals, should be

investigated in an attempt to find a thermocouple that will give a higher emf per degree so that closer control and greater accuracies of measurement will be possible. If a thermocouple can be found that will give twice the emf per degree of Pt-Pt 13% Rh, the accuracy of the determination will be doubled. However, availability, ease of handling, weldability, and resistance to contamination, will still remain a problem.

3. The present lack of accuracy in the calorimeter will necessitate the redetermination of the data presented in this dissertation when a more accurate calorimeter is available. Several things of considerable interest are on the borderline of detection in the present calorimeter. Some of these are the interfacial energy between ferrite and cementite, a change in the specific heat of pearlite with interlamellar spacing, an accurate determination of the heat of partitioning of alloying elements in pearlite, the heat of solution of ferrite and cementite in austenite, the heat of solution of carbon in ferrite, the heat of solution of cementite in austenite, and the determination of the residual energy in a cold worked metal. However, most of the conclusions that may be reached concerning the present data will be essentially unchanged.

BIBLIOGRAPHY

BIBLIOGRAPHY

1. E.S. Davenport and E.C. Bain, "Transformation of Austenite at Constant Sub-Critical Temperatures" Trans. AIMME, 90, 117 (1930)

2. M.A. Grossman, AIMME Technical Paper 1437 (1942)

3. R.F. Mehl, "The Structure and Rate of Formation of Pearlite" Trans. A.S.M., 29, 813 (1941)

4. R.F. Mehl and F. C. Hull "The Structure of Pearlite" Trans. A.S.M., 30, 381 (1942)

5. Pellisier, Hawkes, Johnson, and Mehl "The Interlamellar Spacing of Pearlite" Trans. A.S.M., 30, 1049 (1942)

6. Hull, Colton, and Mehl "Rate of Nucleation and Rate of Growth of Pearlite" Trans. AIMME, 150, 185 (1942)

7. R.F. Mehl and G.A. Roberts "Effect of Inhomogeneity in Austenite on the Rate of the Austenite-Pearlite Reaction in Plain Carbon Steels" Trans. AIMME, 154, 318 (1943)

8. W.A. Johnson and R.F. Mehl "Reaction Kinetics in Processes of Nucleation and Growth" Trans. AIMME, 135, 416 (1939)

9. Smith and Mehl "Lattice Relationships in Decomposition of Austenite to Pearlite" Trans. AIMME, 150, 211 (1942)

10. C. Zener "Kinetics of the Decomposition of Austenite" Trans. AIMME, 167, 550 (1946)

11. F.C. Thompson."The Interfacial Tension Between Carbide of Iron and Iron" Trans. Faraday Society, 17, 391 (1922)

12. J. H. Frye, Jr. Unpublished Report to the Bethlehem Steel Co.

13. J. H. Frye, Jr., E.E. Stansbury, and D.L. McElroy, "Absolute Rate Theory Applied to Rate of Growth of Pearlite" Jnl. Metals, Feb., 1953, 219

14. D.L. McElroy "Isothermal Transformation Studies on the Austenite-Sorbite Reaction in Three High Purity Eutectoid Steels" Master's Thesis, University of Alabama, 1953

15. M.L. Picklesimer "The Austenite-Pearlite Reaction in a 1% Mn High Purity Eutectoid Steel" Master's Thesis, University of Tenn., 1951

16. Darken and Gurry The Physical Chemistry of Metals, New York: McGraw-Hill Book Company, Inc. (1953)

17. Darken and Smith "The Thermodynamics Functions of Iron" Ind. and Eng. Chem., 43, No. 8, 1815, (1951)

18. The Iron and Steel Institute Special Report No. 24, 1939

19. "The Physical Properties of a Series of Steels" Part II of above Report, Jnl Iron and Steel Institute (London), 83, (1946)

20. H. Esser and E. Baerlecken "Die wahre Spezifische Wärme von reinem Eisen und Eisen-Kohlenstoff-Leigierungen von 20° bis 1100°" Archiv für das Eisenhüttenwesen 14 Jahrgang Heft 12 June 1941

21. C. Sykes and H. Evans "Specific Heat/Temperature Curves of Commercially Pure Iron and Certain Plain Carbon Steels" Jnl Iron and Steel Inst. 138, 125 (1938)

22. W. Jellinghaus "An Automatic Arrangement for Drawing the Heat Content Curve and for Thermal Analysis with Small Heating Velocity" Archiv für das Eisenhüttenwesen, 22, 65 (1951)

23. P. R. Pallister "The Specific Heat and Resistivity of High Purity Iron up to 1250°C". Jnl Iron and Steel Institute 87, Feb, 1949

24. P. R. Pallister Section I_B of reference 19

25. J. H. Awberry and E. Griffiths Proceedings of the Royal Society, 174, Series A, page 1 (1940)

26. H. Moser Physikalische Zeitschrift, 37, 529 (1936)

27. H. Quinney and G. I. Taylor "The Emission of Latent Energy due to Previous Cold Working When a Metal is Heated" Proc. Roy. Soc. (London) A163, 157 (1937)

28. G. I. Taylor and H. Quinney Proc. Roy. Soc. A143, 307 (1934)

29. J. H. Awberry and A. Snow "Total Heat at Various Temperatures up to 950°C" Second Alloy Steels Research Committee Report Section IX (3), 216

30. H. E. Cleaves and J. G. Thompson The Metal Iron New York: McGraw Hill Book Co. (1935)

31. E. E. Stansbury, G.E. Elder, and M. L. Picklesimer "A High Temperature Calorimeter for Solid State Measurements" Progress Report Sept. 1951-Sept. 1952 on activities under A.E.C. Research Grant No. AT-(40-1)-1068 from the Metallurgy Division, Dept. of Chem. Eng. University of Tennessee

32. G. E. Elder "The Design and Development of a High Temperature Calorimeter" University of Tennessee, June, 1952

33. H. Ulich and H. Siemonsen Archiv für Eisenhüttwesen 14 27-34 (1940)

APPENDIX A

CALCULATION OF SMOOTHED EMF-TEMPERATURE TABLES FOR Pt-Pt 13%Rh THERMOCOUPLES

The accuracy desired in the operation of the adiabatic calorimeter to obtain the data required, necessitated measurement of the emf of the Pt-Pt 13% Rh thermocouple in tenths of a microvolt. The tables given in Bulletin No. 508, Bureau of Standards were in microvolts and were rounded off to the nearest microvolt.. Preliminary tests of the calorimeter using copper as the test material showed that inexplicible jumps in the specific heat of copper occurred in the neighborhood of 500°C. The tables given in Bulletin No. 508, Bureau of Standards, were plotted on a very large scale and the resulting curve interpolated in tenths of a microvolt. The jumps in the specific heat were still present. A check of the microvolts per 20°C interval in the neighborhood of 500°C showed several discrepancies. Several attempts were made to fit the emf tables with second, third, and fourth degree polynomials. No equations could be found above 300°C that were satisfactory for more than 50°C per equation. It was then decided to attempt to smooth the emf-temperature tables by the process of successive differences. The attempt was successful. Recalculating the temperature interval for the data having jumps in the specific heat by using the smooth tables, resulted in a smooth continuous curve from room temperature to 600° C.

The process of the calculation of the emf-temperature tables by the method of differences is discussed in Chapter IV and an example of the calculation is given. The complete tables are given in the following pages. Also included is a table of differences of emf values between Bulletin No. 508 and the smoothed tables.

TABLE IV

Revised Emf-Temperature Tables for Pt-13%Rh Pt Thermocouples.
Reference Junction - 0°C Temperature in °C Emf in Absolute Microvolts.
Small type gives microvolts per degree for each preceding interval.

°C	0	1	2	3	4	5	6	7	8	9
	5·428	5·422	5·444	5·466	5·488	5·510	5·532	5·554	5·576	5·598
0	0.000	5.422	10.866	16.332	21.820	27.330	32.862	38.416	43.992	49.590
	5·626	5·642	5·664	5·686	5·708	5·730	5·752	5·774	5·795	5·817
10	55.210	60.852	66.516	72.202	77.910	83.640	89.392	95.165	100.960	106.777
	5·838	5·859	5·880	5·901	5·921	5·942	5·963	5·984	6·005	6·026
20	112.615	118.474	124.354	130.255	136.176	142.118	148.081	154.065	160.070	166.096
	6·046	6·067	6·089	6·109	6·130	6·150	6·171	6·192	6·213	6·234
30	172.142	178.209	184.297	190.406	196.536	202.686	208.857	215.049	221.262	227.496
	6·254	6·275	6·295	6·315	6·336	6·356	6·376	6·396	6·416	6·436
40	233.750	240.025	246.320	252.635	258.971	265.327	271.703	278.099	284.515	290.951
	6·456	6·477	6·497	6·517	6·537	6·557	6·577	6·597	6·617	6·637
50	297.407	303.884	310.381	316.898	323.435	329.992	336.569	343.166	349.783	356.420
	6·657	6·677	6·697	6·717	6·736	6·756	6·776	6·796	6·816	6·836
60	363.077	369.754	376.451	383.168	389.904	396.660	403.436	410.232	417.048	423.884
	6·856	6·876	6·896	6·915	6·935	6·955	6·974	6·994	7·014	7·034
70	430.740	437.615	444.510	451.425	458.360	465.315	472.289	479.283	486.297	493.331
	7·053	7·073	7·093	7·113	7·132	7·152	7·172	7·191	7·211	7·230
80	500.384	507.457	514.550	521.663	528.795	535.947	543.119	550.310	557.521	564.751
	7·249	7·268	7·287	7·306	7·325	7·344	7·362	7·381	7·400	7·418
90	572.000	579.268	586.555	593.861	601.186	608.530	615.892	623.273	630.673	638.091
	7·437	7·456	7·474	7·493	7·512	7·530	7·549	7·566	7·584	7·602
100	645.528	652.984	660.458	667.951	675.463	682.993	690.541	698.107	705.691	713.293
	7·619	7·637	7·654	7·673	7·689	7·706	7·722	7·739	7·756	7·772
110	720.912	728.549	736.203	743.875	751.564	759.270	766.992	774.731	782.487	790.259
	7·789	7·805	7·821	7·837	7·852	7·868	7·884	7·899	7·914	7·929
120	798.048	805.853	813.674	821.511	829.363	837.231	845.115	853.014	860.928	868.857
	7·944	7·958	7·973	7·988	8·002	8·017	8·031	8·045	8·059	8·073
130	876.801	884.759	892.732	900.720	908.722	916.739	924.770	932.815	940.874	948.947
	8·087	8·100	8·114	8·128	8·141	8·156	8·166	8·181	8·194	8·208
140	957.034	965.134	973.248	981.376	989.517	997.672	1,005.839	1,014.020	1,022.214	1,030.420
	8·218	8·232	8·244	8·257	8·268	8·281	8·294	8·307	8·320	8·332
150	1,038.639	1,046.871	1,055.115	1,063.372	1,071.641	1,079.922	1,088.216	1,096.523	1,104.843	1,113.175
	8·345	8·358	8·371	8·383	8·396	8·408	8·421	8·434	8·446	8·459
160	1,121.520	1,129.879	1,138.250	1,146.633	1,155.029	1,163.437	1,171.858	1,180.292	1,188.738	1,197.197
	8·471	8·483	8·495	8·507	8·519	8·531	8·543	8·554	8·566	8·576
170	1,205.668	1,214.151	1,222.646	1,231.153	1,239.672	1,248.203	1,256.746	1,265.300	1,273.866	1,282.444
	8·596	8·607	8·619	8·625	8·637	8·648	8·660	8·672	8·684	8·696
180	1,291.034	1,299.636	1,308.249	1,316.874	1,325.511	1,334.160	1,342.820	1,351.492	1,360.179	1,368.874
	8·706	8·717	8·728	8·738	8·750	8·760	8·771	8·782	8·793	8·803
190	1,377.580	1,386.297	1,395.025	1,403.764	1,412.514	1,421.274	1,430.045	1,438.827	1,447.620	1,456.423

TABLE IV (Continued)

Revised Emf-Temperature Tables for Pt-13%RhPt Thermocouples.
Reference Junction - 0°C Temperature in °C Emf in Absolute Microvolts.
Small type gives microvolts per degree for each preceding interval.

°C	0	1	2	3	4	5	6	7	8	9
	9.814	9.823	9.836	9.847	9.857	9.868	9.878	9.888	9.898	9.910
200	1,465.237	1,474.062	1,482.898	1,491.745	1,500.602	1,509.470	1,518.349	1,527.238	1,536.138	1,545.048
	9.920	9.931	9.941	9.951	9.961	9.972	9.982	9.992	10.003	10.012
210	1,553.968	1,562.899	1,571.840	1,580.791	1,589.752	1,598.724	1,607.706	1,616.698	1,625.700	1,634.712
	10.022	10.033	10.043	10.053	10.063	10.073	10.083	10.093	10.103	10.106
220	1,643.734	1,652.767	1,661.810	1,670.863	1,679.926	1,688.999	1,698.082	1,707.175	1,716.278	1,725.391
	10.122	10.131	10.142	10.152	10.162	10.171	10.181	10.191	10.201	10.210
230	1,734.513	1,743.645	1,752.787	1,761.939	1,771.101	1,780.272	1,789.453	1,798.644	1,807.845	1,817.055
	10.220	10.230	10.239	10.249	10.258	10.267	10.276	10.286	10.295	10.304
240	1,826.275	1,835.505	1,844.744	1,853.993	1,863.251	1,872.518	1,881.794	1,891.080	1,900.375	1,909.679
	10.313	10.322	10.331	10.340	10.349	10.359	10.367	10.376	10.384	10.393
250	1,918.992	1,928.314	1,937.645	1,946.985	1,956.334	1,965.692	1,975.059	1,984.435	1,993.819	2,003.212
	10.402	10.411	10.420	10.429	10.437	10.446	10.454	10.463	10.472	10.480
260	2,012.614	2,022.025	2,031.445	2,040.873	2,050.310	2,059.756	2,069.210	2,078.673	2,088.145	2,097.625
	10.489	10.497	10.506	10.514	10.522	10.531	10.539	10.547	10.555	10.563
270	2,107.114	2,116.611	2,126.117	2,135.631	2,145.153	2,154.684	2,164.223	2,173.770	2,183.325	2,192.888
	10.573	10.580	10.588	10.596	10.604	10.612	10.620	10.628	10.636	10.643
280	2,202.460	2,212.040	2,221.628	2,231.224	2,240.828	2,250.440	2,260.060	2,269.688	2,279.324	2,288.967
	10.651	10.659	10.667	10.675	10.682	10.690	10.698	10.706	10.713	10.721
290	2,298.618	2,308.277	2,317.944	2,327.619	2,337.301	2,346.991	2,356.689	2,366.395	2,376.108	2,385.829
	10.729	10.736	10.743	10.751	10.758	10.765	10.773	10.780	10.787	10.794
300	2,395.558	2,405.294	2,415.037	2,424.788	2,434.546	2,444.311	2,454.084	2,463.864	2,473.651	2,483.445
	10.801	10.808	10.815	10.822	10.829	10.836	10.843	10.849	10.856	10.863
310	2,493.246	2,503.054	2,512.869	2,522.691	2,532.520	2,542.356	2,552.199	2,562.048	2,571.904	2,581.767
	10.870	10.876	10.883	10.890	10.897	10.903	10.910	10.917	10.923	10.930
320	2,591.637	2,601.513	2,611.396	2,621.286	2,631.183	2,641.086	2,650.996	2,660.913	2,670.836	2,680.766
	10.936	10.942	10.949	10.955	10.961	10.967	10.974	10.980	10.986	10.992
330	2,690.702	2,700.644	2,710.593	2,720.548	2,730.509	2,740.476	2,750.450	2,760.430	2,770.416	2,780.408
	10.998	11.004	11.010	11.016	11.022	11.028	11.034	11.040	11.046	11.052
340	2,790.406	2,800.410	2,810.416	2,820.428	2,830.450	2,840.478	2,850.512	2,860.552	2,870.598	2,880.650
	11.058	11.064	11.070	11.076	11.081	11.087	11.092	11.098	11.105	11.110
350	2,890.708	2,900.772	2,910.842	2,920.918	2,930.999	2,941.086	2,951.179	2,961.278	2,971.383	2,981.493
	11.116	11.122	11.128	11.133	11.139	11.145	11.151	11.156	11.162	11.168
360	2,991.609	3,001.731	3,011.859	3,021.992	3,032.131	3,042.276	3,052.427	3,062.583	3,072.745	3,082.913
	11.173	11.179	11.184	11.190	11.195	11.201	11.206	11.211	11.217	11.222
370	3,093.086	3,103.265	3,113.449	3,123.639	3,133.834	3,144.035	3,154.241	3,164.452	3,174.669	3,184.891
	11.227	11.233	11.238	11.243	11.248	11.253	11.259	11.264	11.269	11.274
380	3,195.118	3,205.351	3,215.589	3,225.832	3,236.080	3,246.333	3,256.592	3,266.856	3,277.125	3,287.399
	11.279	11.284	11.290	11.295	11.300	11.305	11.310	11.315	11.320	11.326
390	3,297.678	3,307.962	3,318.252	3,328.547	3,338.847	3,349.152	3,359.462	3,369.777	3,380.097	3,390.423

TABLE IV (Continued)

Revised Emf-Temperature Tables for Pt-13%RhPt Thermocouples.
Reference Junction - 0°C Temperature in °C Emf in Absolute Microvolts.
Small type gives microvolts per degree for each preceding interval.

°C	0	1	2	3	4	5	6	7	8	9
		10·331	10·336	10·341	10·346	10·351	10·356	10·361	10·367	10·372	10·377
400	3,400.754	3,411.090	3,421.431	3,431.777	3,442.128	3,452.484	3,462.845	3,473.212	3,483.584	3,493.961
		10·362	10·367	10·372	10·377	10·382	10·387	10·392	10·397	10·402	10·407
410	3,504.343	3,514.730	3,525.122	3,535.519	3,545.921	3,556.328	3,566.741	3,577.159	3,587.582	3,598.010
		10·433	10·438	10·443	10·448	10·453	10·458	10·464	10·469	10·474	10·479
420	3,608.443	3,618.881	3,629.324	3,639.772	3,650.225	3,660.684	3,671.148	3,691.617	3,692.091	3,702.570
		10·484	10·489	10·494	10·499	10·504	10·509	10·514	10·519	10·524	10·529
430	3,713.054	3,723.543	3,734.037	3,744.536	3,755.040	3,765.549	3,776.063	3,786.582	3,797.106	3,807.635
		10·535	10·540	10·545	10·550	10·555	10·560	10·565	10·570	10·575	10·580
440	3,818.170	3,828.710	3,839.255	3,849.805	3,860.360	3,870.920	3,881.485	3,892.055	3,902.630	3,913.210
		10·585	10·590	10·595	10·600	10·605	10·610	10·615	10·620	10·625	10·630
450	3,923.795	3,934.385	3,944.980	3,955.580	3,966.185	3,976.795	3,987.410	3,998.030	4,008.655	4,019.285
		10·635	10·640	10·645	10·650	10·655	10·660	10·665	10·670	10·675	10·680
460	4,029.920	4,040.560	4,051.205	4,061.855	4,072.510	4,083.170	4,093.835	4,104.505	4,115.180	4,125.860
		10·685	10·690	10·695	10·700	10·704	10·709	10·714	10·719	10·724	10·729
470	4,136.545	4,147.235	4,157.930	4,168.630	4,179.334	4,190.043	4,200.757	4,211.476	4,222.200	4,232.929
		10·734	10·739	10·744	10·748	10·753	10·758	10·763	10·768	10·773	10·778
480	4,243.663	4,254.402	4,265.146	4,275.894	4,286.647	4,297.405	4,308.168	4,318.936	4,329.709	4,340.487
		10·783	10·787	10·792	10·797	10·802	10·807	10·812	10·817	10·821	10·826
490	4,351.270	4,362.057	4,372.849	4,383.646	4,394.448	4,405.255	4,416.067	4,426.884	4,437.705	4,448.531
		10·831	10·836	10·841	10·846	10·850	10·855	10·860	10·865	10·870	10·875
500	4,459.362	4,470.198	4,481.039	4,491.885	4,502.735	4,513.590	4,524.450	4,535.315	4,546.185	4,557.060
		10·880	10·884	10·889	10·894	10·899	10·904	10·909	10·914	10·918	10·923
510	4,567.940	4,578.824	4,589.713	4,600.607	4,611.506	4,622.410	4,633.319	4,644.233	4,655.151	4,666.074
		10·928	10·933	10·938	10·943	10·947	10·952	10·957	10·962	10·967	10·972
520	4,677.002	4,687.935	4,698.873	4,709.816	4,720.763	4,731.715	4,742.672	4,753.634	4,764.601	4,775.573
		10·978	10·981	10·985	10·991	10·996	11·001	11·005	11·010	11·015	11·020
530	4,786. 549	4,797.530	4,808.516	4,819.507	4,830.503	4,841.504	4,852.509	4,863.519	4,874.534	4,885.554
		11·025	11·030	11·034	11·039	11·044	11·049	11·054	11·058	11·063	11·068
540	4,896.579	4,907.609	4,918.643	4,929.682	4,940.726	4,951.775	4,962.829	4,973.887	4,984.950	4,996.018
		11·073	11·078	11·082	11·087	11·092	11·097	11·101	11·106	11·111	11·116
550	5,007.091	5,018.169	5,029.251	5,040.338	5,051.430	5,062.527	5,073.628	5,084.734	5,095.845	5,106.961
		11·121	11·125	11·130	11·135	11·140	11·145	11·149	11·154	11·159	11·164
560	5,118.082	5,129.207	5,140.337	5,151.472	5,162.612	5,173.757	5,184.906	5,196.060	5,207.219	5,218.383
		11·169	11·173	11·178	11·183	11·188	11·193	11·197	11·202	11·207	11·212
570	5,229.552	5,240.725	5,251.903	5,263.086	5,274.274	5,285.467	5,296.664	5,307.866	5,319.073	5,330.285
		11·217	11·221	11·226	11·231	11·236	11·241	11·245	11·250	11·255	11·260
580	5,341.502	5,352.723	5,363.949	5,375.180	5,386.416	5,397.657	5,408.902	5,420.152	5,431.407	5,442.667
		11·265	11·269	11·274	11·279	11·284	11·289	11·293	11·298	11·303	11·308
590	5,453.932	5,465.201	5,476.475	5,487.754	5,499.038	5,510.327	5,521.620	5,532.918	5,544.221	5,555.529

TABLE IV (Continued)

Revised Emf-Temperature Tables for Pt-13%RhPt Thermocouples.
Reference Junction - 0°C Temperature in °C Emf in Absolute Microvolts.
Small type gives microvolts per degree for each preceding interval.

°C	0	1	2	3	4	5	6	7	8	9
	11·313	11·317	11·322	11·327	11·332	11·337	11·341	11·346	11·351	11·356
600	5,566.842	5,578.159	5,589.481	5,600.808	5,612.140	5,623.477	5,634.818	5,646.164	5,657.515	5,668.871
	11·361	11·365	11·370	11·375	11·380	11·385	11·389	11·394	11·399	11·404
610	5,680.232	5,691.597	5,702.967	5,714.342	5,725.722	5,737.107	5,748.496	5,759.890	5,771.289	5,782.693
	11·409	11·413	11·418	11·423	11·428	11·433	11·437	11·442	11·447	11·452
620	5,794.102	5,805.515	5,816.932	5,828.356	5,839.784	5,851.217	5,862.654	5,874.096	5,885.543	5,896.995
	11·457	11·461	11·466	11·471	11·476	11·481	11·485	11·490	11·495	11·500
630	5,908.452	5,919.913	5,931.379	5,942.850	5,954.326	5,965.807	5,977.292	5,988.782	6,000.277	6,011.777
	11·505	11·509	11·514	11·519	11·524	11·528	11·533	11·538	11·543	11·547
640	6,023.282	6,034.791	6,046.305	6,057.824	6,069.348	6,080.876	6,092.409	6,103.947	6,115.490	6,127.037
	11·552	11·557	11·562	11·567	11·571	11·576	11·581	11·586	11·590	11·595
650	6,138.589	6,150.146	6,161.708	6,173.275	6,184.846	6,196.422	6,208.003	6,219.589	6,231.179	6,242.774
	11·600	11·605	11·610	11·614	11·619	11·624	11·629	11·634	11·638	11·643
660	6,254.374	6,265.979	6,277.589	6,289.203	6,300.822	6,312.446	6,324.075	6,335.709	6,347.347	6,358.990
	11·648	11·653	11·658	11·662	11·667	11·672	11·677	11·682	11·686	11·691
670	6,370.638	6,382.291	6,393.949	6,405.611	6,417.278	6,428.950	6,440.627	6,452.309	6,463.995	6,475.686
	11·696	11·701	11·706	11·710	11·715	11·720	11·724	11·729	11·734	11·740
680	6,487.382	6,499.083	6,510.789	6,522.499	6,534.214	6,545.934	6,557.659	6,569.388	6,581.122	6,592.861
	11·744	11·748	11·753	11·758	11·762	11·766	11·772	11·777	11·782	11·787
690	6,604.605	6,616.353	6,628.106	6,639.864	6,651.627	6,663.395	6,675.167	6,686.944	6,698.726	6,710.513
	11·791	11·796	11·801	11·806	11·811	11·815	11·820	11·825	11·830	11·834
700	6,722.304	6,734.100	6,745.901	6,757.707	6,769.518	6,781.333	6,793.153	6,804.978	6,816.808	6,828.642
	11·839	11·844	11·849	11·853	11·858	11·863	11·868	11·873	11·877	11·882
710	6,840.481	6,852.325	6,864.174	6,876.027	6,887.885	6,899.748	6,911.616	6,923.488	6,935.365	6,947.247
	11·887	11·891	11·896	11·901	11·906	11·910	11·915	11·920	11·925	11·929
720	6,959.134	6,971.025	6,982.921	6,994.822	7,006.728	7,018.638	7,030.553	7,042.473	7,054.398	7,066.327
	11·934	11·939	11·944	11·948	11·953	11·958	11·963	11·967	11·972	11·977
730	7,078.261	7,090.200	7,102.144	7,114.092	7,126.045	7,138.003	7,149.966	7,161.933	7,173.905	7,185.882
	11·982	11·986	11·991	11·996	12·000	12·005	12·010	12·015	12·020	12·024
740	7,197.864	7,209.850	7,221.841	7,233.837	7,245.837	7,257.842	7,269.852	7,281.867	7,293.887	7,305.911
	12·029	12·034	12·039	12·043	12·048	12·053	12·058	12·062	12·067	12·072
750	7,317.940	7,329.974	7,342.013	7,354.056	7,366.104	7,378.157	7,390.215	7,402.277	7,414.344	7,426.416
	12·077	12·081	12·086	12·091	12·096	12·100	12·106	12·110	12·115	12·119
760	7,438.493	7,450.574	7,462.660	7,474.751	7,486.847	7,498.947	7,510.052	7,523.162	7,535.277	7,547.396
	12·124	12·129	12·134	12·138	12·143	12·148	12·153	12·157	12·162	12·167
770	7,559.520	7,571.649	7,583.783	7,595.921	7,608.064	7,620.212	7,632.365	7,644.522	7,656.684	7,668.851
	12·172	12·176	12·181	12·186	12·191	12·196	12·200	12·205	12·210	12·214
780	7,681.023	7,693.199	7,705.380	7,717.566	7,729.757	7,741.952	7,754.152	7,766.357	7,778.567	7,790.781
	12·219	12·224	12·229	12·233	12·238	12·243	12·248	12·252	12·257	12·262
790	7,803.000	7,815.224	7,827.453	7,839.686	7,851.924	7,864.167	7,876.415	7,888.667	7,900.924	7,913.186

TABLE IV (Continued)

Revised Emf-Temperature Tables for Pt-13%RhPt Thermocouples.
Reference Junction - 0°C Temperature in °C Emf in Absolute Microvolts.
Small type gives microvolts per degree for each preceding interval.

°C	0	1	2	3	4	5	6	7	8	9
800	12·267 7,925.453	12·271 7,937.724	12·276 7,950.000	12·281 7,962.281	12·286 7,974.567	12·290 7,986.857	12·295 7 999.152	12·300 8.011.452	12·305 8,023.757	12·309 8,036.066
810	12·314 8,048.380	12·319 8,060.699	12·324 8,073.023	12·328 8,085.351	12·333 8,097.684	12·338 8,110.022	12·343 8,122.365	12·347 8,134.712	12·352 8,147.064	12·357 8,159.421
820	12·362 8,171.783	12·366 8,184.149	12·371 8,196.520	12·376 8,208.896	12·381 8,221.277	12·385 8,233.662	12·390 8,246.052	12·395 8,258.447	12·400 8,270.847	12·404 8,283.251
830	12·409 8,295.660	12·414 8,308.074	12·419 8,320.493	12·423 8,332.916	12·428 8,345.344	12·433 8,357.777	12·438 8,370.215	12·442 8,382.657	12·447 8,395.104	12·452 8,407.556
840	12·456 8,420.012	12·461 8,432.473	12·466 8,444.939	12·471 8,457.410	12·475 8,469.885	12·480 8,482.365	12·485 8,494.850	12·490 8,507.340	12·494 8,519.834	12·499 8,532.333
850	12·504 8,544.837	12·509 8,557.345	12·513 8,569.858	12·518 8,582.376	12·523 8,594.899	12·527 8,607.426	12·532 8,619.958	12·537 8,632.495	12·541 8,645.036	12·546 8,657.582
860	12·551 8,770.133	12·556 8,682.689	12·560 8,695.249	12·565 8,707.814	12·570 8,720.384	12·574 8,732.958	12·579 8,745.537	12·584 8,758.121	12·588 8,770.709	12·593 8,783.302
870	12·598 8,795.900	12·602 8,808.502	12·607 8,821.109	12·612 8,833.721	12·617 8,846.338	12·621 8,858.959	12·626 8,871.585	12·631 8,884.216	12·635 8,896.851	12·640 8,909.491
880	12·645 8,922.136	12·649 8,934.785	12·654 8,947.439	12·659 8,960.098	12·663 8,972.761	12·668 8,985.429	12·673 8,998.102	12·677 9,010.779	12·682 9,023.461	12·687 9,036.148
890	12·691 9,048.839	12·696 9,061.535	12·701 9,074.236	12·705 9,086.941	12·710 9,099.651	12·715 9,112.366	12·719 9,125.085	12·724 9,137.809	12·729 9,150.538	12·733 9,163.271
900	12·738 9,176.009	12·743 9,188.752	12·747 9,201.499	12·752 9,214.251	12·757 9,227.008	12·761 9,239.769	12·766 9,252.535	12·771 9,265.306	12·775 9,278.081	12·780 9,290.861
910	12·785 9,303.646	12·789 9,316.435	12·794 9,329.229	12·799 9,342.128	12·803 9,354.831	12·808 9,367.639	12·813 9,380.452	12·817 9,393.269	12·822 9,406.091	12·827 9,418.918
920	12·831 9,431.749	12·836 9,444.585	12·841 9,457.426	12·845 9,470.271	12·850 9,483.121	12·855 9,495.976	12·859 9,508.835	12·864 9,521.699	12·869 9,534.568	12·873 9,547.441
930	12·878 9,560.319	12·882 9,573.201	12·887 9,586.088	12·892 9,598.980	12·896 9,611.876	12·901 9,624.777	12·906 9,737.683	12·910 9,650.593	12·915 9,663.508	12·919 9,676.427
940	12·924 9,689.351	12·929 9,702.280	12·933 9,715.213	12·938 9,728.151	12·942 9,741.093	12·947 9,754.040	12·952 9,766.992	12·956 9,779.948	12·961 9,792.909	12·966 9,805.875
950	12·970 9,818.845	12·975 9,831.820	12·979 9,844.799	12·984 9,857.783	12·988 9,870.771	12·993 9,883.764	12·998 9,896.762	13·002 9,909.764	13·007 9,922.771	13·011 9,935.782
960	13·016 9,948.798	13·020 9,961.818	13·025 9,974.843	13·030 9,987.873	13·034 10,000.907	12·039 10,013.946	13·043 10,026.989	12·048 10,040.037	13·053 10,053.090	12·057 10,066.147
970	13·062 10,079.209	13·066 10,092.275	13·071 10,105.346	13·076 10,118.422	13·080 10,131.502	13·085 10,144.587	12·089 10,157.676	12·094 10,170.770	13·098 10,183.869	13·103 10,196.972
980	13·108 10,210.080	13·112 10,223.192	13·117 10,236.309	13·122 10,249.431	13·126 10,262.557	13·131 10,275.688	13·135 10,288.823	13·140 10,301.963	13·145 10,315.108	13·148 10,328. 057
990	13·154 10,341.411	13·159 10,354.570	13·163 10,367.733	13·168 10,380.901	13·172 10,394.073	13·177 10,407.050	13·181 10,420.431	13·186 10,433.617	13·190 10,446.807	12·195 10,460.002

TABLE IV (Continued)

Revised Emf-Temperature Tables for Pt-13 %RhPt Thermocouples.
Reference Junction - 0°C Temperature in °C Emf in Absolute Microvolts.
Small type gives microvolts per degree for each preceding interval.

°C	0	1	2	3	4	5	6	7	8	9
	13·190	13·194	13·200	13·213	13·218	13·223	13·227	13·232	13·236	13·241
1,000	10,473.202	10,486.406	10,499.615	10,512.828	10,526.046	10,539.269	10,552.496	10,565.728	10,578.964	10,592.205
	13·245	13·250	13·254	13·259	13·263	13·268	13·272	13·277	13·281	13·286
1,010	10,605.450	10,618.700	10,631.954	10,645.213	10,658.476	10,671.744	10,685.016	10,698.293	10,711.574	10,724.860
	13·291	13·295	13·300	13·304	13·309	13·313	13·318	13·322	13·327	13·331
1,020	10,738.151	10,751.446	10,764.746	10,778.050	10,791.359	10,804.672	10,817.990	10,831.312	10,844.639	10,857.970
	13·336	13·341	13·345	13·350	13·354	13·359	13·363	13·368	13·373	13·377
1,030	10,874.306	10,884.647	10,897.992	10,911.342	10,924.696	10,938.055	10,951.418	10,964.786	10,978.159	10,991.536
	13·382	13·386	13·391	13·395	13·400	13·404	13·409	13·413	13·418	13·422
1,040	11,004.918	11,018.304	11,031.695	11,045.090	11,058.490	11,071.894	11,085.303	11,098.716	11,112.134	11,125.556
	13·427	13·431	13·436	13·440	13·445	13·449	13·454	13·458	13·463	13·467
1,050	11,138.983	11,152.414	11,165.850	11,179.290	11,192.735	11,206.184	11,219.638	11.233.096	11,246.559	11,260.026
	13·472	13·476	13·481	13·485						
1,060	11,273.498	11,286.974	11,300.455	11,313.940						

TABLE V Emf Differences - Table 4, Bulletin No. 508 Minus Smoothed Tables (Table IV)

°C	0	1	2	3	4	5	6	7	8	9
0	0	−0.422	+0.134	−0.332	+0.180	−0.330	+0.138	−0.416	−0.992	−0.590
10	−0.210	+0.148	−0.516	−0.202	+0.090	−0.640	−0.392	−0.165	+0.040	−0.777
20	−0.615	−0.474	−0.354	−0.255	−0.176	−0.118	−0.081	−0.065	−0.070	−0.096
30	−0.142	−0.209	−0.297	−0.406	−0.536	+0.314	+0.143	−0.049	−0.262	+0.504
40	+0.250	−0.025	−0.320	−0.635	+0.029	−0.327	+0.297	−0.099	+0.485	+0.049
50	+0.593	+0.116	+0.619	+0.102	+0.565	+0.008	+0.431	−0.166	+0.217	+0.580
60	−0.077	+0.246	+0.549	−0.168	+0.096	+0.340	−0.546	−0.232	−0.048	+0.116
70	+0.260	+0.385	+0.490	+0.575	+0.640	+0.685	−0.289	−0.283	−0.297	−0.331
80	−0.384	−0.457	−0.550	−0.663	−0.795	+0.053	−0.119	−0.310	−0.521	+0.249
90	0	−0.268	−0.555	+0.139	−0.186	+0.470	+0.108	−0.273	+0.327	−0.091
100	−0.528	+0.016	−0.458	+0.049	−0.463	+0.007	−0.541	−0.107	−0.691	−0.293
110	+0.088	−0.549	−0.203	+0.125	+0.436	−0.270	+0.008	+0.269	−0.487	−0.259
120	−0.048	−0.853	−0.674	−0.511	−0.363	−0.231	−0.115	−0.014	+0.072	+0.143
130	+1.199	+0.241	+0.268	+0.280	+0.278	+0.261	+0.230	+0.185	+0.126	+0.053
140	−0.034	+0.866	+0.752	+0.624	+0.483	+0.328	+0.161	−0.020	−0.214	+0.580
150	+0.361	+0.129	−0.115	−0.372	−1.359	+0.078	−0.216	−0.523	−0.843	−1.175
160	−0.520	−0.879	−0.250	−0.633	−1.029	−0.437	−0.858	−1.292	−0.738	−1.197
170	−0.668	−1.151	−0.646	−0.153	−0.672	−1.203	−0.746	−0.300	−0.866	−0.444
180	−1.034	−1.636	−1.249	−0.874	−1.511	−1.160	−0.820	−0.492	−1.179	−0.874
190	−0.580	−0.297	−0.025	−0.764	−0.514	−1.274	−1.045	−0.827	−0.620	−0.423
200	−0.237	−1.062	−0.898	−0.745	−0.602	−0.470	−1.349	−1238	−1.138	−1.048
210	−0.968	−0.899	−0.840	−0.791	−0.752	−0.724	−0.706	−0.698	−0.700	−0.712
220	−0.734	−0.767	−0.810	−0.863	−0.926	−0.999	−1.082	−1.175	−1.278	−0.391
230	−0.513	−0.645	−0.787	−0.939	−1.101	−1.272	−1.453	−0.644	−0.845	−1.055
240	−0.275	−0.505	−0.744	−0.993	−0.251	−0.518	−0.794	−1.080	−0.375	−0.679
250	−0.992	−0.314	−0.645	−0.985	−0.334	−0.692	−1.059	−0.435	−0.819	−1.212
260	−0.614	−1.025	−0.445	−0.873	−0.310	−0.756	−1.210	−0.773	−1.145	−0.625
270	−0.114	−0.611	−0.117	−0.631	−0.153	−0.684	−0.223	−0.770	−0.325	−0.888
280	−0.460	−1.040	−0.628	−0.224	−0.828	−0.440	−1.060	−0.688	−0.324	−0.967
290	−0.618	−0.277	−0.944	−0.619	−0.301	−0.991	−0.689	−0.395	−1.108	−0.829
300	−0.558	−0.294	−0.037	−0.788	−0.546	−0.311	−0.084	+.136	−0.651	−0.445
310	−0.246	−0.054	+0.131	−0.691	−0.520	−0.356	−0.199	−0.048	+0.096	−0.767
320	−0.637	−0.513	−0.396	−0.286	−0.183	−0.086	−0.996	−0.913	−0.836	−0.766
330	−0.702	−0.644	−0.593	−0.548	−0.509	−0.476	−0.450	−0.430	−0.416	−0.408
340	−0.406	−0.410	−0.416	−0.428	−0.450	−0.478	−0.512	−0.552	−0.598	−0.650
350	−0.708	−0.772	−0.842	−0.918	−0.999	−1.086	−1.179	−0.278	−0.383	−0.493
360	−0.609	−0.731	−0.859	−0.992	−1.131	−1.276	−1.427	−0.583	−0.745	−0.913

TABLE V (Cont.) Emf Differences – Table 4, Bulletin No. 508 Minus Smoothed Tables (Table IV)

°C	0	1	2	3	4	5	6	7	8	9
370	-1.086	-1.265	-1.449	-1.639	-0.834	-1.035	-1.241	-1.452	-1.669	-1.891
380	-1.118	-1.351	-1.589	-1.832	-2.080	-1.333	-1.592	-1.856	-1.125	-1.399
390	-1.678	-1.962	-1.252	-1.547	-1.847	-2.152	-1.462	-1.777	-2.097	-1.423
400	-1.754	-2.090	-1.431	-1.777	-2.128	-1.484	-1.845	-2.212	-2.584	-1.861
410	-2.343	-2.730	-2.122	-2.519	-1.921	-2.328	-1.741	-2.159	-1.582	-2.010
420	-1.443	-1.881	-2.324	-1.772	-2.225	-1.681	-2.148	-1.617	-2.091	-1.570
430	-1.054	-1.543	-2.037	-1.536	-2.040	-1.549	-2.063	-1.582	-1.106	-1.635
440	-1.170	-1.710	-1.255	-1.805	-1.360	-0.920	-1.485	-1.055	-1.630	-1.210
450	-0.795	-1.385	-0.980	-1.580	-1.185	-0.795	-0.410	-1.030	-0.655	-1.285
460	-0.920	-1.560	-1.205	-1.855	-1.510	-2.170	-1.835	-2.505	-2.180	-2.860
470	-2.545	-2.235	-1.930	-2.630	-2.334	-2.043	-2.757	-2.476	-3.200	-2.929
480	-2.663	-3.402	-3.146	-2.894	-3.647	-3.405	-3.168	-3.936	-3.709	-3.487
490	-3.270	-4.057	-3.849	-3.646	-4.448	-4.255	-4.067	-4.884	-4.705	-4.531
500	-4.362	-4.198	-4.039	-3.885	-4.735	-4.590	-4.450	-4.315	-4.185	-5.060
510	-4.940	-4.824	-4.713	-4.607	-4.506	-4.410	-4.319	-4.233	-4.151	-4.074
520	-5.002	-4.935	-4.873	-4.816	-4.763	-4.715	-4.672	-4.634	-4.601	-4.573
530	-4.549	-4.530	-4.516	-4.507	-4.503	-4.504	-4.509	-4.519	-4.534	-4.554
540	-3.579	-3.609	-3.643	-3.682	-3.726	-3.775	-3.829	-3.887	-3.95	-4.018
550	-3.091	-3.169	-3.251	-3.338	-3.430	-3.527	-3.628	-3.734	-3.845	-2.961
560	-3.082	-3.207	-3.337	-3.472	-3.612	-3.757	-2.906	-3.060	-3.219	-3.383
570	-3.552	-2.725	-2.903	-3.086	-3.274	-3.467	-3.664	-3.866	-3.073	-3.285
580	-3.402	-3.723	-3.949	-4.180	-3.416	-3.657	-3.902	-4.152	-3.407	-3.667
590	-3.932	-4.201	-4.475	-3.754	-4.038	-3.327	-3.620	-3.918	-4.221	-4.529
600	-3.842	-4.159	-3.481	-3.808	-3.140	-3.477	-3.818	-4.161	-3.515	-3.871
610	-3.232	-3.597	-2.967	-3.342	-2.722	-3.107	-2.496	-2.890	-2.289	-2.693
620	-2.102	-2.515	-2.932	-2.356	-2.784	-2.217	-1.654	-2.096	-2.543	-1.995
630	-1.452	-1.913	-1.379	-1.850	-2.326	-1.807	-1.292	-1.782	-1.277	-1.777
640	-1.282	-1.791	-2.305	-1.824	-1.348	-1.876	-1.409	-1.947	-1.490	-1.037
650	-1.589	-1.146	-1.708	-2.275	-1.846	-2.422	-2.003	-1.589	-2.179	-2.774
660	-2.374	-1.979	-2.589	-2.203	-1.822	-2.446	-3.075	-2.709	-3.347	-2.990
670	-2.638	-2.291	-2.949	-2.611	-2.278	-1.950	-2.627	-2.309	-2.995	-2.686
680	-2.382	-2.088	-2.789	-2.499	-2.214	-1.934	-2.659	-2.388	-2.122	-2.861
690	-2.605	-2.353	-2.106	-2.864	-2.627	-2.395	-3.167	-2.944	-2.726	-2.513
700	-2.304	-2.100	-1.901	-1.707	-1.518	-2.333	-2.153	-1.978	-1.808	-1.642
710	-2.481	-2.325	-2.174	-2.027	-1.885	-1.748	-1.616	-1.488	-1.365	-1.247
720	-2.134	-2.125	-1.921	-1.822	-1.728	-1.638	-1.553	-2.473	-2.398	-2.327

TABLE V (Cont.) Emf Differences - Table 4, Bulletin No. 508 Minus Smoothed Tables (Table IV)

°C	0	1	2	3	4	5	6	7	8	9
730	-2.261	-2.200	-2.144	-2.092	-2.045	-2.003	-2.966	-2.933	-2.905	-2.882
740	-2.864	-2.850	-2.841	-2.837	-2.837	-2.842	-2.852	-2.867	-2.887	-2.911
750	-2.940	-2.974	-2.013	-3.056	-2.104	-2.157	-2.215	-2.277	-2.344	-2.416
760	-2.493	-2.574	-2.660	-2.751	-1.847	-1.947	-2.052	-2.162	-2.277	-2.396
770	-2.520	-1.647	-1.783	-1.921	-2.064	-2.212	-1.365	-1.522	-1.684	-1.851
780	-2.023	-1.199	-1.380	-1.566	-1.757	-1.952	-2.152	-1.357	-1.567	-1.781
790	-2.000	-1.244	-1.453	-1.686	-1.924	-1.167	-1.415	-0.667	-0.924	-1.186
800	-1.453	-1.724	-1.000	-1.281	-1.567	-0.857	-1.152	-1.452	-1.757	-1.066
810	-1.380	-1.699	-2.023	-1.352	-1.684	-1.022	-1.365	-0.712	-1.064	-1.421
820	-1.783	-2.149	-2.520	-0.896	-1.277	-1.662	-1.052	-1.447	-1.847	-2.251
830	-1.660	-2.074	-1.493	-1.916	-2.344	-1.577	-1.215	-1.657	-1.104	-1.556
840	-1.012	-1.473	-0.939	-1.410	-0.885	-1.365	-0.850	-0.340	-0.834	-1.333
850	-0.837	-1.345	-0.858	-1.376	-0.899	-1.426	-0.958	-1.495	-1.036	-1.582
860	-1.133	-1.689	-1.249	-1.814	-1.384	-0.958	-1.537	-1.121	-1.709	-1.302
870	-0.900	-1.502	-1.109	-1.721	-1.338	-0.959	-1.585	-1.216	-1.851	-1.491
880	-1.136	-1.785	-1.439	-1.098	-1.761	-1.429	-2.102	-1.779	-2.461	-2.148
890	-1.839	-1.535	-2.236	-1.941	-1.651	-1.366	-2.085	-1.809	-1.538	-2.271
900	-1.009	-0.752	-1.499	-1.251	-1.008	-0.769	-1.535	-1.306	-1.081	-0.861
910	-0.646	-0.435	-1.229	-1.028	-0.831	-0.639	-1.452	-1.269	-1.091	-0.918
920	-0.749	-0.585	-1.426	-1.271	-1.121	-0.976	-0.835	-1.699	-1.568	-1.441
930	-1.319	-1.201	-1.088	-0.980	-1.876	-1.777	-1.683	-1.593	-2.508	-2.427
940	-2.351	-2.280	-2.213	-2.151	-2.093	-2.040	-1.992	-1.948	-2.909	-2.875
950	-2.845	-2.820	-2.799	-2.783	-2.771	-2.764	-2.762	-2.764	-2.771	-2.782
960	-2.798	-1.818	-1.843	-1.873	-1.907	-1.946	-1.989	-2.037	-2.090	-2.147
970	-2.209	-2.275	-2.346	-2.422	-1.502	-1.587	-1.676	-1.770	-1.869	-1.972
980	-2.080	-2.192	-2.309	-2.431	-2.557	-1.688	-1.823	-1.963	-2.108	-2.257
990	-2.411	-2.570	-1.733	-1.901	-2.073	-2.250	-1.431	-1.617	-1.807	-2.002
1000	-2.202	-2.406	-2.615	-2.828	-3.046	-2.296	-2.496	-2.728	-2.964	-3.205
1010	-2.450	-2.700	-2.954	-3.213	-3.476	-2.744	-3.016	-3.293	-2.574	-2.860
1020	-2.151	-3.446	-3.746	-3.050	-3.359	-3.672	-2.990	-3.312	-3.639	-2.970
1030	-2.306	-2.647	-2.992	-2.342	-2.696	-2.055	-2.418	-1.786	-2.159	-2.546
1040	-1.918	-2.304	-1.695	-2.090	-1.490	-1.894	-1.303	-1.716	-1.134	-1.556
1050	-0.983	-1.414	-0.850	-1.290	-1.735	-1.184	-0.638	-1.096	-0.559	-1.026
1060	-0.498	-0.974	-0.455	-0.940						

CALCULATION OF POLYNOMIALS FOR EMF-TEMPERATURE EQUATIONS

The emf-temperature values given in Table 4, Bulletin No. 508, Bureau of Standards, in the neighborhood of 500°C may be approximated by the use of second degree polynomials. The following calculations and equations are given to demonstrate the inadequacy of the derived equations in provided the requisite accuracy (0.1 microvolts) for use in the adiabatic calorimeter and to show that the tables as given in Table 4, Bulletin No. 508, must be in error in the neighborhood of 500°C. It is reasonable to expect that if an equation is fitted over a 100°C range, and will give values agreeing with the published values within 1.5 microvolts, that the curve could be extrapolated 20 to 30°C beyond the ends of the range with the same accuracy. It does not seem reasonable that the true emf-temperature equation could be other than smooth and continuous.

The approximating equation is:

$$E_{T_1}^{T_2} = a + bT + cT^2$$

where

E = the emf of the thermocouple in microvolts
T = temperature in °C
T_1 = lower temperature limit
T_2 = upper temperature limit
a, b, and c = constants of the equation for the given temperature range.

The following emf-temperature values are taken from Table 4, Bulletin No. 508, Bureau of Standards, pages 17 and 18.

°C	Emf	°C	Emf
350	2,890	500	4,455
380	3,194	520	4,672
400	3,194	550	5,004
430	3,712	600	5,563
480	4,241		

The equations derived using these values for evaluation of the constants are:

(1) $E_{350}^{450} = -253.0 + 7.930\ T + 3.0 \times 10^{-3}\ T^2$ (350,400,450)

(2) $E_{380}^{480} = -384.2 + 8.580\ T + 2.2 \times 10^{-3}\ T^2$ (380,430,480)

(3) $E_{500}^{600} = -485.0 + 8.88\ T + 2.0 \times 10^{-3}\ T^2$ (500,550,600)

The temperatures of the prior table were substituted in the above equations to determine the emfs and the smoothness of the equations. The values are given below.

°C	Eq.1	Eq.2	Eq. 3	Table 4
350	2,890.0	2,888.3		2,890
380	3,193.6	3,193.9		3,194
400	3,399.0	3,399.8		3,399
430	3,711.6	3,712.0		3,712
450	3,923.0	3,922.3	3,916.0	3,923
480	4,244.6	4,241.1	4,238.2	4,241
500	4,462.0	4,455.8	4,455.0	4,455
520		4,672.3	4,673.4	4,672
550		5,000.3	5,004.0	5,004
600			5,563.0	5,563

When equation (1) is extrapolated 30°C above its limits, the error is 3.6 microvolts. When extrapolated 50°C, the error is 7.0 microvolts. When equation (2) is extrapolated 30°C below its limits, the error is 1.7 microvolts, and for 20, 40, and 70°C above, the errors are 0.8, 0.3, and 3.7 microvolts. When equation (3) is extrapolated 20°C below, the error is 2.8 microvolts and is 7.0 microvolts for 50°C below. The fit of each equation within its range is within 1.5 microvolts for all values in that range. Thus it is apparent that there must be errors in the tables. It is also apparent that the quadratic equation cannot be used with sufficient accuracy (0.1 microvolts) to calculate the emfs, for which one is to be used?

APPENDIX B

TABLE VI TRUE C_p OF COPPER AND HEAT ABSORBED BY SPECIMEN HEATER

°C	True Mean Specific Heat of Copper		Heat to Specimen Heater (Calculated)				
			Al_2O_3		Nichrome		Heater
	Exp.	Calc.	C_p	Cal/°C	C_p	Cal/°C	Cal/°C
100	0.08640	0.0930	0.2130	0.1404	0.13	0.0592	0.1996
130	0.08735						
150	0.08795						
170	0.08860						
190	0.08920						
200		0.0946	0.2350	0.1549	0.13	0.0592	0.2141
210	0.08981						
230	0.09045						
250	0.09105						
270	0.09158						
290	0.09220						
300		0.0980	0.2552	0.1680	0.13	0.0592	0.2272
310	0.09285						
330	0.09336						
350	0.09407						
370	0.09463						
390	0.09529						
400		0.1010	0.2698	0.1780	0.13	0.0592	0.2372
410	0.09592						
430	0.09650						
450	0.09715						
470	0.09771						
490	0.09828						
500		0.1040	0.2792	0.1839	0.13	0.0592	0.2431
510	0.09893						
530	0.09942						
550	0.10009						
570	0.10075						
590	0.10136						
600		0.1067	0.2860	0.1885	0.13	0.0592	0.2431
610	0.10192						
630	0.10243						
650	0.10304						
670	0.10362						
690	0.10418						
700		0.1095	0.2906	0.1918	0.13	0.0592	0.2510
710	0.10476						
730	0.10529						
750	0.10529						
770	0.10641						
790	0.10702						
800			0.2940	0.1937	0.13	0.0592	0.2529

Experimental specific heats of copper calculated by differences. Calculated specific heats of copper calculated by calculated heater correction. Weight of Al_2O_3 = 0.659 grams, Nichrome = 0.455 grams Al_2O_3 specific heats calculated from data in NBS No. 476, page 11.

TABLE VII FREE ENERGY AND ENTHALPY OF TRANSFORMATION OF A 0.75%C-1% Mn STEEL AT SUBCRITICAL TEMPERATURES

1 °C	2 °K	3 C_p^{pear}	4 C_p^{aus}	5 ΔC_p^{app}	6 ΔC_p^{true}	7 ΔC_p^{true}/mol	8 $\Delta C_p/T$	9 $-\Delta H$	10 $\int \Delta C_p/T$	11 $\iint \Delta C_p/T$	12 ΔT	13 $\frac{\Delta H_o \Delta T}{T_o}$	14 ΔF
710	983	0.2214	0.1550	0.0664	0.0767	4.1686	0.004241	935	0	0	0	0	0
690	963	0.2092	0.1543	0.0549	0.0634	3.4458	0.003578	1011.1	0.0782	0.782	20	-19.0	-19.8
670	943	0.2016	0.1536	0.0480	0.0554	3.0110	0.003193	1075.7	0.1459	3.023	40	038.0	-41.1
650	923	0.1954	0.1529	0.0425	0.0491	2.6686	0.002891	1132.5	0.2067	6.549	60	-57.1	-63.6
630	903	0.1899	0.1522	0.0377	0.0435	2.364	0.002618	1188.1	0.2618	11.235	80	-76.1	-87.3
610	883	0.1856	0.1515	0.0341	0.0394	2.1414	0.0024 5	1233.2	0.3123	16.976	100	-95.1	-112.1
590	863	0.1822	0.1508	0.0314	0.0363	1.9729	0.002286	1274.3	0.3594	23.693	120	-114.1	-137.8
570	843	0.1782	0.1501	0.0281	0.0324	1.7609	0.002089	1311.6	0.4031	31.318	140	-133.2	-164.5
550	823	0.1743	0.1494	0.0249	0.0288	1.5653	0.001902	1344.9	0.4430	39.779	160	-152.2	-192.0
530	803	0.1718	0.1487	0.0231	0.0267	1.4511	0.001807	1375.1	0.4801	49.011	180	-171.2	-220.2

Critical temperature = 710°C
Mol weight = 54.35 grams
Total weight specimen + heater = 19.5217 grams
True weight of specimen = 16.9060 grams
Col. 3 = apparent specific heat of pearlite/gram
Col. 4 = apparent specific heat of austenite/gram
Col. 5 = difference between 4 and 3
Col. 6 = true specific heat difference/gram
Col. 7 = true specific heat difference/mol=54.35 x (col.6)
Col. 8 = col. 7 divided by col. 2

Col. 9 = enthalpy of transformation, cal/mol
$= 9_2 = 9_1 + 20(7_1 + 7_2)/2$
Col. 10= $10_2 = 10_1 + 20(8_1 + 8_2)/2$
Col. 11= $11_2 = 11_1 + 20(10_1 + 10_2)/2$
Col. 12= degree of supercooling °C
Col. 13= $\frac{\Delta H_o \Delta T}{T_o} = \frac{935 \times \Delta T}{983} = 0.95117 \times \Delta T$
Col. 14= free energy of transformation, cal/mol
$14_1 = 13_1 + 11_1$

DATA NEEDED FOR CALCULATIONS IN TABLE VIII

The equation used to perform the calculations in Table VIII is:

$$\Delta H_{T_2} = \Delta H_{T_1} + (T_2 - T_1)\, \Delta C_p^{(\alpha-\gamma)} \times (55.85)$$

where

ΔH = enthalpy of transformation of pure iron, cal/mol
T_2 = lower temperature °C
T_1 = upper temperature °C
ΔC_p = difference in true specific heats per gram

As the enthalpies of transformation were desired at the even temperatures, and the specific heats are mean specific heats at the odd temperatures, the differences of true mean specific heats were not averaged over the temperature interval, but were taken as the mean over the temperature interval of the even temperatures. That is, the mean true specific heat difference between austenite and ferrite at 890°C is 0.1814 cal/gram °C. This then was the mean specific heat difference over the temperature interval from 900 to 880°C. Therefore, in Table VIII,

$$\text{Col. } 14_3 = \text{col. } 13_2 \times 20 \times 55.85 + \text{col. } 14_1$$

where the subscripts are the line numbers in Table VIII

Weight of copper plugs = 1.3566 grams
Weight of heater = 1.2547 grams
Weight of iron specimen = 26.1352 grams
Weight of Fe + heater = 27.2791 grams
Weight of steel specimen = 16.9060 grams
Weight of steel + heater = 19.5217 grams

$$\Delta C_p^{Fe} = C_{p_{app}}^{alpha} \times \frac{wt^{app\ Fe}}{wt_{true\ Fe}} - C_{p_{app}}^{aus(Mn)} \times \frac{wt^{app\ Mn}}{wt_{true\ Mn}} + C_p^{Cu} \times \frac{wt^{Cu}}{wt_{t,Mn}}$$

$$+ C_p^{heater} \times \frac{wt^{heater}}{wt_{t,Mn}} \left(1 - \frac{wt^{h,Fe} \times wt^{t,Mn}}{wt_{h,Mn} \times wt_{t,Fe}}\right)$$

$$\Delta C_p^{Fe} = 1.04377\ C_{p_{app}}^{alpha} - 1.15472\ C_{p_{app}}^{aus(Mn)} + 0.80244\ C_p^{Cu} + 0.03083\ C_p^{heater}$$

TABLE VIII ENTHALPY OF TRANSFORMATION OF PURE IRON AT SUBCRITICAL TEMPERATURES

1	2	3	4	5	6	7	8	9	10	11	12	13	14
910	0.1105	0.1499	0.2550	0.1051	0.08377	0.00258	0.00887	0.1620	0.18706	0.1847	0.19278	0.01717	211
900													220.9
890	0.1099	0.1491	0.2545	0.1054	0.08400	0.00259	0.00882	0.1614	0.18637	0.1850	0.19310	0.01814	
880													241.2
870	0.1094	0.1484	0.2542	0.1058	0.08432	0.00260	0.00878	0.1608	0.18568	0.1869	0.19508	0.02078	
860													264.4
850	0.1088	0.1476	0.2538	0.1062	0.08464	0.00261	0.00873	0.1602	0.18499	0.1909	0.19926	0.02561	
840													293.0
830	0.1082	0.1468	0.2535	0.1067	0.08504	0.00262	0.00868	0.1596	0.18429	0.1956	0.20416	0.03117	
820													327.8
810	0.1077	0.1461	0.2531	0.1070	0.08528	0.00263	0.00864	0.1590	0.18360	0.2010	0.20980	0.03747	
800													369.7
790	0.1071	0.1453	0.2526	0.1073	0.08552	0.00264	0.00859	0.1584	0.18291	0.2081	0.21721	0.04553	
780													420.6
770	0.1065	0.1445	0.2522	0.1077	0.085837	0.00265	0.00855	0.1578	0.18221	0.2460	0.25677	0.08576	
760													516.4
750	0.1060	0.1438	0.2517	0.1079	0.08600	0.00265	0.00851	0.1572	0.18152	0.2518	0.26282	0.09246	
740													619.7
730	0.1054	0.1430	0.2512	0.1082	0.08624	0.00266	0.00846	0.1566	0.18083	0.23195	0.24210	0.07239	
720													700.6
710	0.1048	0.1422	0.2507	0.1085	0.08648	0.00267	0.00841	0.1560	0.18014	0.21907	0.22866	0.05960	
700													767.2
690	0.1042	0.1414	0.2502	0.1088	0.08671	0.00267	0.00836	0.1554	0.17944	0.2088	0.21794	0.04953	
680													822.5
670	0.1036	0.1405	0.2496	0.1091	0.08695	0.00268	0.00831	0.1548	0.17875	0.2014	0.21016	0.04240	
660													869.9
650	0.1030	0.1397	0.2490	0.1093	0.08711	0.00269	0.00827	0.1542	0.17806	0.1938	0.20228	0.03518	
640													909.2
630	0.1024	0.1389	0.2484	0.1095	0.08727	0.00269	0.00822	0.1536	0.17736	0.1873	0.19552	0.02907	
620													941.7
610	0.1018	0.1381	0.2477	0.1096	0.08735	0.00269	0.00817	0.1530	0.17667	0.1820	0.18997	0.02416	

Col. 1 = temperature °C
Col. 2 = true sp. h. copper
Col. 3 = 1.3566 x col. 2
Col. 4 = heat to heater + plugs
Col. 5 = col. 4 - col. 3
Col. 6 = col.5/1.2547
Col. 7 = 0.03083 x col. 6
Col. 8 = 0.08024 x col. 2
Col. 9 = apparent sp. h. aus.
Col.10 = 1.15472 x col. 9
Col. 11 = apparent sp. h. ferrite
Col. 12 = 1.04377 x col. 11
Col. 13 = difference of true sp. h. = (12)-(10) + (8) + (7)
Col. 14 = enthalpy of trans. cal/mol

TABLE IX FREE ENERGY AND ENTHALPY OF TRANSFORMATION OF A 0.87% C Fe-C ALLOY AT SUBCRITICAL TEMPERATURES

1	2	3	4	5	6	7	8	9	10	11	12	13	14
720	993		0.15535					875	0	0	0	0	0
700	973	0.2185	0.15465	0.0638	0.0728	3.9409	0.004050	983.7	0.1106	1.106	20	-17.6	-18.7
690	963	0.2094	0.1543	0.0551	0.0629	3.4035	0.003534	1020.4	0.1485	2.4025	30	-26.4	-28.8
670	943	0.2015	0.1536	0.0479	0.0547	2.9588	0.003138	1084.1	0.2152	6.0391	50	-44.1	-50.1
650	923	0.1940	0.1529	0.0411	0.0469	2.5388	0.002751	1139.0	0.2741	10.9327	70	-61.7	-72.6
630	903	0.1887	0.1522	0.0365	0.0417	2.2546	0.002497	1186.9	0.3266	16.9398	90	-79.3	-96.2
610	883	0.1842	0.1515	0.0327	0.373	2.0199	0.002288	1229.7	0.3744	23.9501	110	-96.9	-120.9
590	863	0.1809	0.1508	0.0301	0.0343	1.8593	0.002155	1268.5	0.4189	31.8831	130	-114.6	-146.4
570	843	0.1767	0.1501	0.0266	0.0304	1.6431	0.0019949	1303.5	0.4599	40.6706	150	-132.2	-172.8
550	823	0.1735	0.1494	0.0241	0.0275	1.4887	0.001809	1334.9	0.4975	50.2442	170	-149.8	-200.0
530	803	0.1701	0.1487	0.0214	0.0244	1.3219	0.0016446	1362.9	0.5320	60.5392	190	-167.4	-228.0

Critical temperature = 720°C
mol weight = 54.13
total weight specimen + heater = 19.7388 grams
true weight of specimen = 17.2973 grams
Col. 1=temperature °C
Col. 2=temperature °K
Col. 3=apparent specific heat of pearlite/gram
Col. 4=apparent specific heat of austenite/gram
Col. 5=difference between 3 and 4
Col. 6=true specific heat difference/gram
=(col. 5) x 19.7388/17.2973 = 1.141149 x (col. 5)

Col. 7 = true specific heat difference/mol
= 54.13 x (col. 6)
Col. 8 = Col. 7 divided by col. 2
Col. 9 = enthalpy of trans., cal/mol $9_2 = 9_1 + 20(7_1 + 7_2)/2$
Col.10 = $\Delta C_p/T$ $10_2 = 10_1 + 20(8_1 + 8_2)/2$
Col.11 = $\Delta C_p/T$ $11_2 = 11_1 + 20(10_1 + 10_2)/2$
Col.12 = ΔT = degree of supercooling °C
Col.13 = $H_o \Delta T/T_o$ = 875 x ΔT/993=0.881168 ΔT
Col.14 = ΔF = free energy of transformation,
= cal/mol = $14_1 = 13_1 + 11_1$

TABLE X

EXPERIMENTAL APPARENT SPECIFIC HEATS OF 0.75%C-1%Mn & 0.87%C STEELS

°C	T-261 620°C	T-262 620°C	T-310 640°C	T-311 640°C	T-270 660°C	T-278 680°C	T-279 680°C	0.87%C Steel
70		0.11277	0.11277			0.11372		
90		0.11455	0.11588	0.11449	0.11450	0.11711		0.11879
110		0.11946	0.12197	0.11951	0.11926	0.12298		0.12210
130		0.12342	0.12636	0.12355	0.12415	0.12604	0.12414	0.12422
150		0.12752	0.12925	0.12727	0.12917	0.12867	0.12663	0.12798
170	0.13134	0.13207	0.13268	0.13130	0.13405	0.13233	0.12965	0.13295
190	0.13299	0.13443	0.13596	0.13365	0.13632	0.13521	0.13299	0.13712
210	0.13587	0.13725	0.13921	0.13713	0.13845	0.13787	0.13538	0.13974
230	0.13914	0.14031	0.14149	0.13988	0.14081	0.14119	0.13887	0.14089
250	0.14249	0.14321	0.14256	0.14257	0.14347	0.14430	0.14213	0.14328
270	0.14499	0.14555	0.14520	0.14513		0.14599	0.14447	0.14554
290	0.14731	0.14781	0.14738	0.14727		0.14697	0.14704	0.14778
310	0.14882	0.14906	0.14946	0.14886		0.15012	0.14882	0.14954
330	0.15060	0.15113	0.15118	0.15077		0.15299	0.15060	0.15145
350	0.15220	0.15274	0.15290	0.15264		0.15494	0.15207	0.15308
370	0.15403	0.15434	0.15495	0.15429		0.15735	0.15408	0.15480
390	0.15518	0.15574	0.15622	0.15547	0.15488	0.15901	0.15563	0.15636
410	0.15693	0.15752	0.15770	0.15724	0.15679	0.16139	0.15697	0.15831
430	0.15852	0.15945	0.15953	0.15903	0.15858	0.16303	0.15916	0.16195
450	0.16070	0.16195	0.16184	0.16146	0.16046	0.16552	0.16099	
470	0.16351	0.16417	0.16438	0.16250	0.16250	0.16742	0.16386	0.16261
490	0.16652	0.16781	0.16713	0.16667	0.16589	0.17025	0.16705	0.16579
510	0.16809	0.16955	0.16881	0.16829	0.16805	0.17273	0.16858	0.16690
530	0.17048	0.17255	0.17183	0.17138	0.17133	0.17518	0.17181	0.17007
550	0.17186	0.17361	0.17364	0.17328	0.17439	0.17803	0.17429	0.17347
570	0.17449	0.17631	0.17680	0.17628	0.17704	0.18211	0.17823	0.17671
590	0.17731	0.17943	0.18034	0.17934	0.18044	0.18648	0.18219	0.18094
610	0.17982	0.18180	0.18280	0.18199	0.18299	0.19043	0.18560	0.18424
630	0.18559	0.18594	0.18696	0.18519	0.18629	0.19439	0.18994	0.18867
650	0.19340	0.19157	0.19095	0.19031	0.19035	0.20014	0.19535	0.19399
670	0.19895	0.19936	0.19832	0.19727	0.10567	0.20611	0.20164	0.20347
690	0.20742	0.20867	0.20713	0.20655	0.20401	0.21369	0.20922	0.20836
710	0.21815	0.22153	0.22009	0.21899	0.21647	0.22466	0.22139	0.24297
730	1.34745	1.39031	1.36609	1.37727	1.35617	1.32727	1.35526	1.32545
735	0.30630	0.30209	0.31225	0.30719	0.30061	0.32741	0.31856	0.35812
750	0.18924	0.17761	0.19170	0.15521	0.17571	0.19467	0.18675	0.17976
770	0.16232	0.15787	0.16099	0.15872	0.15942	0.16734	0.16115	0.17234
790	0.16222	0.15805	0.16013	0.15889	0.15877	0.16623	0.15856	0.16263
810							0.15865	0.16117

All T- specimens are 0.75%C - 1% Mn Steels isothermally transformed from austenite to pearlite at the temperatures indicated. The 0.87%C Fe-C Binary alloy was furnace cooled from the homogenizing temperature of 1100°C.

TABLE XI REPRODUCIBILITY OF SPECIFIC HEATS IN A 0.75% C - 1% Mn STEEL AND SPECIFIC HEATS OF AUSTENITE IN 0.75%C-1%Mn AND 0.87%C STEELS

°C	29 April		1 May		2 May			0.87% C Binary
	Pearlite	Austenite	Pearlite	Austenite	Pearlite	Austenite		Austenite
90					0.12288			
110					0.12044			
130					0.12544			
150					0.12833			
155			0.12948					
165			0.13083		0.12998			
170	0.13028							
175			0.13291		0.13187			
185			0.13262		0.13233			
190	0.13119							
195			0.13388		0.13376			
205			0.13387					
210	0.13416				0.13579			
230	0.13735		0.13919		0.13808			
250	0.14065	0.14167	0.14167		0.14094			
270	0.14338		0.14348		0.14298			
290	0.14618		0.14529		0.14526			
310	0.14737		0.14698		0.14684			
330	0.14972		0.14913		0.14901			
350	0.15147		0.15065		0.15106			
370	0.15343		0.15256		0.15311			
390	0.15545		0.15407		0.15411			
410	0.15724		0.15670		0.15616			
430	0.15964		0.15861		0.15797			
450	0.16024		0.16082		0.16007			
470	0.16231		0.16307		0.16258			
490	0.16505		0.16614		0.16554			
510	0.16666		0.16871		0.16762			
530	0.16953	0.17178	0.17177		0.17117			
550	0.17215		0.17451		0.17387			
570	0.17547		0.17853		0.17790			
590	0.18089		0.18300		0.18143			
610	0.18444		0.18635		0.18528			
630	0.18918		0.19123		0.19034			
650	0.19484				0.19682			
670	0.20146		0.20347		0.20392			
690	0.21004	(cooled	0.20958		0.21217			
710		to 710)	0.22257			(cooled		(cooled
735		0.15641				to 704)		to 725)
750		0.15680				0.15733		0.15802
770	0.16163	0.15797	0.15973		0.16097	0.15883		0.15747
790	0.16011	0.15822	0.15713		0.15969	0.15892		0.15588
810		0.15830	0.15713		0.15969	0.15831		0.15980
830			0.16574		0.16210	0.15921		0.16364
850			0.16377		0.16238 -	0.16043		0.16659
870								0.16171

All specimens were held for 30 to 45 minutes at 850 to 900°C before determining austenite specific heats.

TABLE XII

EXPERIMENTAL APPARENT SPECIFIC HEATS OF PURE IRON

°C	C_p	°C	C_p
70	0.11223	610	0.18201
90	0.11483	630	0.18732
110	0.11836	650	0.19380
130	0.12153	670	0.20135
150	0.12399	690	0.20881
170	0.12684	710	0.21907
190	0.12822	730	0.23195
210	0.13083	745	0.24477
230	0.13369	755	0.26073
250	0.13622	765	0.28136
270	0.13834	775	0.22748
290	0.14072	785	0.20849
310	0.14240	795	0.20668
330	0.14431	805	0.20185
350	0.14616	815	0.19954
370	0.14827	825	0.20440
390	0.14993	835	0.19585
410	0.15239	845	0.18602
430	0.15418	855	0.19111
450	0.15715	865	0.19007
470	0.15958	875	0.18549
490	0.16230	885	0.18467
510	0.16459	895	0.18471
530	0.16784	905	0.18453
550	0.17038	925	0.15946
570	0.17448	935	0.15680
590	0.17837		